Identifying Genetic Factors and Processes Involved in the Cardiac Perinatal Transitional Program

Lara Kouri
Hon. B.Sc., Minor B.A.

Thesis submitted to the Faculty of Graduate and Postdoctoral Studies, in partial fulfillment of the requirements for the M.Sc. degree in Biochemistry

Department of Biochemistry, Microbiology and Immunology

Faculty of Medicine

University of Ottawa

ABSTRACT

Cardiomyocyte perinatal development is characterized by the transition from a hyperplastic to a hypertrophic growth. We hypothesize that genetic factors and processes in the cardiac perinatal transitional program can be identified by a systematic analysis of different stages in heart development. Microarray expression patterning of mRNAs and microRNAs uncovered a perinatal cardiogenomic switch between 5 and 7 days post-birth. Gene ontology analysis revealed cellular and metabolic processes as highly representative Biological Processes. Moreover, approximately 40% of known mice transcription factors are significantly ($p<0.05$) fluctuating between embryonic day 19 and 10 days post-birth. As the heart matures, cardiomyocytes progressively exit cell cycle with day 5 as a pivotal point. Hypertrophy entails cardiomyocyte binucleation which may be promoted by Protein Regulator of Cytokinesis (Prc1) and its interactors. Temporal cardiac transcription expression analysis provides insight into underlining effectors within the cardiac perinatal transitional program as well as cardiac pathology.

ACKNOWLEDGEMENTS

First and foremost, I would like to thank my Supervisor, Dr. Patrick Burgon, for wholeheartedly welcoming me into his lab and for his continuous involvement and guidance throughout my Master's research project. You have given me the opportunity to explore an exciting field in amazing company.

I would like to express my gratitude to my thesis advisory committee, Dr. Jocelyn Côté and Dr. Balwant Tuana, for their constructive feedback and support. You have been key in the development of this project.

I would like to acknowledge the funding provided by the Ontario Graduate Scholarship (OGS) and the CIHR Frederick Banting and Charles Best Canada Graduate Scholarship Master's Award.

I am particularly indebted to my fellow lab mates and friends: Karen Soueidan, Shelley Deeke, Seham Rabaa, Elmira Ahmady, Allen Teng, Branka Vulesevic, and Jennifer Kasbary. I cannot stress enough how much your smiles, encouragement, help, brainstorming, care and kindness, have been my motivational factor. Also a great big thank you to my study buddies at SITE. I would also like to thank Dr. Alexandre Stewart, Lan Vo, Yanqing Wang, and Robbie Davies for their help during my microarray deciphering days.

I must express my gratitude to my neighbouring lab members Dr. Adolfo de Bold, Dr. Mercedes de Bold, Linda Connor, Asna Choudhry, Monica Forero, Amy Martinuk,

Cassandra Roeske and Shahreen Amin. Thank you for your advice, support and great stories. Our lab office events are not the same without you.

Last but certainly not least, I must express my gratitude to my family for all their infinite love, support and encouragement. Unfortunately I still have not solved heart disease; however you may continue calling me Dr. Lara.

Without you all, my Master's project would not have been possible or enjoyable.

Thank you!

TABLE OF CONTENTS

LIST OF ABBREVIATIONS

ASB15: Ankyrin repeat and SOCS Box-containing 15
ANOVA: Analysis Of Variance
bp: base pair
BP: Biological Processes
CDC2: Cell Division Cycle 2 (Cyclin-Dependent Kinase 1 – CDK1)
CDK4: Cyclin-Dependent Kinase 4
cDNA: Complementary DNA
CT: Cycle Threshold
d: Day
DAPI: 4', 6-diamidino-2-phenylindole
DMEM: Dulbecco's Modified Eagle's Medium
DNA: Deoxyribonucleic Acid
EDTA: Ethylenediaminetetraacetic acid
EPAS1: Endothelial PAS domain protein 1
ES: Enrichment Score
FBS: Fetal bovine serum
FBXW7: F-Box and WD repeat domain containing 7
FDR: False-Discovery Rate
GAPDH: Glyceraldehyde-3-Phosphate Dehydrogenase
GO: Gene Ontology
HDAC: Histone Deacetylase
HEPES: 4-(2-hydroxyethyl)-1-piperazineethanesulfonic acid
HIF3α: Hypoxia Inducible Factor 3, alpha
HRP: Horseradish Peroxidase
kDa: KiloDalton
MAD2l1: MAD2 mitotic arrest deficient-like 1 (yeast)
MHC: Myosin Heavy Chain
MOP: Multicellular Organismal Process
mRNA: Messenger Ribonucleic Acid
miRNA: microRNA
NEB: New England Biolabs
NLS: Nuclear localization signal
NP-40: Nonidet P-40
N.S.: Non-Significant
PBS: Phosphate-Buffered Saline
pCDC2(Tyr15): Phosphorylated CDC2 at Tyrosine 15
PCR: Polymerase Chain Reaction
PFKM: Phosphofructokinase, muscle
PGK2: Phosphoglycerate kinase 2
PLIER: Probe Logarithmic Intensity Error
PLN: Phospholamban
PPIA: Peptidylprolyl isomerase A (cyclophilin A)
pRB(Ser780): Phosphorylated Rb at Serine 780
PRC1: Protein Regulator of Cytokinesis 1
PVDF: Polyvinylidene Fluoride
O/N: Over Night
OR: Olfactory Receptor
RB: Retinoblastoma
RMA: Robust Multi-Array Average
RNA: Ribonucleic Acid
RT: Room Temperature
RT-PCR: Reverse-Transcriptase PCR
RXRγ: Retinoid X Receptor, gamma
SDS-PAGE: Sodium Dodecyl Sulfate Polyacrylamide Gel Electrophoresis
TBE: Tris Borate EDTA
TBST: Tris-Buffered Saline Tween-20
TF: Transcription Factor

LIST OF FIGURES

LIST OF TABLES

INTRODUCTION, RATIONALE, HYPOTHESIS, AND EXPERIMENTAL AIMS

HEART DEVELOPMENT

The heart progresses through different developmental stages (embryogenesis, postnatal development, maturity, and senescence) and responds to environmental and pathological stimuli (Fuster & King, 2008). The heart is composed of a complex arrangement of cardiomyocytes, fibroblasts, as well as smooth muscle, endothelial, endocardial, neuroendocrine and hematopoietic cells, with spatial and regional specialization (Sehl et al., 2000). Cardiomyocytes evolve through three cellular and growth factor-dependent developmental phases: proliferation, binucleation, and hypertrophy (Ahuja et al., 2007).

Normal heart development is regulated by growth programs, mechanical load, plus endo- and paracrine factors (Forssmann et al., 1989; Molkentin & Dorn, 2001). Conversely pathological cardiac growth results as an adaptive response to increased wall stress (i.e. myocardial injury) (Francis & McDonald, 1992). Molecular pathways that modulate the switch between physiological and pathological cardiac growth remain unclear.

At the cellular level, the mammalian heart develops through two main growth phases: i) hyperplasia, and ii) hypertrophy. Hyperplasia principally occurs during prenatal heart development and entails cardiomyocyte proliferation and mononucleation (Oparil et al., 1984; **Figure 1A, B,** and **D**). Hypertrophy predominantly characterizes postnatal cardiac growth whereby cardiomyocyte cellular division is nearly absent and replaced by volume increase and enhanced binucleation (Soonpaa et al., 1996; **Figure 1A, B, C** and **D**). As a result, although cardiomyocytes constitute only about 20% of all cardiac cells within the human myocardium, they contribute 90% of the volume and mass of the heart (Field, 2004).

Cardiomyocytes undergo dynamic growth patterns, however the heart-to-body weight ratio remains relatively constant throughout development and into maturity (**Figure**

1E; Li et al., 1996; Leu et al., 2001). The switch between hyperplasia and hypertrophy suggests that genetic factors regulating cardiomyocyte proliferation and expansion are likely expressed differentially during prenatal and neonatal life.

Transitioning Toward Maturation

Certain physiological, cellular, and anatomical properties in the perinatal heart have been identified whereas genetic regulatory factors remain poorly understood. Morphological parameters that are altered during the transition from a prenatal to a postnatal heart include enhanced myofibril density, mature intercalated discs, and binucleated cardiomyocytes (Winick & Noble, 1965). Physiologically, the heart rate steadily increases with age but then levels off at 14 days postnatally in rats (Wu & Wu, 2009). Conversely, ejection fraction (EF) in rats fluctuates with age whereby for the first four days EF is high, declines until day 7, rises until day 21 then stabilizes into adulthood (Dowell, 1984). In addition, left ventricle size increases with age signifying increased stroke volume and cardiac output (Hopkins et al., 1973).

Temporal cardiomyocyte analysis in the mouse revealed particular developmental parameters: 1) **Day 0-4**: cardiomyocyte volume is constant with an increase in heart weight; 2) **Day 5-14**: cardiomyocyte volume substantially increases; 3) **Day 14**: cardiomyocyte volume increments decreases; 4) **3 months**: cardiomyocytes reach volume maturity (Leu et al., 2001). These phenotypic changes were defined as hyperplasia (at day 0 and 4) and hypertrophy (beginning at day 5).

Figure 1: Cardiomyocyte terminal differentiation occurs shortly after birth and is characterized by a transition from a hyperplastic to a hypertrophic growth. A) Cardiomyocyte DNA synthesis and binucleation during murine development. Proliferation index (black circles) determined via autoradiography of isolated tritiated thymidine cell preparations. Binucleation index (red circles) identified by DAPI immunofluorescence assay of isolated cells. [Adaptation of "Cardiomyocyte DNA synthesis and binucleation during murine development" by Soonpaa et al., 1996 that appeared in *The American Journal of Physiology* of the American Physiological Society. The American Physiological Society has not endorsed the content of this adaptation or translation, or the context of its use.] **B)** Mouse neonatal cardiomyocytes isolated from 3 day and 10 day old hearts illustrating mono- and binucleated phenotypes. Nuclei labeled with propidium iodide (red) and F-actin with phalloidin (green). **C)** Hearts isolated from mice at 1 and 10 days post-birth demonstrate the increase in heart volume with age. **D)** Mouse cardiomyocyte nuclei count per cell (±Standard Deviation), at 3 and 10 days post-birth. **E)** Murine heart and body mass (±Standard Deviation) increases in parallel during development. Panels **B**, **C**, **D**, and **E** are provided by the Burgon lab (unpublished data).

A.

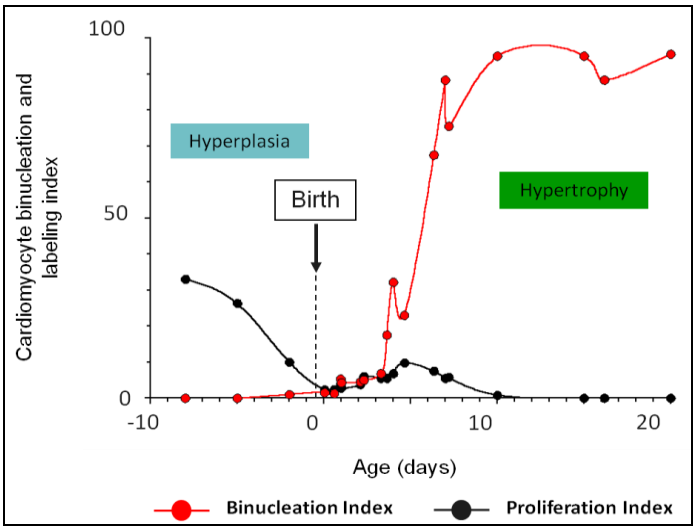
100
50
0
-10
0
10
20
Cardiomyocyte binucleation and labeling index
Hyperplasia
Birth
Hypertrophy
Age (days)
Binucleation Index
Proliferation Index

B.

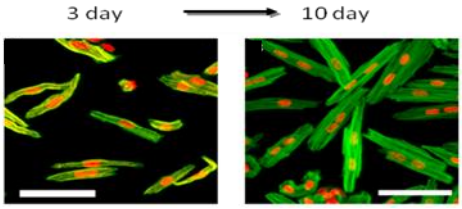
3 day
10 day

C.

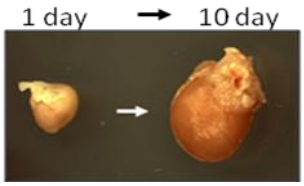
1 day
10 day

D.

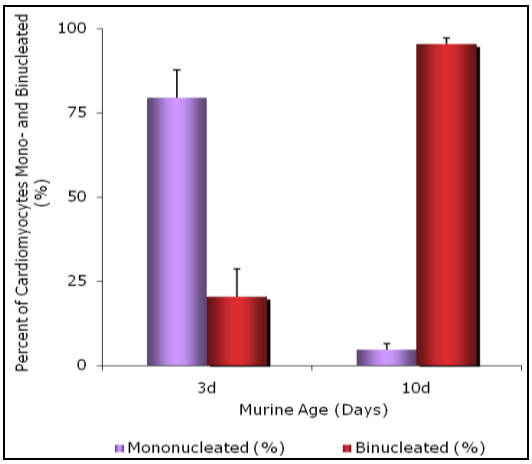
100
75
50
25
0
Percent of Cardiomyocytes Mono- and Binucleated (%)
3d
10d
Murine Age (Days)
Mononucleated (%)
Binucleated (%)

E.

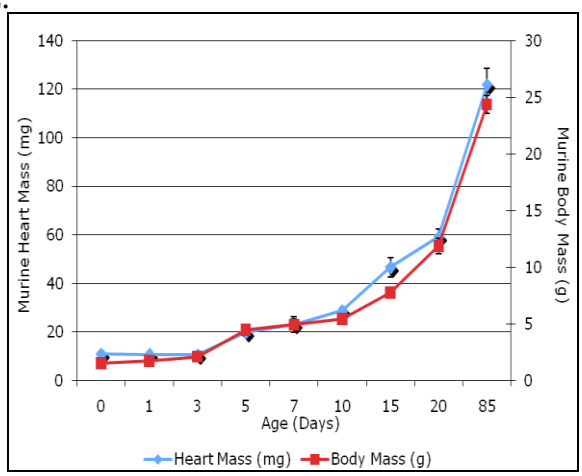
140
120
100
80
60
40
20
0
30
25
20
15
10
5
0
Murine Heart Mass (mg)
Murine Body Mass (g)
0
1
3
5
7
10
15
20
85
Age (Days)
Heart Mass (mg)
Body Mass (g)

Radiolabeling mouse cardiomyocytes with tritiated thymidine demonstrates the gradual decrease in proliferation which coincides with the appearance of binucleation, characterizing the hyperplastic and hypertrophic growth patterns (**Figure 1A**; Soonpaa et al., 1996). Thus far, analysis of Sprague-Dawley rat cardiac development narrowed the switch from hyperplastic and hypertrophic growth to 3 and 4 days post-birth (Li et al., 1996; Poolman & Brooks, 1998) whereas the shift is known to manifest in humans between 3 to 6 months of age (Tam et al., 1995).

Regenerating Muscle

The adult heart has long been believed to be incapable of regenerating injured muscle (Tam et al., 1995; Zak, 1974). That ability is thought to be lost during the perinatal transition, when cardiomyocytes exit the cell cycle and become terminally differentiated (Armstrong et al., 2000). The heart's restricted capacity to regenerate is reinforced by the knowledge that primary cardiac sarcomas are rare (Simpson et al., 2008). In fact, some evidence has emerged proving that the heart may possess limited ability to renew cardiomyocyte pools.

Bergmann et al. (Bergmann et al., 2009) reported that 50% of human cardiomyocytes are renewed during a normal life span. The Frisén group proved that human cardiomyocytes are restored at a 1% turnover rate per year until the age of 25 followed by a decrease to 0.45% at the age of 75. This work capitalized on the release of ^{14}C generated by nuclear bomb testing during the Cold War to radiocarbon date human cardiomyocytes.

Moreover, the majority of cardiomyocytes originating from a mature heart are said to be terminally differentiated, keeping in mind that a fraction of younger cardiomyocytes (15-

20% in rat myocardium) retain their replicative capacity (Kajstura et al., 2000; Leri et al., 2000).

The heart predominantly responds to myocardial injury by scar formation (Mallory et al., 1939). Recently, studies have focused on myocardial regenerative therapies in the hopes of reversing the damage. Such studies include implantation of multipotent cardiac stem cells which illustrated a renewal of rat myocardium after an acute injury (Anversa & Nadal-Ginard, 2002). Furthermore, populations of cardiac, embryonic, and induced pluripotent stem cells have widely been assessed for their potential to repair and regenerate the injured myocardium (Bolli & Chaudhry, 2010). Nevertheless, stem cell transplantation therapies present conflicting and inconclusive results (Orlic et al., Nature, 2001; Orlic et al., PNAS, 2001; Chien, 2004; Balsam et al., 2004; Murry et al., 2004). Determining the ideal cell type limits the progression of the field (Bolli & Chaudhry, 2010).

Alternative investigations demonstrated the importance of defining different cardiac adaptive responses to environmental stimuli. For instance, during the onset of pathological hypertrophy or dilated cardiomyopathies, fetal heart genes and microRNAs are partially reactivated (Taegtmeyer et al., 2010; Thum et al., 2007). Concurrently, a murine study on the survival rates 8 weeks following a myocardial infarction illustrated that younger hearts recover better and have less scaring than older hearts (Gould et al., 2001). A recent study by Porrello et al. revealed that a 1 day mouse retains the capacity to regenerate after partial surgical resection of the myocardium; however the regenerative potential is lost at 7 days post-birth (Porrello et al., 2011) at which point rat cardiomyocytes exit cell cycle and become increasingly binucleated (Li et al., 1996). Interestingly, lower vertebrates possess cardiomyocytes with retained ability to divide postnatally (Nag et al., 2005 and Oberpriller

et al., 1995). Identifying the differentiating factors between higher and lower vertebrates may be a promising lead in reverse engineering damaged myocardium.

Given the importance of cardiomyocyte developmental capacity, understanding the factors involved in remodeling events, in particular in the transition from a hyperplastic- to hypertrophic-based growth, may provide insight for potential therapies in myocardial repair and regeneration after injury.

Genetically Engineered to Grow

The initiation of cardiac growth *in utero* and the maintenance of adult cardiac function are mediated by cardiogenetic programs (Fuster & King, 2008). Cardiac development research has mainly been regarded in the literature as two separate entities, that of prenatal and adult heart growth, with little known about the transition between the two types of growth patterns.

Key players controlling both prenatal development and adult homeostasis include Wnt (Grigoryan et al., 2008) and Notch signaling (Nemir & Pedrazzini, 2008). Loss- and gain-of-function mutations of the Wnt pathway (through mutations of β-catenin) were shown to cause defects in heart formation and ventricular outflow tract (Ai et al., 2007; Baurand et al., 2007; Chen et al., 2006; Cohen et al., 2007; Kioussi et al., 2002; Klaus et al., 2007; Kwon et al., 2007; Lickert et al., 2002; Liebner et al., 2004; Lin et al., 2007; Qu et al., 2007; Qyang et al., 2007; Zamora et al., 2007; Zhou et al., 2007). Moreover, loss- and gain-of-function mutations in the Notch pathway (notably Notch1, Notch2, RBP-J, Jagged1, Dll4, Hey1, Hey2, and HeyL) resulted in impaired cardiac development, hypoplasia, pericardial edema, enlarged hearts, ventricular defects, and malfunctioning hypertrophy (Swiatek et al.,

1994; McCright et al., 2001; Xue et al., 1999; Timmerman et al., 2004; Grego-Bessa et al., 2007; Duarte et al., 2004; Watanabe et al., 2006; Xin et al., 2007; Donovan et al., 2002; Gessler et al., 2002; Kokubo et al., 2005; Kokubo et al., 2004; Fischer et al., 2004; Xiang et al., 2006; Conlon et al., 1995; Krebs et al., 2003; Oka et al., 1995; McCright et al., 2002; Fischer et al., 2007).

The Prenatal Heart

The prenatal heart is exposed to a hypoxic environment and mainly depends on carbohydrates (lactate and glucose) as a source of adenosine triphosphate (ATP) (Bartelds et al., 2000). Interestingly, the heart expresses different genetic isoforms of a particular protein dependent upon the developmental stage. In accordance, the fetal heart expresses α-skeletal actin and compliant titin isoforms (i.e. N2BA1/N2BA2) (Lahmers et al., 2004; Schwartz et al., 1992) as well as other factors associated with tolerance of low levels of oxygen (Bishop, 1990).

Transcription factors (TF) have been extensively studied and identified as regulators of differentiation and growth of the developing heart. In particular, β-MHC is regulated by Nkx2.5, MEF2C, and GATA4/5/6, and then inhibited by thyroid hormone to give rise to α-MHC at maturity (Morkin, 2000). Other TFs encompass different stages of heart development, as studied in the mouse (**Table 1**; Nemer, 2008).

Table 1: Transcription Factors Mediating Prenatal Cardiac Development.

Cardiac Development Stage	Age	Transcription Factors
Cardiac Crescent	E7.5	GATA4, Mesp1/2, Nkx2.5
Linear Heart	E8	GATA4
Chamber Formation	E8.5 to E12	GATA4, Nkx2.5, Tbx5, dHand, eHand, Pitx2, MEF2C
Maturation and Septation	E12 to birth	GATA4, Nkx2.5, Tbx5, Rxrα, FOG-2, TEF-1, Sox4, NF-Atc, Pitx2, CITED, ZIC3, Hey2, Tbx1

Olson et al. focus on a "core cardiac network" involving NK2, MEF2, GATA, Tbx and Hand as essential genes in cardiomyocyte differentiation and cardiac morphogenesis, claiming that this "heart kernel" is evolutionary inflexible (Olson, 2006). Other factors associated with prenatal heart development include positive cell cycle regulators (ie. cyclins, Cdks…) which coincides with a known increase in cardiomyocyte cell cycle activity (Pasumarthi & Field, 2002).

The Perinatal Heart

The perinatal heart undergoes anatomical, physiological and biochemical changes to promote the conversion from a hyperplastic to hypertrophic heart. Knowledge concerning the transitional cardiac period is slowly developing, albeit with several gaps. The transitional cardiac period in mice is believed to span embryonic day 19 until 10 days post-birth (Soonpaa et al., 1996).

Thyroid hormone (TH) is known to be a major regulator of normal heart function (Brent, 2000). Coined as the "Master Maturator", thyroid hormone acts to promote (i.e. α-MHC and sarcoplasmic reticulum calcium ATPase) and prevent (β-MHC and phospholamban) expression of cardiac genes (Danzi & Klein, 2004; Ojamaa et al., 1992;

Kahaly & Dillmann, 2005). Mice have rapidly beating hearts which invokes a pressure overload and consequently a transcriptional switch from β- to α-MHC (Fuster & King, 2008). Both isoforms are present in the heart, however the beta isoform predominates during embryogenesis and fetal development followed by a shift to the alpha isoform soon after birth. Transcript expression levels of both isoforms drastically plunges until one day after birth whereby α-MHC is established and remains elevated throughout adulthood (Ng et al., 1991).

Additionally, HDAC1 and HDAC2 were found to be associated with perinatal development through deletion experiments. Cardiac-specific deletion of either HDAC1 or HDAC2 in mice did not demonstrate cardiac defects, whereas mice lacking both HDAC1 and HDAC2 illustrated dilated cardiomyopathy, arrhythmia, and neonatal lethality. Furthermore, global deletion of HDAC2 in mice did not cause any discernable effects until the perinatal period where mice presented cardiac defects (elimination of the right ventricle lumen, pathological hyperplasia, apoptosis of cardiomyocytes, and bradycardia) (Montgomery et al., 2007). Lastly, cell cycle regulators are dysregulated during the transition from a developing to a senescent heart (Brooks et al., 1997; Poolman & Brooks, 1998).

The Adult Heart

Genetic programs in the adult heart involve many homeostatic and adaptive mechanisms including maintenance of calcium influx, calcium handling, contraction, and myocardium survival (Cartwright et al., 2005).

Myocardin appears to be a leading factor in heart function and cardiomyocyte survival as the deletion of Myocardin in the adult heart caused rapid-onset heart failure, dilated cardiomyopathy and death within a week (Huang et al., 2009). The adult heart endures a more stringent hemodynamic load when compared to a fetal heart which causes the switch in metabolic pathways from glucose oxidation to fatty acid oxidation (Taegtmeyer et al., 2010). Similar to the perinatal heart, the adult heart takes part in isoform switching, in particular with the abundance of α-cardiac actin and adult titin isoforms (Lahmers et al., 2004; Schwartz et al., 1992). Transcription factors regulating cardiac hypertrophy include GATA4, NFAT, Csx/Nkx2.5, SRF, MEF2, Hand1/2, and Smad (Akazawa & Komuro, 2003).

Hormones play a vital role in normal physiological development, barring no exception to the heart. Hypertrophic growth of the heart is suggested to be regulated by multiple factors including hormones such as fibroblast growth factor (FGF) (Topper, 2000) and adrenergic receptors for norepinephrine (Barki-Harrington et al., 2004). Other common hormones include Insulin-like Growth Factor-1 (IGF-1) (McMullen et al., 2004) and thyroid hormone (TH) (Brent, 2000). Studies have shown the importance of IGF-1 in physiological cardiac hypertrophy. Essentially, IGF-1 receptors are tyrosine kinases present on the sarcolemmal membrane of cardiomyocytes involved in inducing growth signals to the nucleus and protein synthesis machinery by activating the PI3-K/PDK1/Akt-dependent signal transduction pathway (McMullen et al., 2004).

Conversely certain negative cell cycle regulatory genes (i.e. Cdk inhibitors) are increased in the adult heart which coincides with decreased cardiomyocyte cell cycle activity (Pasumarthi & Field, 2002).

Cardiomyocyte Cellular Regulation

The interplay between hyperplastic and hypertrophic cardiac growth entails a heterogeneous population of mono- and binucleated cardiomyocytes as a result of cardiomyocytes undergoing a final round of karyokinesis (nuclear division) in the absence of cytokinesis (cell division) (Li et al., 1997; Li et al., 1997). Karyokinesis and cytokinesis are generally tightly coupled processes but are inexplicably dissociated in cardiomyocytes. The majority of late neonatal (after day 4 in the rat) and adult cardiomyocytes withdraw from cell cycle and are blocked in G_0/G_1 or G_2/M (Brooks et al., 1997; Poolman & Brooks, 1998). Specifically, 85% of adult cardiomyocytes arrest in G_0/G_1 and the remaining 15% in G_2/M (Li et al., 1998). It is believed that adult cardiomyocytes lose the capacity to divide due to negative regulators of cell cycle (Capasso et al., 1992).

Furthermore cardiogenetic programs are differentially expressed between a prenatal and an adult heart. Late neonatal and adult hearts have depleted expression of factors involved in cell cycle progression and growth whereas structural proteins and stress response factors are upregulated, as determined by microarray gene expression profiles (Chen et al., 2004).

Generally, cell cycle includes positive (cyclin and cyclin-dependent kinases) and negative (cyclin-dependent kinase inhibitors) cell cycle regulators (McGill & Brooks, 1995). Cell cycle progression is regulated by the interplay between cyclins and cyclin-dependent kinases (CDKs). Moreover cyclins are classified by cell cycle phase (**Table 2**).

Table 2: Cyclins Modulating Cell Cycle Stages.

Cell Cycle	Associated Cyclin	Reference
G_1	Cyclin D1, D2, D3, and E	Hunter & Pines, 1991 and 1994; Murray & Hunt, 1993
S	Cyclin E and A	
G_2	Cyclin A and B	
M	Cyclin B	

D-type cyclins bind to CDK4 and CDK6 whereas cyclin E associates with CDK2, in order to control progression through G_1/S (Kang et al., 1997). Cyclin A interacts with CDK2 or cdc2 to allow S/G_2 phase transition (Kang & Koh, 1997). Lastly, cyclin B associates with cdc2 and regulates entry into mitosis (Lees, 1995; Morgan, 1995).

Cyclin/CDK function is controlled by cyclin availability and the phosphorylated state of CDK residues (Morgan, 1995). In mammals, the cyclin B1/cdc2 complex is inactivated by the Wee1 kinase which phosphorylates cdc2 on tyrosine 15 and threonine 14; conversely, the complex is activated by the phosphatase Cdc25A, B or C (Morgan, 2007). Wee1 and Cdc25 mediate cell cycle by preventing premature mitosis when DNA is unreplicated or damaged (Morgan, 2007). Therefore cyclins involved in G_1 and S are expressed in parallel with DNA synthesis (embryonic and early neonatal cardiac development); however G_2 and M phase cyclins decline with an arrest in DNA synthesis (late neonatal heart development).

Previous reports have stressed the importance of studying genetic expression patterns in the developing heart, with a focus on positive and negative cell cycle factors (Chen et al., 2004; Sehl et al., 2000). During early neonatal development (at 2, 3, 4 and 5 days of age in Wistar rats), cardiomyocytes are increasingly in G_0 or G_1 and decreasingly in S and G_2/M

phases of cell cycle (Poolman & Brooks, 1998). Particularly, cyclins and CDKs have been reported to be highly expressed during embryonic development but decrease with age; G_2/M phase cyclins are depleted more rapidly than G_1/S cyclins and CDKs (Kang et al., 1997).

In the rat, cyclin D1 expression decreases when comparing hearts aged 0, 7, and 14 days post-birth as well as adult hearts (Chen et al., 2004). G_1 cyclins (D2 and D3) slightly increase between 2 and 5 days post-birth while S phase cyclins (cyclin A and E) decrease with development (Yoshizumi et al., 1995; Brooks et al., 1997). M phase cyclin B transcript expression oscillates whereby the abundance of B1 is highest at day 0, decreases at 7 days, slightly increases at 14 days, then redescends at adulthood (Chen et al., 2004).

Cdc2 and CDK2 proteins have been shown to decrease while CDK4 and CDK6 are slightly enhanced during the transitional period (Poolman & Brooks, 1998). In fact, cell cycle activators, cdc2, cdc25, cdc42 are downregulated from day 0 to 7 and 14 days post-birth as well as adulthood (Chen et al., 2004). In contrast, CDK inhibitors (p18, p57, p21, p27) are upregulated in cardiomyocytes through the late gestational and neonatal period (Poolman & Brooks, 1996 and 1998; Chen et al., 2004).

It is believed that cyclin B1 and cdc2 complex formation and activation influences entry into mitosis (Bicknell et al., 2004; Kang et al., 1997). Hypertrophic growth entails G_2/M arrest which is suggested to be mediated by the absence of the cyclin B1/cdc2 complex (Bicknell et al., 2004). Interestingly, Carmena et al. illustrated that downregulation of cyclin B1 and cells exiting the M phase correlate with multinucleation of *Drosophila* spermatids (Carmena & Riparbelli, 1998).

G_1 phase CDKs mainly target the retinoblastoma protein (Rb). Cyclin D/CDK4 complex phosphorylates members of the Rb family in late G_1 preventing Rb's inhibitory role

on growth which promotes the transition to the S phase (Kang & Koh, 1997). The synthesis and abundance of D-type cyclins is highly dependent upon the stimulation of growth factors (Sherr, 1993 and 1994). Rb, p107 and p130 make up the mammalian "pocket protein" family responsible for governing biological processes through interactions with cellular proteins (Poznic, 2009). Rb associates with members of the E2F family, which are responsible for activating transcription of genes involved in DNA synthesis and cell cycle progression (Field, 2004). The unphosphorylated state of Rb promotes binding with E2F, while phosphorylation of Rb disrupts Rb/E2F binding. E2F may initiate transcription when unbound to Rb. Hence, phosphorylated Rb accumulates in S phase while the unphosphorylated form is predominantly in G_1 (Poznic, 2009). There appears to be conflicting and inconclusive results for Rb expression during perinatal heart development (Kim et al., 1994; Jiang et al., 1997; MacLellan et al., 2005).

microRNA IN HEART DEVELOPMENT AND DISEASE

Recent findings dispute the unidirectional central dogma whereby the genetic flow of DNA to RNA to protein is transformed into a complex system of intertwined networks. Therefore genetic regulation should be viewed keeping in mind that the supposed 'junk' DNA in fact includes RNA-based regulatory factors (non-coding RNAs such as microRNA, piRNA, rasiRNA etc.) (Condorelli and Dimmeler, 2008). Emerging studies highlight the importance of a new class of small non-coding RNAs, microRNAs, in the regulation of post-transcriptional gene expression. A single microRNA (miRNA) is estimated to target and modulate more than 200 coding genes (Krek et al., 2005). miRNAs are abundant in most tissues (1,000-30,000 copies per cell (Allawi et al., 2004)) and are believed to mediate a

wide variety of normal and pathological cellular processes. In particular, these small RNAs are expressed in the heart and have been shown to modulate myogenesis, cardiac development, cardiac performance, cardiomyocyte hypertrophy, cardiac ion channels, myocardial growth, electrical balance, and angiogenesis (Zorio et al., 2009). Although miRNA knowledge has seen a great growth spurt, its involvement in cardiac development remains largely unknown.

microRNA Discovery

First described in 1993 by Victor Ambros and colleagues during an investigation of *C. elegans*, lin-4, a small RNA pair that did not code for a protein, was suggested to regulate gene expression. At the same time, Gary Ruvkun and colleagues demonstrated lin-14 as the first miRNA target gene, describing a novel post-transcriptional gene regulation method. It was not until seven years later that Ruvkun identified the second miRNA named let-7, another *C. elegans* gene encoding the RNA that promotes the transition from late-larval to adult cell fates. Strong conservation of the latter miRNA caused a widespread interest into the miRNA world. miRNAs may be found in various organisms ranging from protozoans to humans (Appasani et al., 2007).

Despite the strong conservation of miRNAs between kingdoms, there are important differences in terms of the specialized miRNA activity. The majority of plant miRNAs have perfect homology to their target messenger RNA (mRNA), and they act through the RNAi pathway to cause mRNA degradation (Rhoades et al., 2002). Similar to animal miRNAs, some plant miRNAs base-pair imperfectly with their target sites. In plants and yeast there is also evidence that miRNAs are involved in repression of transcription by guiding chromatin methylation (Gonzalez et al., 2008).

microRNA Biogenesis and Silencing Activity

Encoded in introns of non-coding or coding genes and in exons of non-coding genes (Chu & Rana, 2007), miRNAs are estimated to be 22 nucleotide(nt)-long single-stranded regulatory elements (Ambros, 2004). miRNAs originate from the transcription of precursor molecules, known as pri-miRNA, by RNA polymerase II in the nucleus. The primary transcripts are then cleaved by Drosha-DGCR8, an RNase III family endonuclease, to generate stem-loop structured precursors (pre-miRNA) of 70-100nt long (Srivastava & Cordes, 2009). This short hairpin-structured RNA is recognized by the nuclear export factor, Exportin-5 which partners with Ran-GTP-binding protein to form a nuclear transport complex that translocates pre-miRNAs into the cytoplasm (Thum et al., 2008). Once in the cytoplasm, premature miRNAs are processed by Dicer, the second RNase III endonuclease, into 22nt duplexes of mature miRNAs. One strand of the mature miRNA duplex is then loaded onto the RISC (RNA-Induced Silencing Complex) and the other is degraded. A miRNA combined with the RISC, entitled miRISC, may exert gene silencing on its target via a perfect or imperfect base pairing interaction (Chu & Rana, 2007). It is believed that the miRISC mainly targets the 3'UTR of transcripts but it has been recently shown that the coding sequence and the 5'UTR may be alternative miRNA target sites (Tay Y, 2008; Lee et al., 2009). Gene silencing is performed by: 1) repressing protein translation; 2) accelerating mRNA degradation; or 3) sending mRNA to P-bodies for storage. These procedures depend on the level of complementarity between the miRNA and the transcript (Song, 2006). Messenger RNAs sequestered to storage compartments may be released and translated as a result of an environment change or stimuli induction (Chu & Rana, 2007).

Mice Versus Humans

Mice and humans have extensively been shown to have high genetic conservation through linkage groups (DeBry and Seldin, 1996; Eppig and Nadeau, 1995), with no exceptions to miRNA expression. There are presently 851 cloned or computer-predicted human miRNAs in the NIH miRNA database, miRBase (Wellcome Trust Genome, 2007); however, it is thought that there are more likely 1000 human miRNAs (Griffiths-Jones et al., 2008). Mice have approximately 793 predicted miRNAs, 70 are suggested to be primarily acting in the heart (Shahi et al., 2006).

microRNA and Heart Disease

Many studies have demonstrated the great involvement of miRNA in disease. In particular, a cardiac-specific deletion of Dicer, the miRNA processing enzyme, led to rapid progression of dilated cardiomyopathy, heart failure, and postnatal lethality (Chen et al., 2008) which highlights the vital role of miRNAs in normal development and survival. In addition, a microarray study showed that 87% of the miRNAs that were downregulated in the failing human hearts were also found to be downregulated in fetal heart tissue, a signature of hypertrophied and failing myocardium (Divakaran & Mann, 2008). Further analysis of miRNAs revealed miRNA-specific involvement in cardiac disease including miR-195, whose expression is known to be upregulated during cardiac hypertrophy and can induce hypertrophic growth in cultured cardiomyocytes and transgenic mice (van Rooij et al., 2006). Other miRNAs have also been identified in mice and human to have concurrent roles in cardiac hypertrophy (Shahi et al., 2006). van Rooij et al. demonstrated that the miR-29 family plays a role in cardiac fibrosis after myocardial infarction (van Rooij et al., 2008). **Figure 2** classifies miRNAs into various cardiac defects.

Figure 2: microRNA Involvement in Cardiac Disease. Summary of microRNAs and their processing enzyme Dicer shown to be implicated in cardiac disease progression (ventricular septation defect, arrhythmia, apoptosis, contractility, fibrosis, myocyte hypertrophy, dilated cardiomyopathy) and recovery (angiogenesis post-myocardial infarction (MI) and hyperplasia). [Adapted with permission by The Journal of Cell Science, "microRNAs and Muscle Disorders", Chen, J., Callis, T., Wang, D., (2009) Vol. 122 (Pt 1), 13-20; in combination with an adaption from van Rooij, E., Marshall, W., & Olson, E., "Toward microRNA-Based Therapeutics for Heart Disease: The Sense in Antisense", Circulation Research, Vol. 103, Issue 9, 919-928, 2008, with permission from Wolters Kluwer Health.]

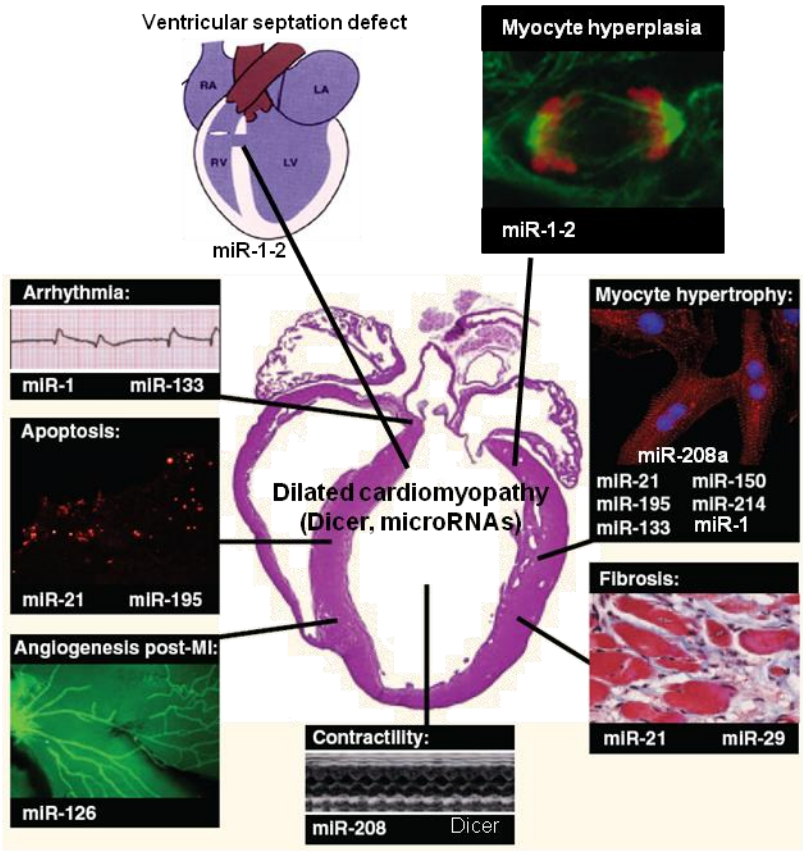
Ventricular septation defect
RA
LA
RV
LV
miR-1-2
Myocyte hyperplasia
miR-1-2
Arrhythmia:
miR-1
miR-133
Apoptosis:
miR-21
miR-195
Angiogenesis post-MI:
miR-126
Dilated cardiomyopathy
(Dicer, microRNAs)
Myocyte hypertrophy:
miR-208a
miR-21
miR-150
miR-195
miR-214
miR-133
miR-1
Fibrosis:
miR-21
miR-29
Contractility:
miR-208
Dicer

CARDIOMYOCYTE MULTINUCLEATION

Multinucleation is the product of cardiomyocytes proceeding through nuclear division with the absence of cytokinesis (Clubb and Bishop, 1984). Kang and Koh determined that binucleation of rat cardiomyocytes increases from 2.5% at day 2, 14% at day 4, 50% at day 8, and reaches a plateau of 80% at day 14. In general, 60 to 90% of mammalian cardiomyocytes become binucleated during hypertrophy (Jackson et al. 1998; Soonpaa et al., 1996).

Cardiomyocytes, like all cell types, progress through cell cycle during proliferation. Key cytoskeletal remodeling events promote cytokinesis to generate two daughter cells (**Figure 3**; Glotzer et al., 2005). Between metaphase and anaphase, a network of antiparallel nonkinetochore interdigitating microtubules are formed linking chromatid pairs, termed the spindle midzone. The assembly of the midzone is essential in spindle architecture and elongation as well as proper cleavage furrow alignment (D'Avino et al., 2005; McCollum, 2004). During late anaphase, each set of chromatid is bound to a dense network of overlapping antiparallel microtubules to form a central mitotic spindle (Mastronarde et al., 1993). Several proteins including INCENP, survivin, polo, aurora B, Rho and CENP-E gather at the midzone of mammalian mitotic spindles to regulate cellular cleavage during late mitosis (Drechsel et al., 1997; Lee et al., 1995; Mackay et al., 1998; Skoufias et al., 2000; Takada et al., 1996; Terada et al., 1998; Uren et al., 2000; Yen et al., 1992). In addition, a novel protein named protein regulator of cytokinesis 1 (PRC1) has been shown to be associated to the central mitotic spindle (Jiang et al., 1998).

Recent evidence has emerged highlighting the potential roles of cyclin D1, cyclin G1 and calcyclin binding protein (through CacyBP/SIP) in cardiomyocyte multinucleation (Au et al., 2006; Liu et al., 2010; Soonpaa et al., 1997).

Figure 3: Cytoskeletal Remodeling during Cytokinesis. Animal cells initiate cytokinesis by forming a contractile ring linked to the plasma membrane, termed the cleavage furrow. The contractile ring is composed of a complex network of actin and myosin filaments, whereby the myosin motor displaces actin and causes cellular constriction. The central spindle defines the region at the constriction site composed of antiparallel microtubules that are bundled between chromatid sisters during anaphase as well as key regulators of cytokinesis. The formation of the central spindle serves as a marker for the initiation of cytokinesis in anaphase [Adapted with permission from AAAS; Glotzer, M., *Science*, 2005, Vol. 307 (5716), 1735-1739.]

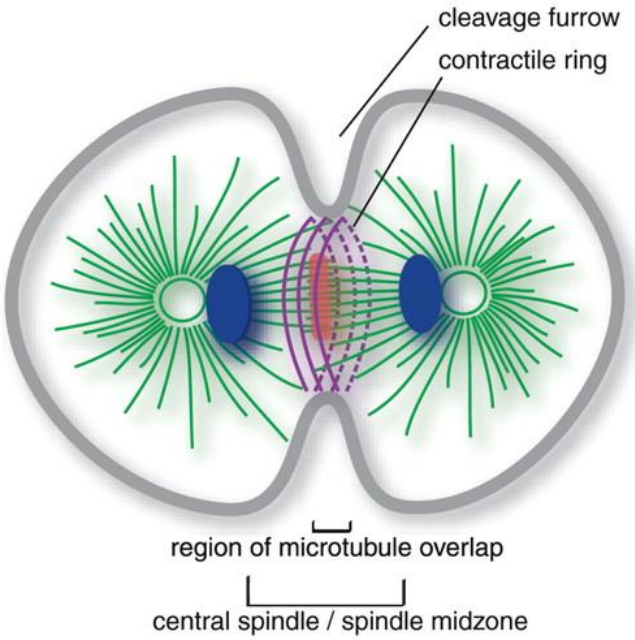
cleavage furrow
contractile ring
region of microtubule overlap
central spindle / spindle midzone

RATIONALE

The heart undergoes various age-dependent growth stages. In mammals, cardiomyocyte terminal differentiation occurs shortly after birth and is characterized by a transition from a hyperplastic to a hypertrophic growth. Hypertrophy entails binucleation of cardiomyocytes prior to marked cellular volume increase. Genetic networks modulating prenatal and adult heart development have been separately studied. Anatomical, physiological, and cellular observations have been revealed within the highly dynamic cardiac perinatal transition; however key molecular mechanisms and pathways regulating the cardiac perinatal transition have yet to be elucidated. Chen et al. first introduced global gene expression analysis of postnatal cardiac development in the mouse; however they focused on large intervals and disregarded the finer steps in perinatal development. Taking advantage of this knowledge, the goal of the proposed research is to provide additional depth into the cardiogenomic perinatal program in the mouse.

HYPOTHESIS

Genetic factors and processes in the cardiac perinatal transitional program can be identified by systematic analysis of different stages in murine heart development.

EXPERIMENTAL AIMS

1) Determine transcriptional patterns of mRNA and microRNA during the murine cardiac perinatal transitional program through microarray expression profiles and gene ontologies.
2) Elucidate key factors involved in cardiomyocyte maturation and binucleation.

MATERIALS AND METHODS

MOUSE MODEL

Wild-type 129/SV-E mice were utilized to study the molecular mechanisms and factors in perinatal cardiac development. Mice were maintained at the University of Ottawa Heart Institute animal facility. All experiments were conducted in conformity with the ethical standards set by the University of Ottawa Animal Care Committee and Animal Care and Veterinary Service (ACVS). Mice were inbred and studied at embryonic day 19, as well as 1, 3, 4, 5, 6, 7, 10 days and 6 to 8 weeks post-birth.

RNA ISOLATION, QUANTIFICATION AND QUALIFICATION

RNA Isolation

Hearts were excised from 129/SV-E mice at embryonic day 19 (E19), day 1, 3, 4, 5, 6, 7 and 10 as well as 6-7 weeks post-birth and washed with 1xPBS before being snap-frozen in liquid nitrogen and stored at -80°C. Total RNA was extracted using appropriate RNase-free laboratory equipment and environment. Isolation was carried out via Qiagen miRNEasy Mini Kit (Cat.# 217004) as per manufacturer's recommendation (using the bench-top Polytron Homogenizer with a 7mm generator). Volume of QIAzol is as follows: 700µL for E19, 1 day (1d), 3 day (3d), 4 day (4d), 5 day (5d), 6 day (6d), 7 day (7d), and 10 day (10d); and 2100µL for adult. RNA was eluted from the column with nuclease-free water then with the former eluant. E19 to 10d RNA was eluted with 50µL but adult RNA was eluted with 150µL spread over three columns.

RNA Quantity and Quality

After isolation, the RNA purity and yield was determined using the NanoDrop® ND-1000 spectrophotometer via the Nucleic Acid function (Agilent Technologies). The optical density (OD) measurements were analyzed at wavelengths of 230, 260 and 280. RNA was considered pure when the OD 260/280 ratio was approximately 2.0 and the 260/230 ratio between 2.0 and 2.2. Further evaluation of RNA quality was performed for microarray processing using the Agilent 2100 Bioanalyzer and RNA Nano Chips (Cat.# 5067-1511). Electropherograms and RNA Integrity Numbers (RIN) were generated from the Total Nano Eukaryote setting to detect RNA degradation. The RIN is calculated based on the ratio of 28S/18S bands and were between 8.0 and 10. Freeze-thaw cycles were limited as much as possible.

MICROARRAYS

Gene Expression Microarray

One microgram of total RNA was processed in-house through the Affymetrix GeneChip® Whole Transcript (WT) Sense Target Labeling Assay kit using Affymetrix GeneChip® Mouse Exon 1.0 ST Arrays (3/timepoint) which covers approximately 1 million exons. There are approximately four probes per exon and 40 probes per gene which allows to analyze expression at the gene and exon level.

For the exon microarrays, three hearts were pooled for each timepoint of interest (E19, 1d, 3d, 5d, 7d, 10d, adult), processed into experimental triplicates, for a total of 63 hearts analyzed over 21 chips.

microRNA Expression Microarray

Profiling was performed in duplicate per timepoint by the Genetic Analysis Facility – The Center for Applied Genomics (TCAG) at The Hospital for Sick Children. The Illumina microarray platform contains 656 miRNAs probe set (611 excluding Solexa microRNAs) based on the Sanger software, Version 12.0. These panels cover approximately 97% of the microRNAs described by the miRBase database.

For the microRNA microarrays, three hearts were pooled for each timepoint of interest (E19, 1d, 3d, 5d, 7d, 10d, adult), processed into experimental duplicates, for a total of 42 hearts analyzed over 14 chips.

Microarray Quality Control

Initially, a general visual inspection of each chip was performed after scanning. There were no white speckles, holes, smudges or areas of saturation. No outliers were found between replicates for both the exon and microRNA microarrays.

The microRNA microarray quality control was calculated by TCAG prior to receiving the Illumina data (.txt) (see **Appendix – Suppl. Figure 1**).

The exon microarray Quality Assurance/Quality Control (QA/QC) was fulfilled through the Affymetrix Expression Console™. Quality controls include the following tests: 1) Labeling controls whereby Lys<Phe<Thr<Dap; 2) Signal Histogram; 3) Pearson's Correlation for RMA Core, PLIER Core, Controls, and RMA Extended; 4) Log Expression Signal; 5) Relative Signal Box Plot; 6) Relative Log Expression Signal; 7) Box Plot of Probe Cell Intensity; 8) Relative Probe Cell Intensity; 9) External Spike Controls whereby

BioB<BioC<BioD<Cre; 10) Report Metrics (Core and Extended): All_mean, PM_mean, All_rle_mean, Pos_vs_neg_auc, Bgrd_mean whereby RMA, PLIER, Extended, Core, Controls, and Samples are within bounds.

Quality of microRNA and exon intensity files were further assessed through Partek® Principal Component Analysis (PCA) transformation.

Microarray Analysis

Data was analyzed using Partek® Genomics Suite. cDNA was normalized through Robust Multi-Array Average (RMA) and gene level analysis was run through a 1-way Analysis Of Variance (ANOVA). microRNA data was processed through a Log2 transformation and a 1-way ANOVA. Exon and microRNA expression arrays were normalized differently because of the dissimilar microarray platforms. Data was examined by contrasting one timepoint to the following (i.e. E19 versus 1 day). All statistical results were run through the False Discovery Rate (FDR) algorithm to correct for effects introduced by multiple testing (FDR≤0.05). Post-hoc analysis was performed using the Tukey's biweight function.

The 1-way ANOVA provides analytical information including p-values and fold-changes. Volcano plots were generated with total genes or microRNAs found on the microarrays, using the Partek® software. To determine the number of significantly differentially expressed genes and microRNAs, lists were filtered at a p-value≤0.05 and ranked by fold-change. Gene lists were manually compared to known and predicted mouse transcription factors (TF) (Riken Transcription Factor Database (TFdb), 2004; Kanamori et al., 2004) to determine the TFs found on the chip and of those significantly changing (p≤0.05). Filtered gene lists (p≤0.05) with a FDR≤0.05 were input into the Partek® Gene

Ontology (GO) algorithms (Chi-square test and restricted analysis to functional groups with more than 2 genes and using a default mapping file) to generate GO profiles limited to Biological Processes and thresholds at an Enrichment Score≥3 and an Age Score≥3. GO profiles were visualized as Pie Charts (total significantly changing genes) and Forest Plots (significantly downregulated and upregulated genes). All processes that were not found to be significant, according to the criteria above, were manually removed.

microRNA and genetic lists were combined to assess *in silico* microRNA target predictions, utilizing TargetScan (TargetScanMouse, 2006-2009). GeneMANIA allowed to localize Prc1 within an *in silico* association network (Warde-Farley et al., 2010).

After analyzing the microarray data, days 4 and 6 post-birth were included in the study for the following experiments in order to see if they possess a role in the transitional program.

Microarray Validation

Reverse Transcriptase Polymerase Chain Reaction (RT-PCR)

Transcripts were semi-quantified from wild-type 129/SV-E mice hearts at embryonic day 19 and 1, 3, 4, 5, 6, 7, 10 days post-birth as well as from adult mice (6-7 weeks). RNA was isolated then DNase-treated using the Promega RQ1 RNase-Free DNase kit (Cat.# M6101) according to manufacturer's recommendation. One microgram of RNA was reverse transcribed via the New England BioLabs (NEB) M-MuLV Reverse Transcriptase System (Cat.# M0253L). cDNA was amplified using the NEB Taq DNA polymerase (Cat.# M0267L) protocol and primers designed through UCSC Blat and IDT (**Table 3**). All primers were designed to span two separate exons with the exception of Pln, to prevent amplifying

residual genomic DNA. Thermocycler conditions were set as follows: 1 cycle at 95°C for 1min; 35 cycles at 95°C, annealing temperature (T_M), and 72°C, for 30sec each; then, 72°C for 5mins. Annealing temperature for each primer set was optimized through melting curve experiments. Ten microliters of PCR products were confirmed by size and charge electrophoresis using a 3% agarose gel in 1X Tris/Borate/EDTA buffer stained with 0.005% ethidium bromide. Amplification products were approximately 200 base pairs (bp). Gene products were analyzed and visualized throughout three independent experiments.

Quantitative Real-Time PCR

Transcripts were quantified by relative Real-Time PCR using the Roche LightCycler® 480 Multiwell PCR System, the LC480 machine and the LightCycler® 480 SYBR Green I Master kit (Cat.# 0470751600), as per manufacturer's indication. Real-Time PCR experiments were realized using 96-well PCR plates (Cat.# 04729692001). RNA was isolated then DNase-treated using the Promega RQ1 RNase-Free DNase kit (Cat.# M6101) according to manufacturer's recommendation. One microgram of RNA was reverse-transcribed via the New England BioLabs (NEB) M-MuLV Reverse Transcriptase System (Cat.# M0253L). Reaction mix was halved to 10µL with: 1.5µL PCR-grade water, 0.5µL Forward and Reverse PCR primer (5µM), 5µL 2X conc. Master Mix, and, 2.5µL cDNA (diluted 1:5). Annealing temperature and primer sequences may be found within **Table 3**. PCR primer efficiency was calculated with the slope of a standard curve of known cDNA concentrations at a standard deviation of 0.04 over 4 log quantity differences, run in technical triplicates. CT values from experimental triplicates were normalized to a calibrator (adult heart cDNA), reference gene (Ppia), and no-template control (NTC), diluted at 1:5.

Table 3: List of Primer Sequences with their Corresponding Optimized Melting Temperature (T_M). Each gene was amplified with their respective forward (F) and reverse (R) primer.

Gene Name	Sequence	Melting Temperature (T_M)
Asb15	F: 5'- TGGATTACGTCCCTCTGTGTGCAA-3' R: 5'- AATAAGTATCTTCGCATCG-3'	60°C
Cdk4	F: 5'- ATTGGATTGCCTCCAGAAGACGAC -3' R: 5'- AGGCAGAGATTCGCTTATGTGGGT -3'	60°C
Epas1 (Hif2α)	F: 5'- CTATGCCTCCCAGTTCCAGGACTA-3' R: 5'- GGCACGTTCACCTCACAGTCATATCT-3'	60°C
Fbxw7	F: 5'- ACACGCTAACAGGACACCAGTCAT-3' R: 5'- TCTCCAATGTGACGAGGTTTCGGA-3'	60°C
Gapdh	F: 5'- GTGAAGGTCGGTGTGAACG -3' R: 5'- ATTTGATGTTAGTGGGGTCTCG-3'	60°C
Hif3α	F: 5'- AAGTTCACATACTGCGACGAGA -3' R: 5'- CGAGTATGTTGCTCCGTTTG -3'	55°C
Mad2l1	F: 5'- GTCCCAGAAAGCCATACAGGATGA -3' R: 5'- TGAGCGTAGACGGACTTCTTCACA -3'	60°C
Pfkm	F: 5'- AAAGAACAGTGGTGGCTGAAGCTG-3' R: 5'- GCTTCCCAGACCGTTTCCTTGAA -3'	60°C
Pgk2	F: 5'- CATTTGGCGCAGCAAGTAGCAGTA -3' R: 5'- GTGGCCCAAGCAAAGCTGATAGTT -3'	60°C
Pln	F: 5'- AAAGTGCAATACCTCACTCGCTCG -3' R: 5'- CAGCAGCAGACATATCAAGATGAGGC -3'	60°C
Ppia	F: 5'- AGCATACAGGTCCTGGCATCTTGT -3' R: 5'- AAACGCTCCATGGCTTCCACAATG -3'	60°C
Prc1	F: 5'- CCTGTGGAGGCAATTATGACTGGA -3' R: 5'- TCTCGGCATCATGAAGATGGAGCA -3'	60°C
Rxrγ	F: 5'- AGAGAAGGTTTATGCCACCCTGGA-3' R: 5'- TGGGAGTGTCTCCAATGAGCTTGA -3'	60°C

CELL CYCLE AND PRC1 IMMUNOBLOTTING

Protein expression was assessed through immunoblotting. Wild-type mouse heart, brain and skeletal muscle were lysed with lysis buffer and a handheld glass dounce homogenizer. Complete lysis buffer was prepared with: 10mL stock lysis buffer (50mM Tris HCl (pH 8),

200mM NaCl, 20mM NaF, 20mM β-glycerophosphate, 0.5% NP-40), 5µL sodium vanadate, 1 tablet phosphoStop (Roche, Cat.# 04906837001), 1 tablet complete Mini (Roche, Cat.# 11836153001), 10µL 1M dithiothreitol (DTT). Volume of lysis buffer is as follows: 100µL for E19 and 1d; 300µL for 3d; 400µL for 4d; 500µL for 5d; 600µL for 6d; 700µL for 7d; 1000µL for 10d; and 3000µL for adult. After thorough homogenization, lysate was transferred into a 1.5mL centrifuge tube and placed on ice for 15mins, with 5min vortexing intervals. Lysates were centrifuged at 10,000xg for 10mins at 4°C. Protein samples were preserved from the supernatant and the precipitate was discarded. Protein concentrations were calculated using the Bio-Rad Protein Assay system (Cat.# 500-0006) in 96-well flat-bottom plates. Concentrations were read with a spectrophotometer at 595nm and calculated through a standard curve with known concentrations of bovine serum albumin (NEB, Cat.# B9001S). Samples were diluted to 5 or 10µg with sample buffer and 1M DTT (5:1 ratio), as well as complete lysis buffer, prior to denaturing at 95°C for 5mins.

Protein samples were resolved on 4-15% Biorad Miniprotean TGX precast polyacrylamide gels (Cat.# 456-1096) in 1X SDS/Tris/Glycine buffer along with GeneDireX® BLUeye prestained protein ladder (Cat.# PM007-0500). Gels were run for 30mins at 200V prior to transferring to an activated PVDF membrane (Immobilon-P Transfer Membrane, Millipore) for an hour at 100V (Bio-Rad Criterion Gel Apparatus) in transfer buffer (190mM glycine, 25mM Tris base, 20% chilled methanol). The gels were subjected to Coomassie staining (0.2% Coomassie Blue, 7.5% acetic acid, 50% ethanol) for 1 hour at room temperature (RT) followed by overnight (O/N) destaining (50% methanol, 10% acetic acid) to visualize MHC. Blots were incubated with blocking buffer in 1XTBST (500mM Tris, 1.5M NaCl and 0.05% Tween-20) for one hour at RT on shaker. Blocking

buffer utilized was 5% fat-free milk (for Cdc2, Rb, Cyclin B1, and Prc1) or a mix of 1% milk and 1% BSA (for pCdc2(Tyr15) and pRb(S780)). Membranes were incubated with primary and secondary antibody with either 1% fat-free milk (Cdc2, Rb, Cyclin B1, and Prc1) or a mix of 1% milk and 1% BSA (pCdc2(Tyr15) and pRb(S780)) with gentle shaking. After washing 3 times with 1XTBST, membranes were incubated O/N with primary antibody at 4°C. The primary antibody dilutions were as follows: 1:500 for Cyclin B1 (Santa Cruz Biotechnology (SCB), sc-245) and pRb(S780) (SCB, sc-12901); 1:1000 for Rb (SCB, sc-50), Cdc2 (SCB, sc-747), pCdc2(Tyr15) (SCB, sc-7989); and 1:10 000 of Prc1 (Abcam, ab51248). Prior to incubating the blots with α-Prc1, the rabbit monoclonal antibody was incubated for 30mins with a blocking peptide at double the amount of Prc1 antibody, according to manufacturer's suggestions. After washing, membranes were incubated with secondary antibody for 45mins at RT: 1:3000 α-mouse IgG-HRP (Cell Signaling, #7076) for Cyclin B1; 1:2000 donkey α-goat IgG-HRP (SCB, sc-2020) for pCdc2(Tyr15); α-rabbit IgG-HRP (Cell Signaling, #7074) for Prc1, Cdc2, Rb, pRb(S780). Immunoblot signals were detected using a SuperSignal West Pico Chemiluminescent kit (Thermo Scientific, Cat.# 34080) and developed on X-Ray Film (Thermo Scientific Pierce* CL-XPosure, Cat.# 34093,) per manufacturer's protocol.

Protein from mouse HL-1 cells was isolated and quantified by Shelley Deeke. Briefly, the cells were cultured in Claycomb medium supplemented with 10% fetal bovine serum, 1% v/v penicillin-streptomycin, and 2mM L-glutamine at 37°C, in 5% CO_2. HL-1 cells were lysed in 10mM HEPES (pH 7.4), 50mM NaCl, 0.5mM EDTA, 2mM $MgCl_2$, protease inhibitor cocktail (Roche) and 20mM N-ethylmaleimide. Cell lysates were cleared and protein concentration was determined as described above.

EXPERIMENTAL RESULTS

Murine hearts were investigated at different ages within the perinatal cardiogenomic program utilizing microarray bioinformatic tools. As defined by Soonpaa et al., the transition from hyperplasia to hypertrophy spans late embryogenesis to 10 days post-birth, which we refer to as the **cardiac perinatal transitional program**. As a result, hearts were investigated prior and after birth, hence during cardiac remodeling and into early maturation. We chose to analyze hearts initially at embryonic day 19, knowing that mouse gestational period is between 19 and 21 days, and finally at 6-7 weeks post-birth, when mice have reached early adulthood. In particular, we sought to determine the changes within small intervals of the program, thus: E19 versus 1 day (d), 1d versus 3d, 3d versus 5d, 5d versus 7d, 7d versus 10d, and 10d versus adult. Narrowing the analysis permits us to identify factors and networks regulating each step of the cardiac perinatal transitional program.

AIM 1: DETERMINE TRANSCRIPTIONAL PATTERNS OF MRNA AND MICRORNA DURING THE MURINE CARDIAC PERINATAL TRANSITIONAL PROGRAM

Initially, transcripts were isolated from embryonic day 19 (E19) as well as 1, 3, 5, 7, 10, and 42-49 days (6-7 weeks) post-birth. Transcriptional expression levels were investigated with exon and microRNA microarrays. After normalizing the data signals, volcano plots were generated to illustrate the abundance of transcripts and microRNAs changing at different points in development (**Figure 4** and **5**). Volcano plots permit a clear visualization of the number of factors significantly ($p \leq 0.05$) upregulated (positive fold-change) and downregulated (negative fold-change) when comparing one age to another. Our focus is on small intervals within the transitional period therefore we chose the following intervals: E19 vs. 1d; 1d vs. 3d; 3d vs. 5d; 5d vs. 7d; 7d vs. 10d; and 10d vs. adult.

At the gene level, the volcano plots include the p-value and fold-change for all 16,655 genes found on the microarray (**Figure 4**). Contrasts between E19 and 10 day have the same X and Y axes in order to study each contrast in addition to gaining an overall perspective. It appears that a smaller number of genes are expressed when comparing 1d vs. 3d (**B**), 3d vs. 5d (**C**), and 5d vs.7d (**D**), also there is a similar number of genes significantly up- and downregulated. On the other hand, the largest cohort of genes significantly changing is found at E19 vs. 1d (**A**) and 7d vs. 10d (**F**). Since an adult heart is markedly different from a developing heart, the volcano plot for 10d vs. adult had an independent X and Y axis to avoid misinterpretation of the other plots. As expected, genes were significantly changing when comparing 10d to adult, with comparable amounts of genes up- and downregulated.

At the microRNA level (**Figure 5**), volcano plots summarize microRNA expression patterns for the 655 microRNAs found on the Illumina microarray. All the panels [**A** (E19 vs. 1d), **B** (1d vs. 3d), **C** (3d vs. 5d), **D** (5d vs. 7d), **E** (7d vs. 10d) and **F** (10d vs. adult)] appear to have more microRNAs significantly upregulated than downregulated ($p \leq 0.05$). When comparing 5d and 7d (**D**), there is a striking reduction in the number of microRNAs significantly changing ($p \leq 0.05$). Panel **F** further demonstrates the dramatic abundance of significantly upregulated microRNAs when analyzing a heart aged at 10d versus adulthood ($p \leq 0.05$).

Microarray profiling revealed numerous microRNAs changing during perinatal heart development including the microRNAs with proven roles in heart development and disease (**Table 4**). Lists of varying microRNAs during the transition were generated after filtering at a p-value≤ 0.05; results were reduced to the microRNAs with the largest and significant fold-changes as well as heart-related microRNAs. The largest fold-changes are observed for upregulated microRNAs at 3d vs. 5d, 5d vs. 7d, and 10d vs. adult.

Figure 4: Cardiogenetic Perinatal Expression is Highly Dynamic. Volcano plots of genes summarized from the Affymetrix GeneChip Mouse Exon 1.0 ST Array when contrasting a wild-type mouse heart of a certain age to the following age. The Y axis represents the p-value for each gene within the volcano plot. Each gene is colour-coded according to significance of differential expression whereby blue, grey, and red signify a p-value of 0, 0.5, and 1.0, respectively (see colour scale). The X axis represents the fold-change whereby the center line (N/C) signifies no contrast when comparing the two ages. All genes that fall on the right are upregulated while the ones on the left are downregulated when comparing an age to another. Panels **A** to **E** have the same X and Y axis boundaries while **F** differs. The contrasts analyzed are: **A)** E19 versus 1 day; **B)** 1 day versus 3 day; **C)** 3 day versus 5 day; **D)** 5 day versus 7 day; **E)** 7 day versus 10 day; **F)** 10 day versus Adult.

A.

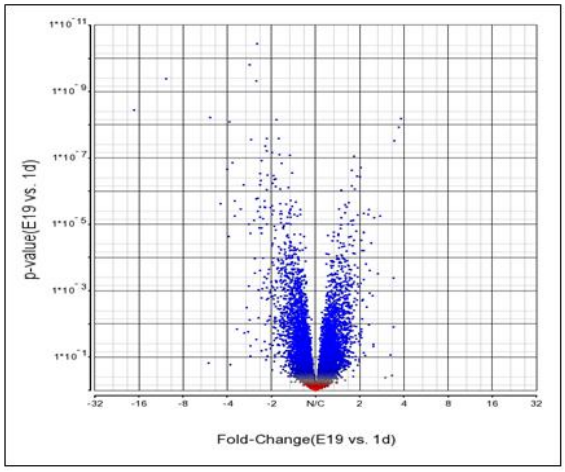
p-value(E19 vs. 1d)
Fold-Change(E19 vs. 1d)

B.

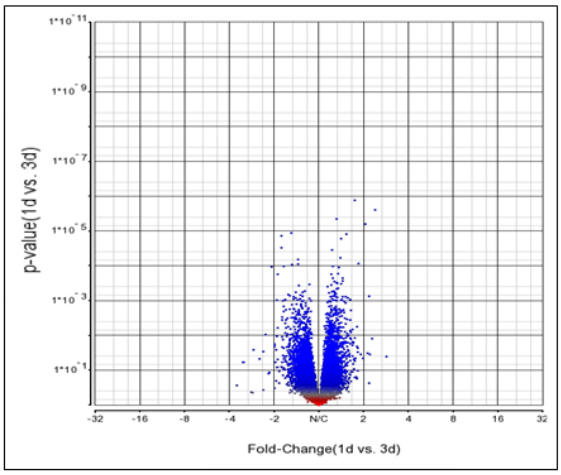
p-value(1d vs. 3d)
Fold-Change(1d vs. 3d)

C.

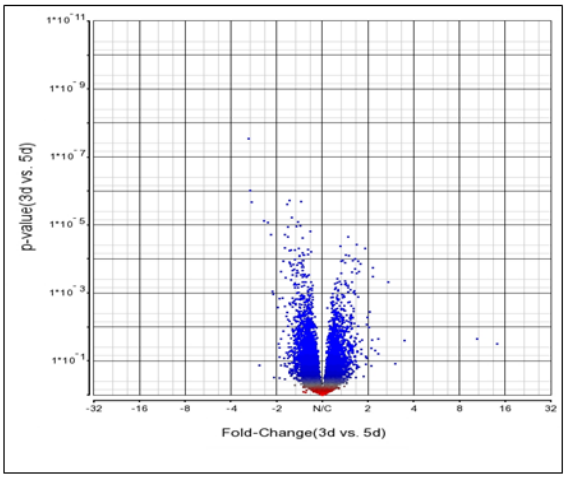
p-value(3d vs. 5d)
Fold-Change(3d vs. 5d)

D.

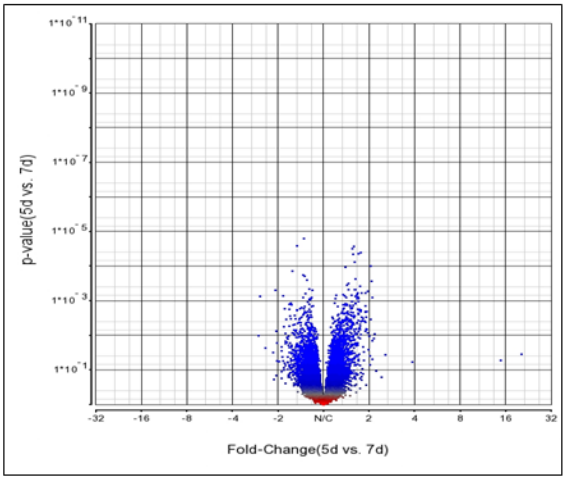
p-value(5d vs. 7d)
Fold-Change(5d vs. 7d)

E.

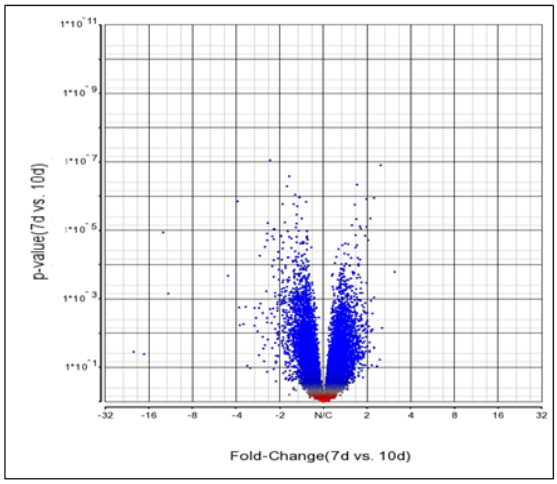
p-value(7d vs. 10d)
Fold-Change(7d vs. 10d)

F.

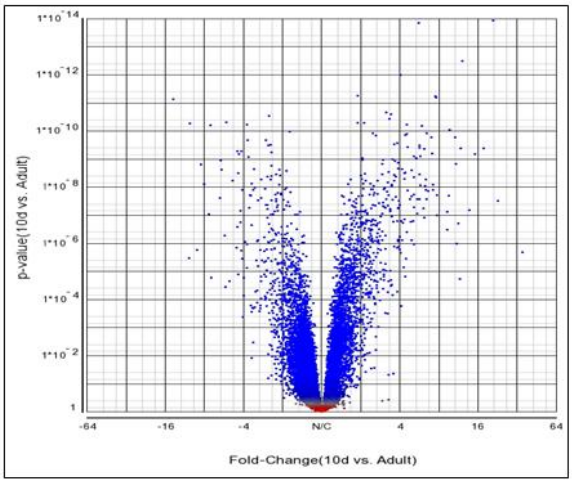
p-value(10d vs. Adult)
Fold-Change(10d vs. Adult)


0
0.5
1.0

Figure 5: Cardiac microRNA Perinatal Expression Patterns are Dispersed. Volcano plots of microRNAs from the Illumina microarray platform when contrasting a wild-type mouse heart of a certain age to the following age. The Y axis represents the p-value for each microRNA within the volcano plot. Each microRNA is colour-coded according to significance of differential expression whereby blue, grey, and red signify a p-value of 0, 0.5, and 1.0, respectively (see colour scale). The X axis represents the fold-change whereby the center line (N/C) signifies no contrast when comparing the two ages. All microRNAs that fall on the right of N/C are upregulated while the ones on the left are downregulated when comparing an age to another. Panels **A** to **E** have the same X axis while **F** differs. The contrasts analyzed are: **A)** E19 versus 1 day; **B)** 1 day versus 3 day; **C)** 3 day versus 5 day; **D)** 5 day versus 7 day; **E)** 7 day versus 10 day; **F)** 10 day versus Adult.

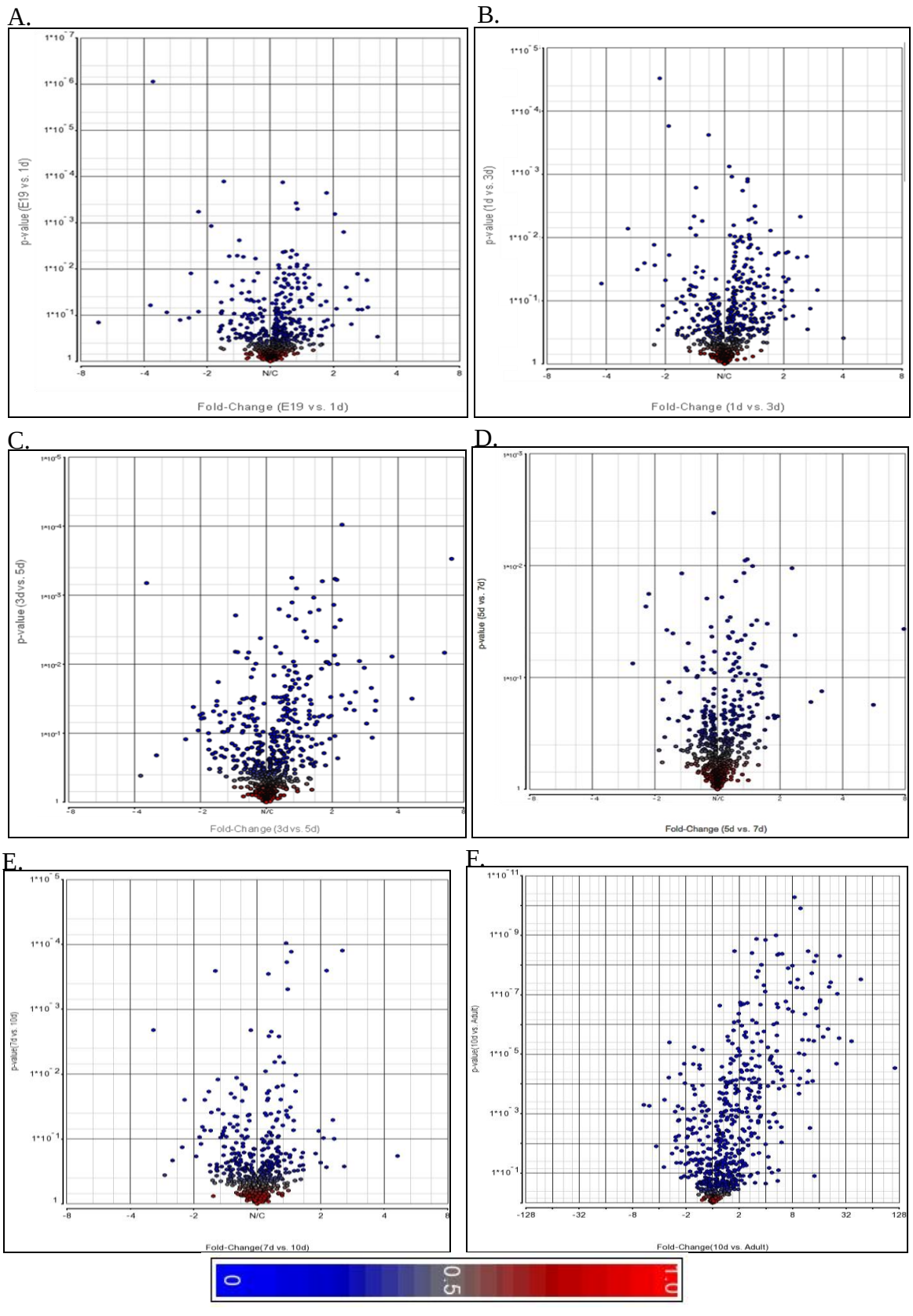
A.
B.
C.
D.
E.
F.
p-value (E19 vs. 1d)
Fold-Change (E19 vs. 1d)
p-value (1d vs. 3d)
Fold-Change (1d vs. 3d)
p-value (3d vs. 5d)
Fold-Change (3d vs. 5d)
p-value (5d vs. 7d)
Fold-Change (5d vs. 7d)
p-value(7d vs. 10d)
Fold-Change(7d vs. 10d)
p-value(10d vs. Adult)
Fold-Change(10d vs. Adult)
N/C
0
0.5
1.0

Table 4: Highly Expressed Mouse microRNAs within the Cardiac Perinatal Period. Illumina normalized (Log2) microRNA microarray results highlighting the wild-type mouse microRNAs (mmu-miR) with the highest and most significant fold-changes (p-value≤0.05) as well as the microRNAs with known involvement in heart development and disease (purple), with their respective p-value and fold-change. Contrasts span from E19 to adult.

	Mouse microRNA	p-value	Fold-Change	Mouse microRNA	p-value	Fold-Change
E19 versus 1 day	**Downregulated**			**Upregulated**		
	mmu-miR-200c	8.77E-07	-3.62	mmu-miR-702	2.50E-02	2.30
	mmu-miR-338-5p	1.24E-02	-2.39	mmu-miR-21*	4.62E-02	2.39
	mmu-miR-150	5.15E-03	-1.44	mmu-miR-325*	1.27E-02	2.61
	mmu-miR-29a	2.39E-03	-1.40	mmu-miR-216a	1.75E-02	2.89
1 day versus 3 day	**Downregulated**			**Upregulated**		
	mmu-miR-34b-3p	7.23E-03	-3.10	mmu-miR-29b	1.74E-02	1.88
	mmu-miR-429	3.21E-02	-2.78	mmu-miR-1-2-as	1.69E-02	2.10
	mmu-miR-34c*	2.53E-02	-2.56	mmu-miR-19a	2.07E-02	2.35
	mmu-miR-150	1.73E-04	-1.92	mmu-miR-301b	1.99E-02	2.62
3 day versus 5 day	**Downregulated**			**Upregulated**		
	mmu-miR-144:9.1	4.17E-02	-2.15	mmu-miR-29b*	9.02E-03	2.66
	mmu-miR-19b	4.81E-02	-1.74	mmu-miR-292-5p	3.16E-02	4.63
	mmu-miR-497	4.00E-02	-1.68	mmu-miR-686	6.82E-03	6.52
	mmu-miR-34a	3.41E-02	-1.68	mmu-miR-705	2.98E-04	7.03
5 day versus 7 day	**Downregulated**			**Upregulated**		
	mmu-miR-29b*	2.32E-02	-2.21	mmu-miR-105	3.31E-02	1.73
	mmu-miR-713	1.80E-02	-2.14	mmu-miR-1-2-as	1.06E-02	2.28
	mmu-miR-196b	3.76E-02	-1.76	mmu-miR-344	4.19E-02	2.36
	mmu-miR-29c*	1.17E-02	-1.49	mmu-miR-509-3p	3.69E-02	7.88
7 day versus 10 day	**Downregulated**			**Upregulated**		
	mmu-miR-689	2.09E-03	-3.11	mmu-miR-450-5p	1.85E-02	1.51
	mmu-miR-15a*	2.50E-02	-2.21	mmu-miR-380-5p	1.03E-02	1.52
	mmu-miR-743a	2.50E-02	-1.77	mmu-miR-302b	2.53E-04	2.13
	mmu-miR-509-5p	2.50E-02	-1.69	mmu-miR-302d	1.24E-04	2.53
10 day versus Adult	**Downregulated**			**Upregulated**		
	mmu-miR-705	5.08E-04	-5.96	mmu-miR-208a	2.02E-02	1.96
	mmu-miR-29b*	5.47E-04	-5.16	mmu-miR-214*	2.40E-05	2.35
	mmu-miR-684	1.25E-02	-4.31	mmu-miR-1-2-as	1.28E-03	3.44
	mmu-miR-7b	6.12E-05	-3.11	mmu-miR-301b	2.09E-05	25.08
	mmu-miR-155	4.01E-06	-3.07	mmu-miR-431	9.33E-08	25.60
	mmu-miR-138*	2.19E-02	-3.11	mmu-miR-376a*	2.89E-06	26.82
	mmu-miR-29a	2.10E-05	-2.09	mmu-miR-496	4.96E-09	27.26
	mmu-miR-150	9.45E-05	-2.05	mmu-miR-154*	3.66E-06	37.03
	mmu-miR-29b	1.31E-02	-1.96	mmu-miR-377	3.04E-08	47.08
	mmu-miR-29c*	1.68E-03	-1.78	mmu-miR-380-3p	2.92E-05	114.1

Overall expression profiles were assessed by plotting the number of significantly changing genetic factors over time (**Figure 6**). Panel **A** illustrates the trends of significantly ($p \leq 0.05$) changing transcripts (mRNAs) and microRNAs (miRNAs, excluding the Solexa sequences) within different intervals during perinatal cardiac development. The profiles follow one another with an inflection point between 5 and 7 day for mRNAs and 5 and 10 day for miRNAs. Thus, the number of changing genes and microRNAs slightly varies until the inflection point, at which point a dramatic increase in variability takes place. The percentage linked to the profiles provides the amount of genetic factors increasing over time (i.e. from the total number of microRNAs changing between E19 and 1d, 28% are downregulated at E19 when compared to 1d, which translates to 28% of microRNAs increasing over time, from E19 to 1d). Intriguingly, a comparable amount of transcripts are up- and downregulated (~50%) while there is nearly double the number of microRNAs upregulated than downregulated at each interval (i.e. 72% of microRNAs are upregulated at E19 when compared to 1d).

Figure 6B stratifies genes to transcription factors, whereby out of 16,655 genes on the array, 606 are known or predicted murine transcription factors (TF) (Riken Transcription Factor Database (TFdb), 2004), of which 258 (42.6%) are significantly changing ($p \leq 0.05$) between E19 and 10 days post-birth. The graph and table summarizes the ratios representing the number of genes (or TFs) significantly increasing divided by those significantly decreasing over time. A TF expression ratio of 0.61 (<1) at E19 vs. 1d refers to a greater number of upregulated genes and a smaller number of downregulated genes at E19 as compared to 1d. Furthermore, this ratio signifies an overall decrease of TFs at 1d. Conversely, a ratio greater than 1 (>1) represents an increase in gene or TF expression over

time. When evaluating the ratios of increased to decreased gene and TF expression, we notice that the pattern switches at each contrasting point. That is, at the TF level there are more TFs decreasing at E19 vs. 1 day but then the pattern alternates at 1 day vs. 3 day, and proceeds in that manner. Interestingly, the expression ratio profiles of genes and TFs result in a W and M pattern, respectively. Similar to the volcano plots, the largest cohort of total significantly changing genes (including TFs) appears at E19 vs. 1d and 7d vs. 10d while the least variable expression pattern is at 5d vs. 7d ($p \leq 0.05$), as seen in the table below panel **B**.

Figure 6: Genomic Patterning Promoting Heart Maturation. Genetic expression profile during the cardiac perinatal transitional program determined by the number of significantly ($p \leq 0.05$) changing genes and microRNAs when comparing a wild-type mouse heart of a certain age to another. **A)** Profiles of the number of significantly changing mRNAs (blue) and microRNAs (red) over time. The percentages linked to the data points represent the percentage of increasing genes or microRNAs to total number of changing genes or microRNAs. **B)** Expression ratio of significantly increased genes (red) or transcription factors (blue) to the number of decreased genes or TFs over time. The green and yellow trend lines outline the gene and transcription factor ratio patterns, respectively. Values are summarized in the table below the graph.

A.

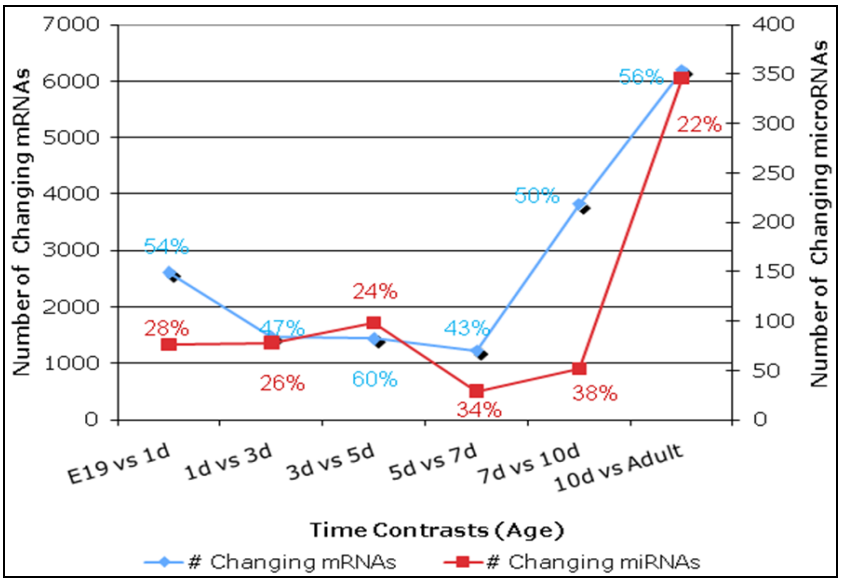

B.

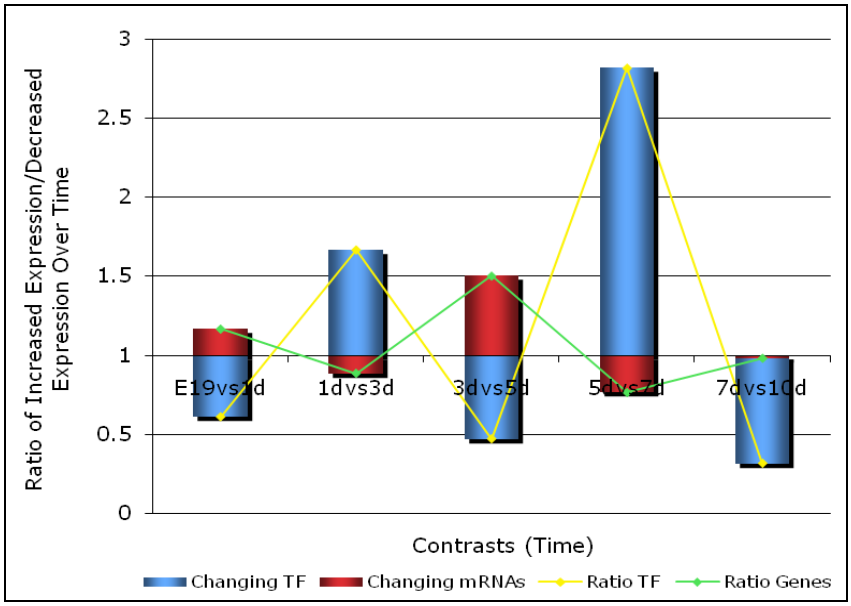

	Transcription Factors				Genes (mRNAs)			
Contrast	**Total**	**# Up**	**# Down**	**Ratio #Down/#Up**	**Total**	**#Up**	**# Down**	**Ratio #Down/#Up**
E19 vs. 1d	95	59	36	0.61	2606	1203	1403	1.17
1d vs. 3d	48	18	30	1.67	1460	774	686	0.89
3d vs. 5d	50	34	16	0.47	1439	575	864	1.50
5d vs. 7d	42	11	31	2.82	1226	695	531	0.76
7d vs. 10d	146	111	35	0.32	3818	1927	1891	0.98

Genetic expression patterns were mapped to gene ontology (GO) profiles to gain a global perspective, in addition to knowing which processes are activated or inactivated during heart maturation (**Figure 7** and **8**). Partek® was used to generate GO profiles from gene lists filtered at a p-value≤0.05 and FDR≤0.05. Generally, GO profiles are divided into Biological Processes (BP), Cellular Components (CC), and Molecular Function (MF). Analysis was limited to Biological Processes because our interest lies within organismal events that encompass regulatory processes involved in genetic expression and interactions. The BP with an Enrichment Score (ES)≥3 and an Age Score≥3 were considered as significant and were used to create Forest Plots and Pie Charts. The ES and Age Score are a measurement of the degree at which a gene is overrepresented within BP (i.e. with an increasing score, a gene becomes more representative within a functional group) (Subramanian et al., 2005). As a result, the following three processes persist within our analysis: Cellular Process, Metabolic Process, and Biological Adhesion. In addition, Developmental Process, Biological Regulation, and Multicellular Organismal Process appear to play a role within certain contrasting groups (e.g. 7d vs. 10d). **Figure 7** and **8** enumerate the gene ontologies, however each Biological Process may be further stratified into specific functional groups. A secondary level of analysis predominantly revealed the following functional groups within the BP:

1) Cellular Process: *cell cycle, cell division, cell cycle process, chromosome segregation, microtubule-based process*;

2) Metabolic Process: *macromolecule metabolic process, primary metabolic process, oxidation reduction, biosynthetic process*;

3) Biological Adhesion: *cell adhesion*;

4) Developmental Process: *anatomical structure morphogenesis and development, multicellular organismal development, cellular developmental process, developmental maturation*;

5) Biological Regulation: *regulation of cellular process, regulation of response to stimulus, regulation of developmental process, regulation of metabolic process, regulation of growth*; and,

6) Multicellular Organismal Process: *system process, cytokine production, tissue remodeling*.

Figure 7 illustrates the Forest Plots for contrasts between E19 and adult. Each bar displays the number and percentage of genes within the group (up- or downregulated) as well as the corresponding ES or an indication of non-significance (N.S.). It is important to note that a large cohort of genes found within a process does not necessarily imply significance. When comparing an E19 to a 1 day heart (**A**), Cellular Process, Metabolic Process and Developmental Process are three prominent BP with nearly equal abundance of genes up- and downregulated; however Cellular and Developmental process contain upregulated genes with the strongest Enrichment Scores. At 1d versus 3d (**B**), Biological Regulation, Cellular Process, Metabolic Process and Developmental Process are overrepresented but significantly changing genes within Cellular and Metabolic process are solely upregulated at 1d. Panel **C** highlights Cellular Process, Biological Regulation, Metabolic Process and Developmental Process as functional categories involved within 3 to 5 days post-birth. In contrast to the three former groups, the genes upregulated within Developmental Process are further committed at an ES of 24.6. Although 5d versus 7d has

the shortest list of significantly changing genes (**Figure 6**), there are several highly represented genes involved in the BP, in particular within Cellular Process, Biological Regulation and Metabolic Process (**D**), with the majority being upregulated at 5d. Analyzing panel **E** and **F** revealed the importance of day 10 post-birth. That is, genes involved in BP at 7d are largely downregulated when compared to 10d while genes are mainly upregulated at 10d as compared to adult. Therefore, it appears that certain processes are being downregulated before and after day 10. Overall, E19 vs. 1d, 7d vs. 10d, and 10d vs. adult illustrated the largest cohort of genes significantly mediating Biological Processes. Note, Biological Adhesion is present throughout every contrast, but the gene abundance and/or ES (and Age Score) are minor.

Pie Charts summarize the Biological Processes as seen in the Forest Plots without discriminating between up- and downregulated genes (**Figure 8**). These figures are imperfect representations of Forest Plots because generating a Pie Chart causes certain functional groups to be omitted. This is a result of a new background created by merging two gene lists (up- and downregulated genes). Pie Charts are essentially an alternative method to study global GO profiles that may influence cardiac growth, via short intervals. As Pie Charts provide a wealth of information, only Biological Processes with prominent roles (ES and Age Score ≥ 3) in each interval will be discussed. Panel **A** illustrates the importance of Multicellular Organismal Process, Cellular Process, Biological Adhesion, and Metabolic Process between E19 and 1d. On the other hand, functional groups that differ a 1d and 3d heart have small Enrichment Scores (**B**). Comparing a 3d to a 5d heart mainly highlights Metabolic Process, Multicellular Organismal Process and Cellular Process (**C**).

The most intriguing Pie Charts are that of 5d versus 7d and 7d versus 10d whereby Cellular Process and Metabolic Process, respectively, constitutes approximately 50% of the Biological Processes (**D**). Finally, a 10d heart differs largely from that of an adult heart as depicted in Panel **F**.

Further analysis of the BP demonstrated functional groups with strong representation (i.e. high Enrichment Scores (ES)) that may have been missed at a first pass. In particular, when comparing 5d versus 7d (**D**), Cellular Process is largely upregulated at 5d and is composed of the following functional groups (with their respective ES and percentage of distribution): *cell cycle* (182.2, 33.2%), *cell division* (154.6, 28.2%), *chromosome segregation* (35.3, 6.43%), *microtubule-based process* (23.5, 4.3%), *cell motion* (3.32, 0.61%), and *cellular metabolic process* (13.2, 2.4%). In addition, *mitosis* represents 86.7% of the *cell cycle process* at an Enrichment Score of 164 (data not shown). Similar Cellular Process functional groups are upregulated at 10d when compared to adult (**F**) but with slightly smaller ES. Therefore, Cellular Processes are markedly enhanced at 5d and 10d.

Figure 7: Gene Ontology Processes Altering During Heart Development. Forest Plots of Biological Processes (BP) at contrasting cardiac ages from E19 to adulthood generated with gene lists significantly changing over time ($p \leq 0.05$, $FDR \leq 0.05$). BP significance includes an Enrichment Score and Age Score above 3, otherwise denoted as N.S. (non-significant). The number of genes downregulated (left, red) and upregulated (right, green) are represented on the X axis. Numbers within bars (in black) represent the Enrichment Score. The percentage in green or red outside the bar graphs represent the percentage of genes within the up- or downregulated genes, respectively, as compared to the total number of genes significantly changing. The contrasts analyzed are: **A)** E19 versus 1 day; **B)** 1 day versus 3 day; **C)** 3 day versus 5 day; **D)** 5 day versus 7 day; **E)** 7 day versus 10 day; **F)** 10 day versus Adult.

A.

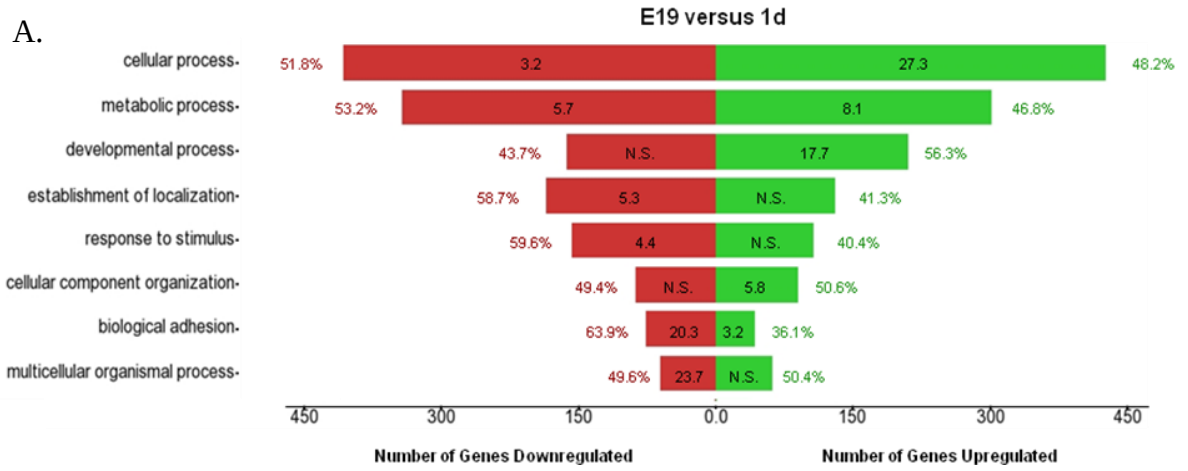
E19 versus 1d
cellular process
metabolic process
developmental process
establishment of localization
response to stimulus
cellular component organization
biological adhesion
multicellular organismal process
51.8%
3.2
27.3
48.2%
53.2%
5.7
8.1
46.8%
43.7%
N.S.
17.7
56.3%
58.7%
5.3
N.S.
41.3%
59.6%
4.4
N.S.
40.4%
49.4%
N.S.
5.8
50.6%
63.9%
20.3
3.2
36.1%
49.6%
23.7
N.S.
50.4%
450
300
150
0.0
150
300
450
Number of Genes Downregulated
Number of Genes Upregulated

B.

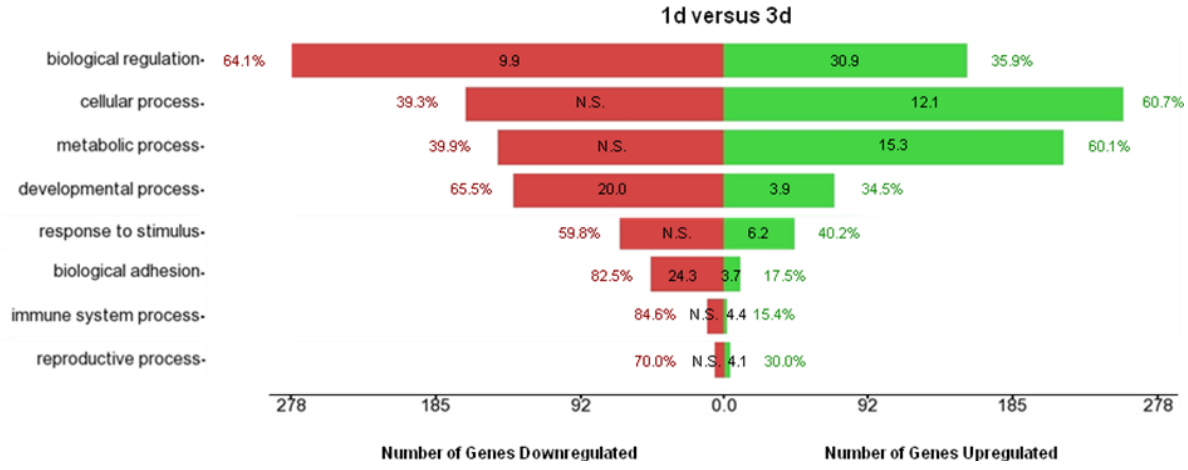
1d versus 3d
biological regulation
cellular process
metabolic process
developmental process
response to stimulus
biological adhesion
immune system process
reproductive process
64.1%
9.9
30.9
35.9%
39.3%
N.S.
12.1
60.7%
39.9%
N.S.
15.3
60.1%
65.5%
20.0
3.9
34.5%
59.8%
N.S.
6.2
40.2%
82.5%
24.3
3.7
17.5%
84.6%
N.S.
4.4
15.4%
70.0%
N.S.
4.1
30.0%
278
185
92
0.0
92
185
278
Number of Genes Downregulated
Number of Genes Upregulated

C.

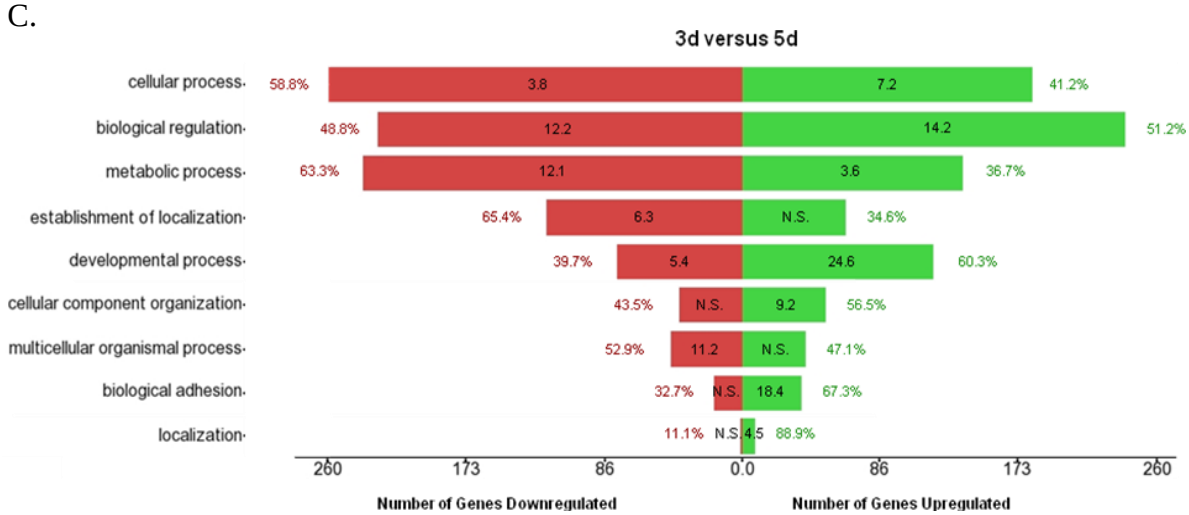
3d versus 5d
cellular process
biological regulation
metabolic process
establishment of localization
developmental process
cellular component organization
multicellular organismal process
biological adhesion
localization
58.8%
3.8
7.2
41.2%
48.8%
12.2
14.2
51.2%
63.3%
12.1
3.6
36.7%
65.4%
6.3
N.S.
34.6%
39.7%
5.4
24.6
60.3%
43.5%
N.S.
9.2
56.5%
52.9%
11.2
N.S.
47.1%
32.7%
N.S.
18.4
67.3%
11.1%
N.S.
4.5
88.9%
260
173
86
0.0
86
173
260
Number of Genes Downregulated
Number of Genes Upregulated

D.

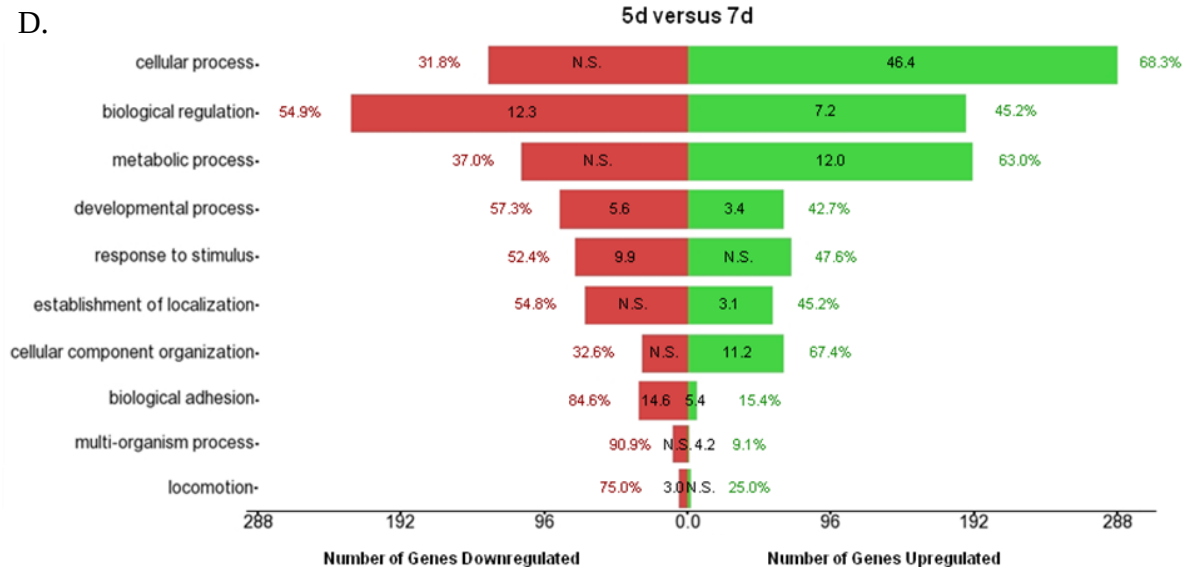
5d versus 7d
cellular process
biological regulation
metabolic process
developmental process
response to stimulus
establishment of localization
cellular component organization
biological adhesion
multi-organism process
locomotion
31.8%
N.S.
46.4
68.3%
54.9%
12.3
7.2
45.2%
37.0%
N.S.
12.0
63.0%
57.3%
5.6
3.4
42.7%
52.4%
9.9
N.S.
47.6%
54.8%
N.S.
3.1
45.2%
32.6%
N.S.
11.2
67.4%
84.6%
14.6
5.4
15.4%
90.9%
N.S.
4.2
9.1%
75.0%
3.0
N.S.
25.0%
288
192
96
0.0
96
192
288
Number of Genes Downregulated
Number of Genes Upregulated

E.

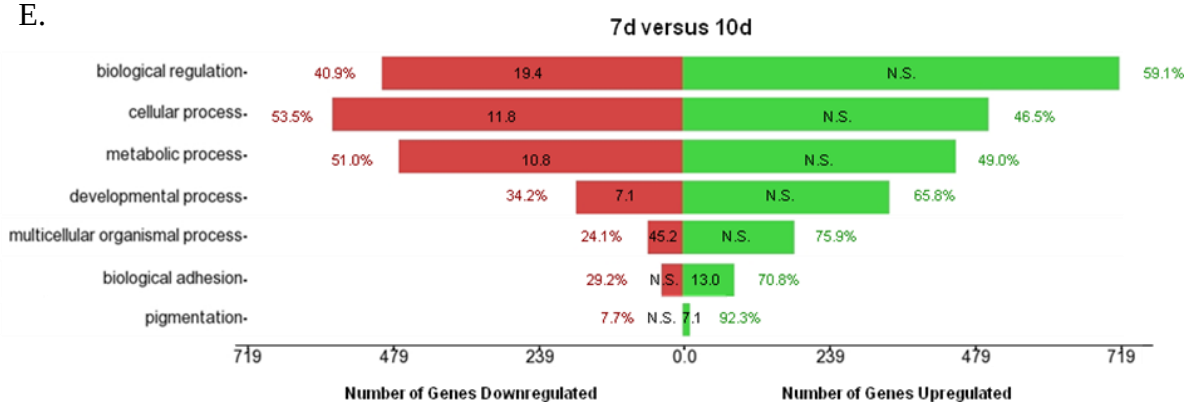
7d versus 10d
biological regulation
cellular process
metabolic process
developmental process
multicellular organismal process
biological adhesion
pigmentation
40.9%
19.4
N.S.
59.1%
53.5%
11.8
N.S.
46.5%
51.0%
10.8
N.S.
49.0%
34.2%
7.1
N.S.
65.8%
24.1%
45.2
N.S.
75.9%
29.2%
N.S.
13.0
70.8%
7.7%
N.S.
7.1
92.3%
719
479
239
0.0
239
479
719
Number of Genes Downregulated
Number of Genes Upregulated

F.

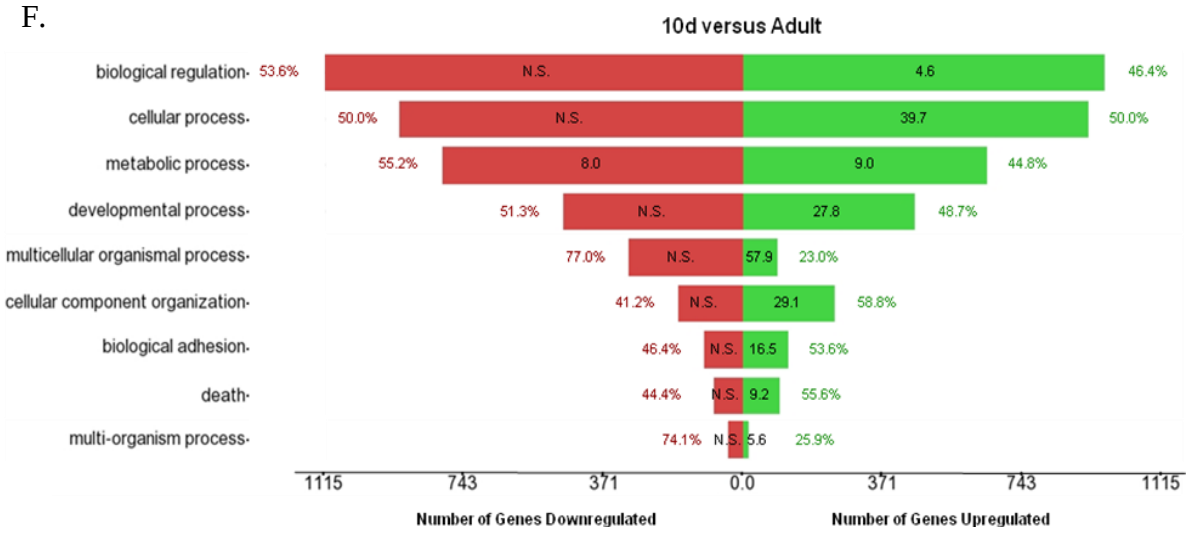
10d versus Adult
biological regulation
cellular process
metabolic process
developmental process
multicellular organismal process
cellular component organization
biological adhesion
death
multi-organism process
53.6%
N.S.
4.6
46.4%
50.0%
N.S.
39.7
50.0%
55.2%
8.0
9.0
44.8%
51.3%
N.S.
27.8
48.7%
77.0%
N.S.
57.9
23.0%
41.2%
N.S.
29.1
58.8%
46.4%
N.S.
16.5
53.6%
44.4%
N.S.
9.2
55.6%
74.1%
N.S.
5.6
25.9%
1115
743
371
0.0
371
743
1115
Number of Genes Downregulated
Number of Genes Upregulated

Figure 8: Overall Biological Processes Significantly Involved in the Heart. Pie Charts of Biological Processes (BP) significantly changing ($p \leq 0.05$, $FDR \leq 0.05$, Enrichment Score and Age Score ≥ 3) at different stages during perinatal heart development. BP are assessed through a gene list of all genes significantly changing over time, including down- and upregulated genes. Each BP contains a corresponding Enrichment Score and percentage distribution found within parentheses. The contrasts analyzed are: **A)** E19 versus 1 day; **B)** 1 day versus 3 day; **C)** 3 day versus 5 day; **D)** 5 day versus 7 day; **E)** 7 day versus 10 day; **F)** 10 day versus Adult.

A.

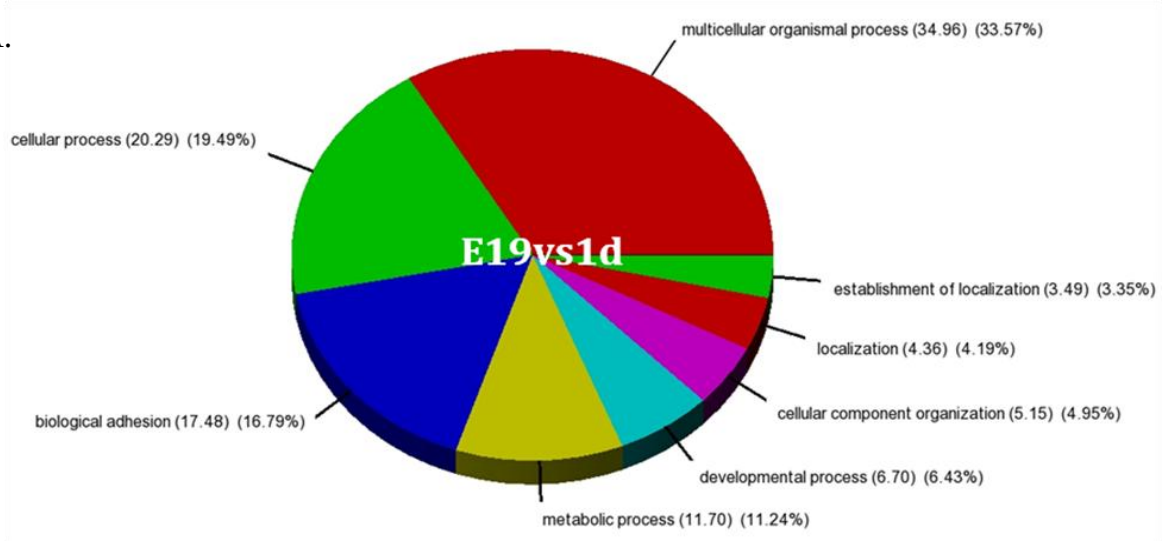
multicellular organismal process (34.96) (33.57%)
cellular process (20.29) (19.49%)
E19vs1d
establishment of localization (3.49) (3.35%)
localization (4.36) (4.19%)
cellular component organization (5.15) (4.95%)
biological adhesion (17.48) (16.79%)
developmental process (6.70) (6.43%)
metabolic process (11.70) (11.24%)

B.

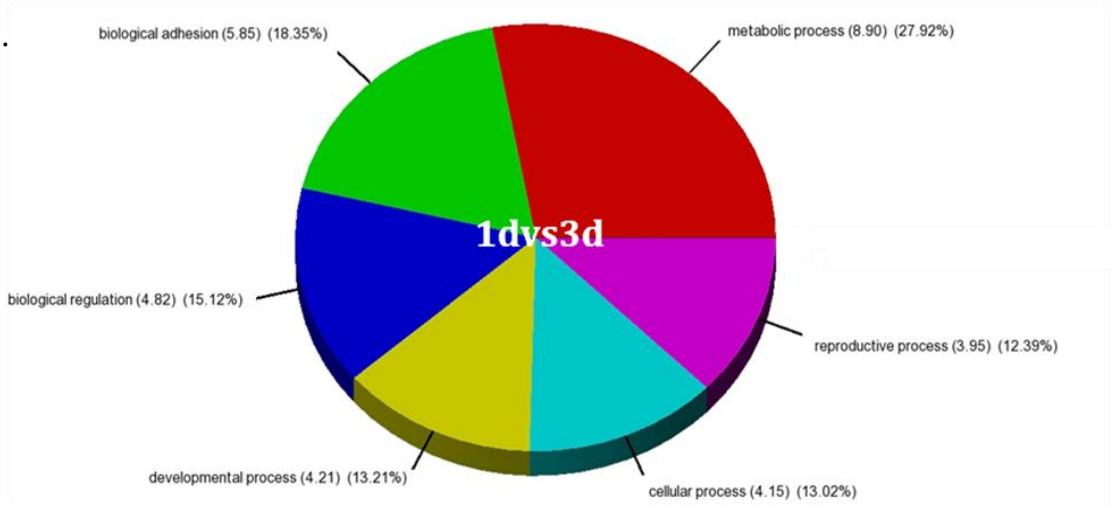
biological adhesion (5.85) (18.35%)
metabolic process (8.90) (27.92%)
1dvs3d
biological regulation (4.82) (15.12%)
reproductive process (3.95) (12.39%)
developmental process (4.21) (13.21%)
cellular process (4.15) (13.02%)

C.

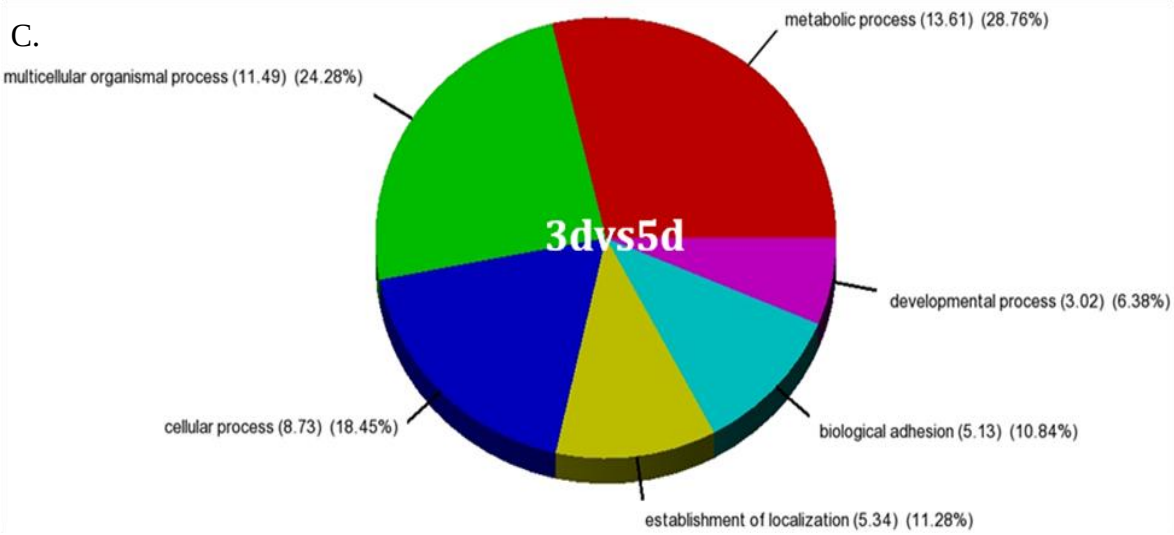
metabolic process (13.61) (28.76%)
multicellular organismal process (11.49) (24.28%)
3dvs5d
developmental process (3.02) (6.38%)
cellular process (8.73) (18.45%)
biological adhesion (5.13) (10.84%)
establishment of localization (5.34) (11.28%)

D.

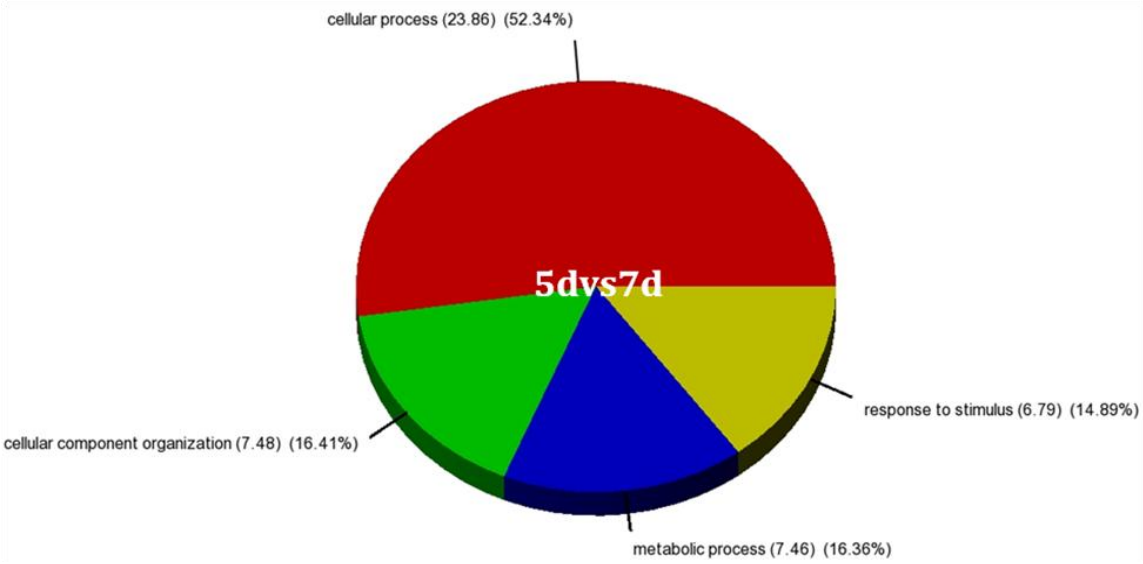
cellular process (23.86) (52.34%)
5dvs7d
response to stimulus (6.79) (14.89%)
cellular component organization (7.48) (16.41%)
metabolic process (7.46) (16.36%)

E.

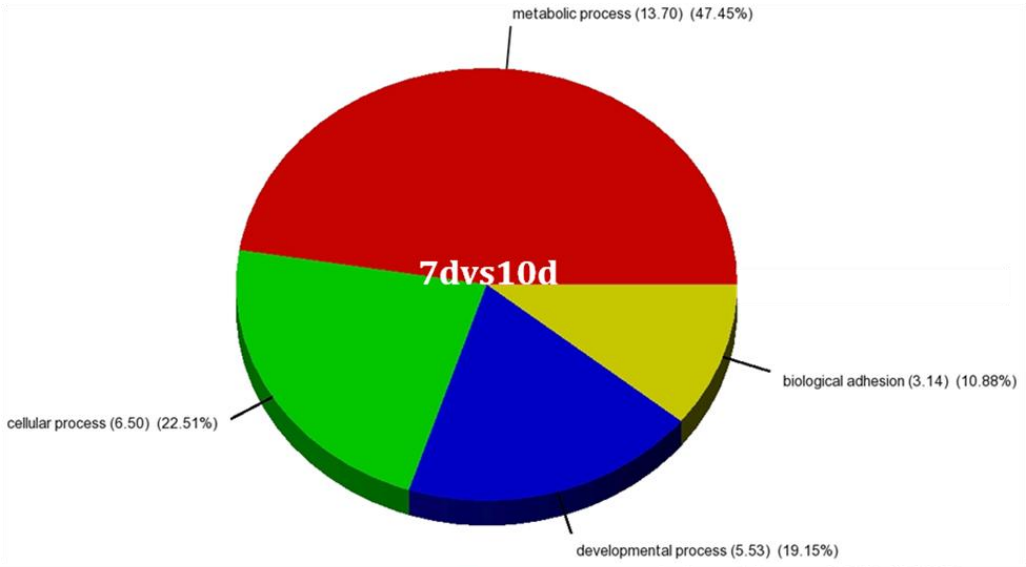
metabolic process (13.70) (47.45%)
7dvs10d
biological adhesion (3.14) (10.88%)
cellular process (6.50) (22.51%)
developmental process (5.53) (19.15%)

F.

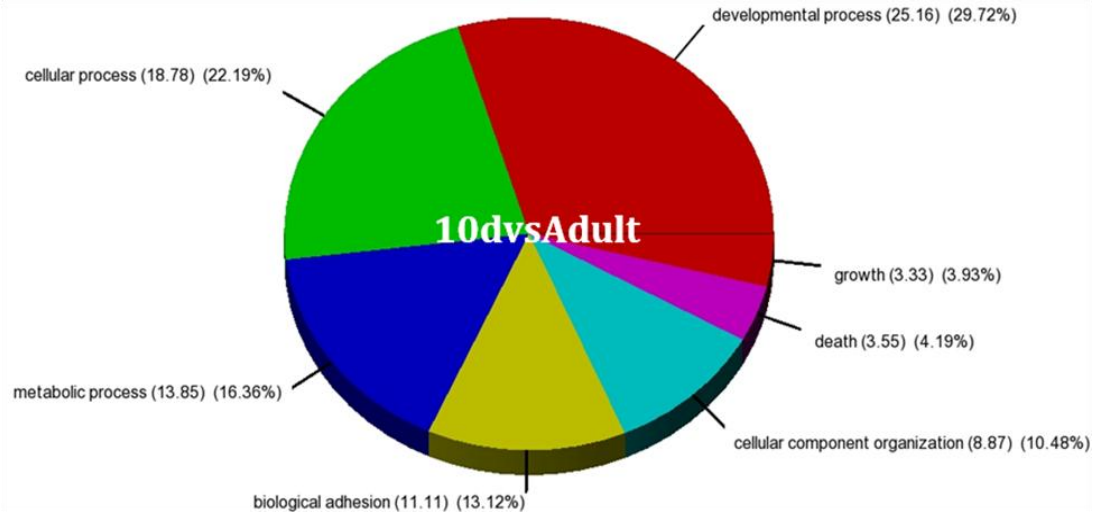
developmental process (25.16) (29.72%)
cellular process (18.78) (22.19%)
10dvsAdult
growth (3.33) (3.93%)
death (3.55) (4.19%)
metabolic process (13.85) (16.36%)
cellular component organization (8.87) (10.48%)
biological adhesion (11.11) (13.12%)

In order to validate the quality of the cDNA microarray datasets, semi-quantitative and quantitative PCR experiments were undertaken. Prior to validating the microarrays, we searched for a reference gene that remained unchanged during the cardiac perinatal transitional program. Structural genes, such as those expressing proteins involved in the cytoskeleton and extra-cellular matrix, were not chosen since the heart undergoes dynamic remodeling events (Chen, et al., 2004). Instead the processing genes Ppia, Pgk2, and Gapdh were selected as their expression remained unchanged in the microarray data. Peptidylprolyl isomerase A (Ppia) encodes enzymes responsible for cis-trans isomerization of proline imidic peptide bonds in oligopeptides and for the acceleration of protein folding. Phosphoglycerate kinase 2 (Pgk2) mediates glycolysis by catalyzing the conversion of 1,3-diphosphoglycerate to 3-phosphoglycerate and releasing one molecule of ATP. Last, glyceraldehyde-3-phosphate dehydrogenase (Gapdh) phosphorylates glyceraldehyde-3-phosphate in the presence of inorganic phosphate and nicotinamide adenine dinucleotide during carbohydrate metabolism (NCBI, 2011). All three genes are frequently amplified in the literature as reference genes for RNA quantitation. **Figure 9** illustrates transcript expression profiles after RT-PCR. Ppia appears to be the sole gene with constant expression at E19, 1d, 3d, 4d, 5d, 6d, 7d, 10d and adult.

Once Ppia was assessed as the reference gene, 9 genes (Rxrγ, Pln, Mad2l1, Epas1, Asb15, Cdk4, Hif3α, Fbxw7, Pfkm) were chosen at random plus Prc1 as validation genes. Protein regulator of cytokinesis 1 (Prc1) was selected since it possessed one of the highest fold-changes when comparing 10d to adult. The False Discovery Rate (FDR) was set at 0.20, therefore an error of 20% was deemed acceptable. It is important to note that day 4 and

6 heart transcripts were added to the validation experiments after uncovering the inflection point between 5d and 7d in the transcriptional profiling, as a precaution of missing vital results. After RT-PCR, eight genes (Prc1, Rxrγ, Mad2l1, Cdk4, Asb15, Pfkm, Hif3α, and Fbxw7) followed the microarray mean expression trend while two genes (Pln and Epas1) deviated from the expected expression profile, which fulfills an FDR of 20% (**Figure 10**). Prc1, Rxrγ and Pln were further analyzed by Real-Time PCR and the resulting fold-change had the same directionality as the fold-change calculated and considered significant with the microarray data. The RT-PCR and Real-Time PCR results do not converge for Pln, albeit the microarray fold-changes hover between -1.1 and 1.0 so it is difficult to say if -1.0 is different from 1.0.

Figure 9: Ppia Remains Constantly Expressed during the Perinatal Cardiac Program. Reference gene expression assessed by reverse-transcribing and PCR amplifying mRNA from differently aged wild-type mouse hearts (E19, 1d, 3d, 4d, 5d, 6d, 7d, 10d, adult) and run on 3% agarose gels supplemented with 0.005% ethidium bromide. Ppia, Pgk2 and Gapdh are commonly used reference genes which were tested to assess which would remain stably expressed during the transitional program. Ppia appears to be the ideal reference gene for this study (N=3).

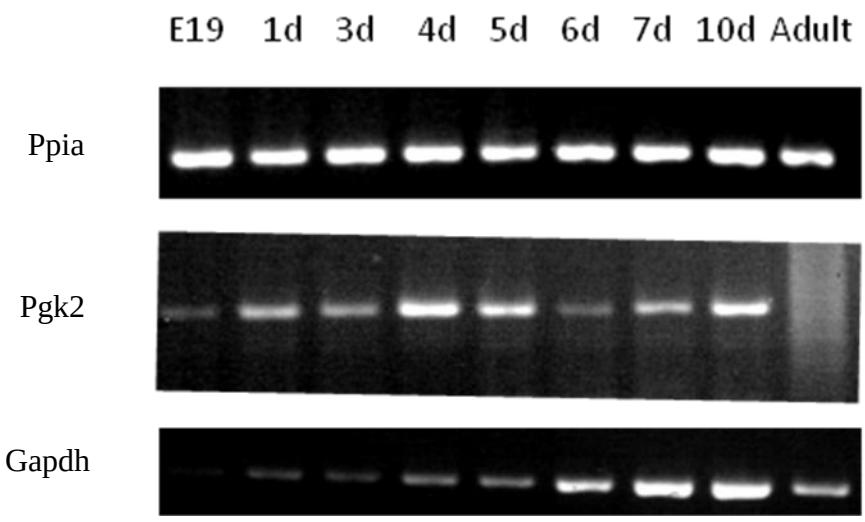
E19
1d
3d
4d
5d
6d
7d
10d
Adult
Ppia
Pgk2
Gapdh

Figure 10: Successful Validation of Exon Microarray Results through RT-PCR and Real-Time PCR. Gene expression profiles assessed by semi-quantitative PCR and Real-Time PCR mimicking the Affymetrix GeneChip Mouse Exon 1.0 ST Array trends at an FDR of 0.20. Transcripts for validation were isolated from wild-type mouse hearts at E19, 1d, 3d, 4d, 5d, 6d, 7d, 10d and adulthood. The following genes were investigated: **A)** Prc1, **B)** Rxrγ, **C)** Pln, **D)** Mad2l1, **E)** Epas1, **F)** Asb15, **G)** Cdk4, **H)** Hif3α, **I)** Fbxw7, **J)** Pfkm.

For **A)**, **B)** and **C)**, the first panel on the left is the normalized (RMA) mean expression signal of a gene generated from the exon microarray data (E19, 1d, 3d, 5d, 7d, 10d, adult) with corresponding standard errors (±Std. Err.). The panel on the right represents the fold-change calculated with Real-Time PCR (white bars) and microarray (black bars) data when comparing differently aged mouse hearts. Asterisks (*) denote the fold-change deemed significant (p-value≤0.05) after a 1-way ANOVA of the microarray data. The relative fold-change of a gene produced by Real-Time PCR is normalized to Ppia expression. The fold-change values are found beneath the bar graph. The third panel illustrates the semi-quantitative PCR of genes run on 3% agarose gels supplemented with 0.005% ethidium bromide (N=3).

Panels **D** to **J** demonstrate the exon microarray normalized (RMA) mean expression signal (±Std. Err.) of a gene followed by a semi-quantitative PCR image (N=3). Note that the FDR (0.20) results include Pln (**C**) and Epas1 (**E**).

A.

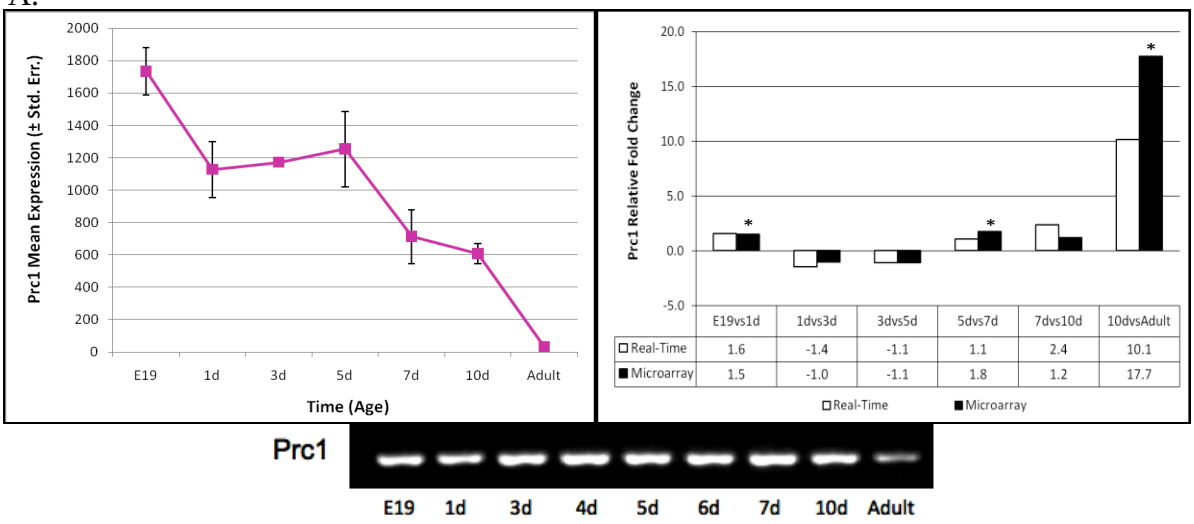
Prc1 Mean Expression (± Std. Err.)
2000
1800
1600
1400
1200
1000
800
600
400
200
0
E19 1d 3d 5d 7d 10d Adult
Time (Age)
Prc1 Relative Fold Change
20.0
15.0
10.0
5.0
0.0
-5.0
*
E19vs1d 1dvs3d 3dvs5d 5dvs7d 7dvs10d 10dvsAdult
Real-Time 1.6 -1.4 -1.1 1.1 2.4 10.1
Microarray 1.5 -1.0 -1.1 1.8 1.2 17.7
Real-Time
Microarray

Prc1
E19 1d 3d 4d 5d 6d 7d 10d Adult

B.

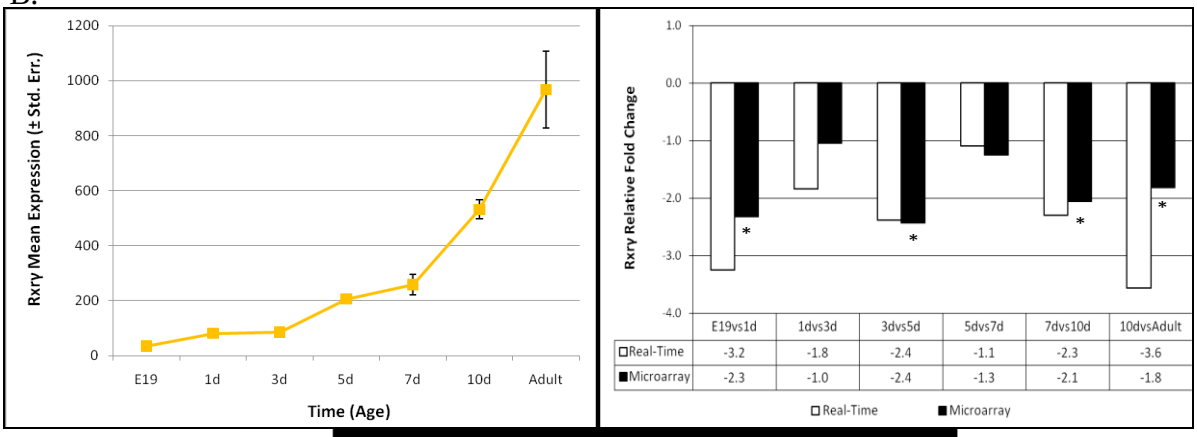
Rxrγ Mean Expression (± Std. Err.)
1200
1000
800
600
400
200
0
E19 1d 3d 5d 7d 10d Adult
Time (Age)
Rxrγ Relative Fold Change
1.0
0.0
-1.0
-2.0
-3.0
-4.0
*
E19vs1d 1dvs3d 3dvs5d 5dvs7d 7dvs10d 10dvsAdult
Real-Time -3.2 -1.8 -2.4 -1.1 -2.3 -3.6
Microarray -2.3 -1.0 -2.4 -1.3 -2.1 -1.8
Real-Time
Microarray

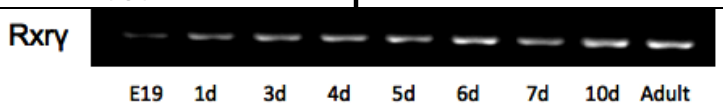
Rxrγ
E19 1d 3d 4d 5d 6d 7d 10d Adult

C.

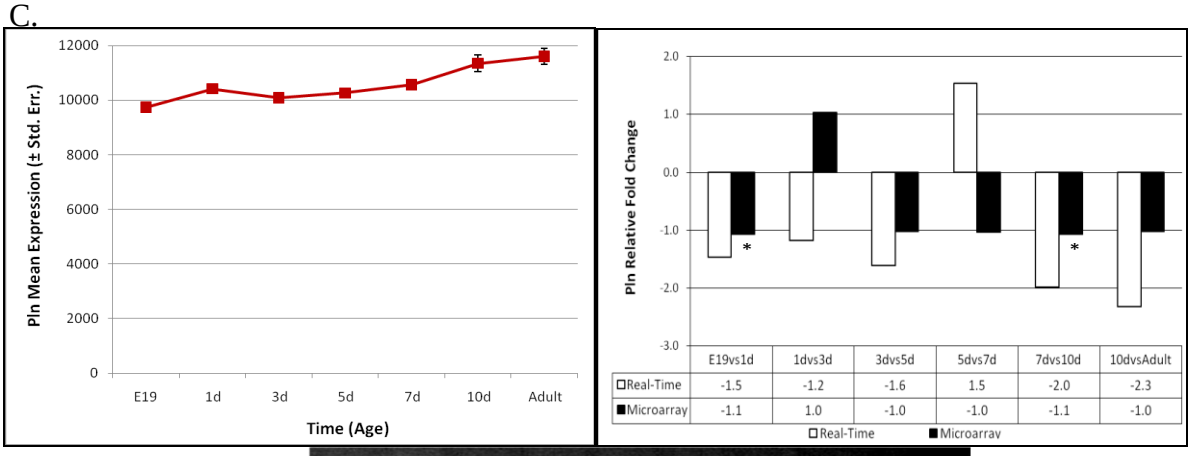
Pln Mean Expression (± Std. Err.)
12000
10000
8000
6000
4000
2000
0
E19 1d 3d 5d 7d 10d Adult
Time (Age)
Pln Relative Fold Change
2.0
1.0
0.0
-1.0
-2.0
-3.0
*
E19vs1d 1dvs3d 3dvs5d 5dvs7d 7dvs10d 10dvsAdult
Real-Time -1.5 -1.2 -1.6 1.5 -2.0 -2.3
Microarray -1.1 1.0 -1.0 -1.0 -1.1 -1.0
Real-Time
Microarray

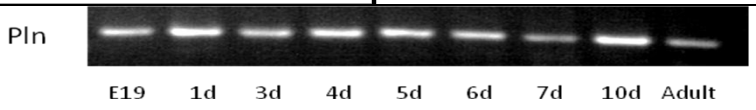
Pln
E19 1d 3d 4d 5d 6d 7d 10d Adult

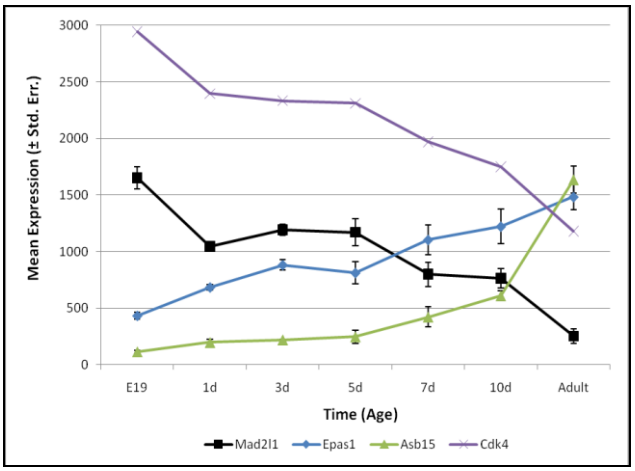
Mean Expression (± Std. Err.)
3000
2500
2000
1500
1000
500
0
E19
1d
3d
5d
7d
10d
Adult
Time (Age)
Mad2l1
Epas1
Asb15
Cdk4

D.

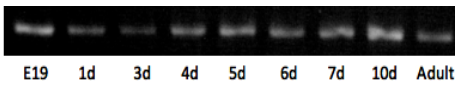
Mad2l1
E19 1d 3d 4d 5d 6d 7d 10d Adult

E.

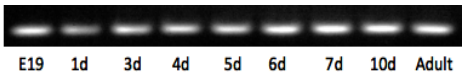
Epas1
E19 1d 3d 4d 5d 6d 7d 10d Adult

F.

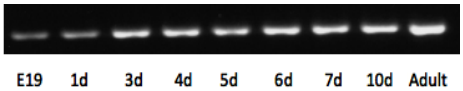
Asb15
E19 1d 3d 4d 5d 6d 7d 10d Adult

G.

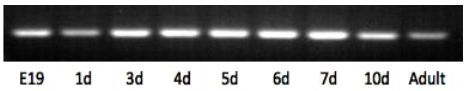
Cdk4
E19 1d 3d 4d 5d 6d 7d 10d Adult

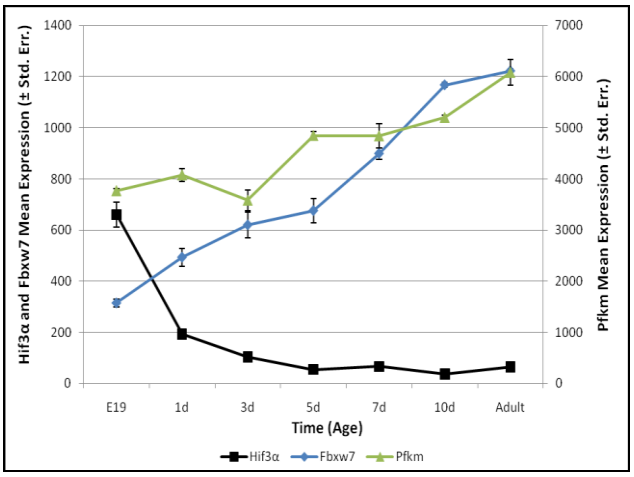
Hif3α and Fbxw7 Mean Expression (± Std. Err.)
1400
1200
1000
800
600
400
200
0
Pfkm Mean Expression (± Std. Err.)
7000
6000
5000
4000
3000
2000
1000
0
E19
1d
3d
5d
7d
10d
Adult
Time (Age)
Hif3α
Fbxw7
Pfkm

H.

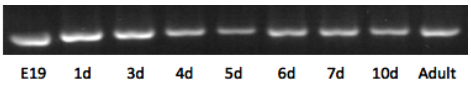
Hif3α
E19 1d 3d 4d 5d 6d 7d 10d Adult

I.

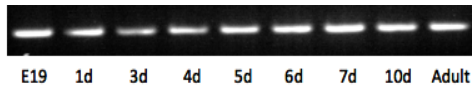
Fbxw7
E19 1d 3d 4d 5d 6d 7d 10d Adult

J.

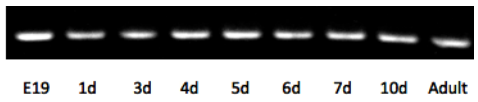
Pfkm
E19 1d 3d 4d 5d 6d 7d 10d Adult

AIM 2: ELUCIDATE KEY FACTORS INVOLVED IN CARDIOMYOCYTE MATURATION AND BINUCLEATION

Cardiomyocyte binucleation is a marker to define the switch from a hyperplastic to a hypertrophic growth (Chung et al., 2010); therefore multinucleation is a vital process in perinatal cardiac transition. Gene level microarray analysis was performed to define factors which may regulate maturation and ploidy. Thus, gene lists were examined at pivotal periods within the transitional program and so the data was sorted sequentially at 10d versus adult, 5d versus 7d, then E19 versus 1d. Consequently, Prc1 was amongst the most significantly and differentially expressed genes ($p \leq 0.05$). Intriguingly, Prc1 is known to mediate cytokinesis (Mollinari et al., 2002) and depletion of Prc1 resulted in binucleated HeLa cells (Jiang et al., 1998). Binucleation characterizes maturing cardiomyocytes hence Prc1 was further investigated. **Figure 11** demonstrates the expression profile of Prc1 along with the fold-changes at each contrast. Interestingly, a 10 day old heart is nearly 18 times more abundant in Prc1 transcript than an adult heart. RT-PCR and quantitative PCR validation confirmed the depletion of Prc1 at adulthood (**Figure 10**) which coincides with our knowledge that the majority of cardiomyocytes cease to divide during hypertrophy**.**

Figure 11: Prc1 Expression Profile Decreases Throughout Perinatal Cardiac Maturation. Exon microarray expression analysis of Prc1. **A)** Normalized (RMA) mean expression signal of Prc1 from wild-type mouse hearts at E19, 1d, 3d, 5d, 7d, 10d and adulthood, with the corresponding standard error (±Std. Err.). **B)** Fold-change and p-value of Prc1 when contrasting the ages. P-values highlighted in blue indicate significant values at $p \leq 0.05$ while grey is non-significant; red and green highlighting signify a decrease and increase in expression, respectively.

A.

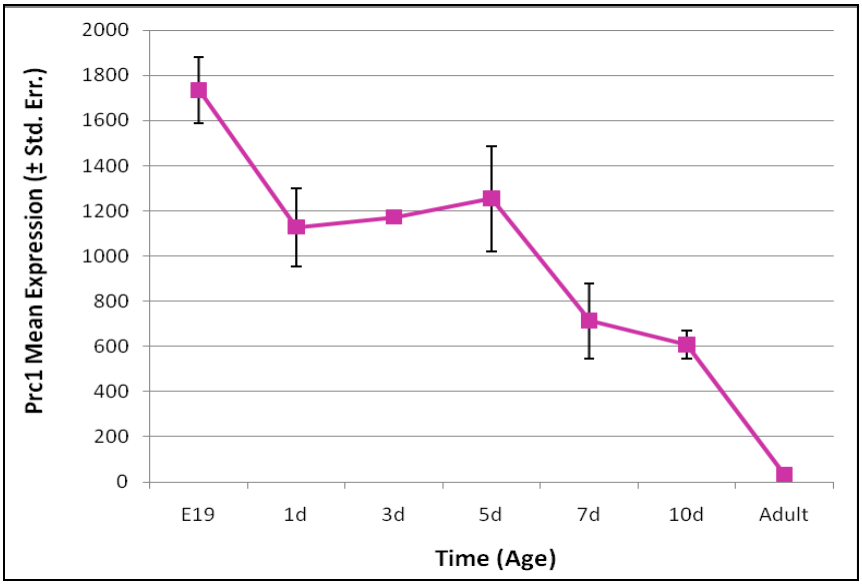

B.

Contrast	p-value	Fold-Change
E19 vs. 1d	0.0384	1.54
1d vs. 3d	0.840	-1.04
3d vs. 5d	0.725	-1.07
5d vs. 7d	0.00952	1.76
7d vs. 10d	0.416	1.17
10d vs. Adult	0.000000000403	17.7

To further investigate Prc1, an antibody and blocking peptide were purchased and utilized. Peptide neutralization experiments proved that the antibody was specific to endogenous cardiac Prc1 (**Figure 12**). Immunoblotting demonstrated that Prc1 protein expression is the inverse of mRNA expression pattern. In essence, Prc1 protein expression increased while transcript expression decreased with cardiac maturation, although the loading control (Myosin Heavy Chain – MHC) was of fairly equal abundance. As expected, skeletal muscle had abundant MHC expression, however both HL-1 and brain had undetectable MHC at 5μg of total protein lysate. HL-1, as well as wild-type adult mouse brain and skeletal muscle lysates were loaded as controls. All three controls were not detected at 5μg.

Isolating mRNA and protein from wild-type murine hearts at different ages proved to be highly erratic whereby the amount of mRNA drops while the amount of protein increased substantially at adulthood (**Figure 13**). Moreover, transcript abundance slightly increased with age, however returned to baseline at adulthood. On the other hand, protein expression appeared relatively constant until 6-7 weeks post-birth when the heart portrays a burst in protein abundance. Comparing the amount of protein to that of mRNA shows virtually no changes from E19 until 10d but a large variability at adulthood.

Figure 12: PRC1 Monoclonal Rabbit Antibody is Specific to Endogenous Cardiac PRC1. Immunoblotting of PRC1 throughout the perinatal heart development. Five micrograms of wild-type mouse heart aged E19, 1d, 3d, 4d, 5d, 6d, 7d, 10d and adult were probed with: Prc1 peptide neutralized **(A)** and rabbit monoclonal PRC1 antibody (Abcam) **(B)**. Five micrograms of undifferentiated HL-1 as well as wild-type adult mouse brain and skeletal muscle protein were used as controls. After transferring, gels were stained with Coomassie-Blue to visualize MHC as loading control. Numbers on left of blot indicate protein weight (kDa) assessed with the GeneDirex® BLUeye prestained protein ladder. The theoretical molecular weight of PRC1 in mouse is 70kDa.

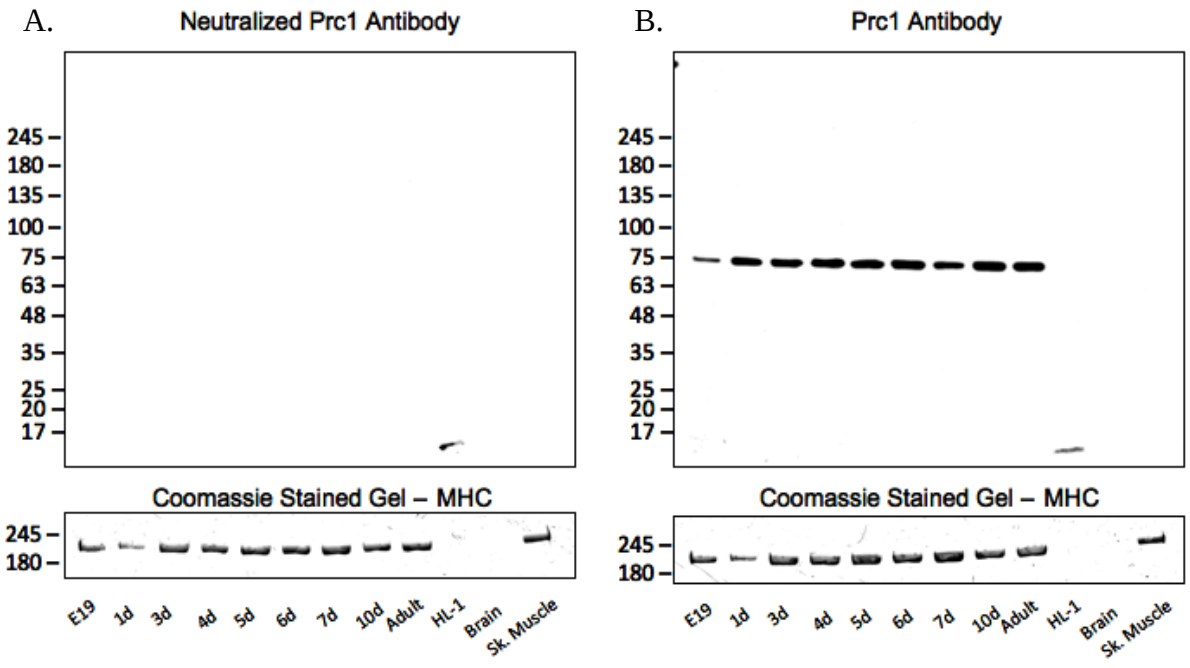
A.
Neutralized Prc1 Antibody
245
180
135
100
75
63
48
35
25
20
17
Coomassie Stained Gel – MHC
245
180
E19
1d
3d
4d
5d
6d
7d
10d
Adult
HL-1
Brain
Sk. Muscle
B.
Prc1 Antibody
245
180
135
100
75
63
48
35
25
20
17
Coomassie Stained Gel – MHC
245
180
E19
1d
3d
4d
5d
6d
7d
10d
Adult
HL-1
Brain
Sk. Muscle

Figure 13: Murine Heart Transcript and Protein Abundance Have Dissimilar Trends. Analyzing the mean amount of mRNA and protein isolated from differently aged mice hearts. **A)** Total mRNA (μg) and protein (μg) were isolated using the QIAzol® miRNEasy kit and lysis buffer, respectively, from wild-type mouse hearts aged at E19, 1d, 3d, 5d, 7d, 10d, and adulthood. The mean amount of total mRNA (μg) and protein (μg), with their corresponding standard deviation (±Std. Dev.), were calculated from nine and three hearts for each age, respectively. **B)** The ratio of the amount of total protein (μg) to the amount of total mRNA (μg) over time.

A.

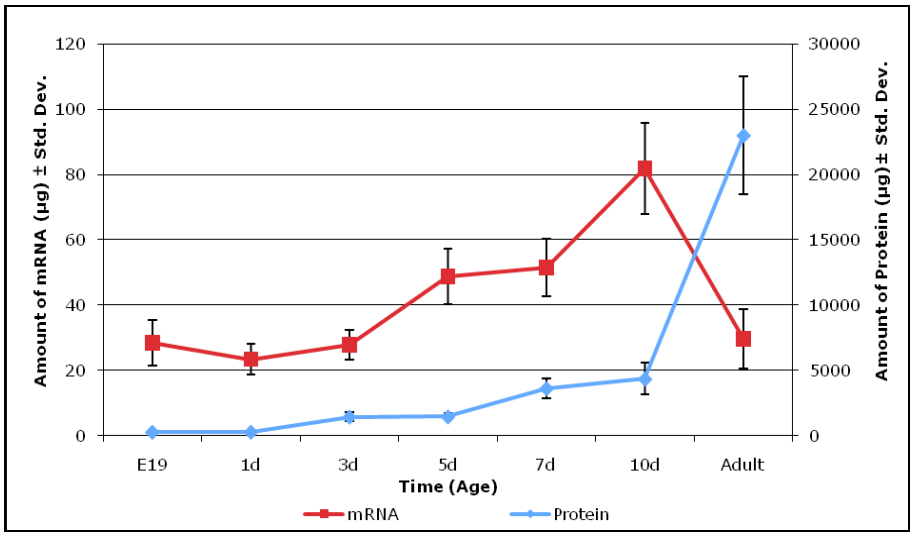
120
100
80
60
40
20
0
30000
25000
20000
15000
10000
5000
0
Amount of mRNA (µg) ± Std. Dev.
Amount of Protein (µg)± Std. Dev.
E19
1d
3d
5d
7d
10d
Adult
Time (Age)
mRNA
Protein

B.

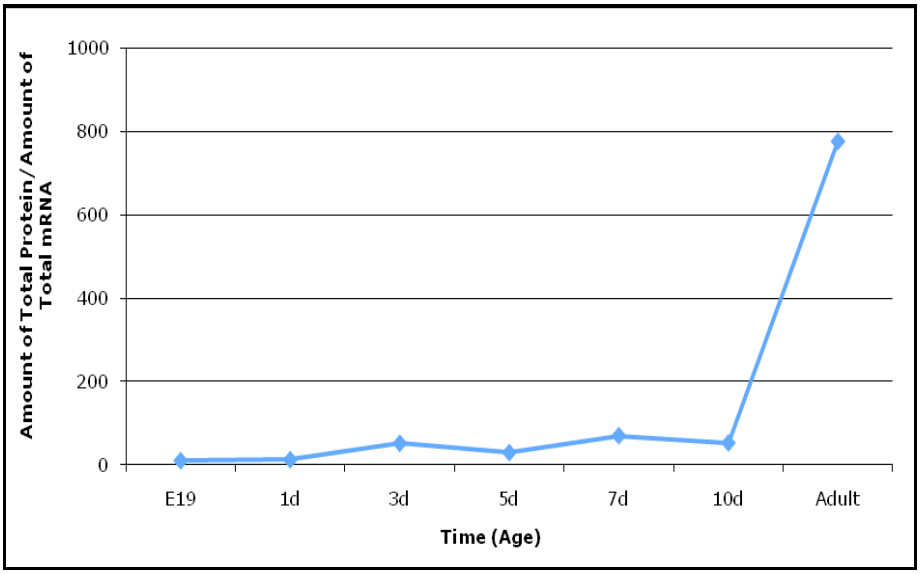
1000
800
600
400
200
0
Amount of Total Protein/Amount of Total mRNA
E19
1d
3d
5d
7d
10d
Adult
Time (Age)

With microRNA microarray expression profiles at our disposal, we aimed to determine if microRNAs are targeting Prc1, causing its dysregulation. Through TargetScan, Partek® algorithms summarized a list of microRNAs putatively targeting Prc1 (**Figure 14**). The software merges the significantly changing genes and microRNAs and matches the microRNAs to their potential targets. This allowed us to see if a change in microRNA expression may affect the expression of its putative targets, namely Prc1. Effectively certain microRNAs that are predicted to target Prc1 are significantly changing between E19 and 1d as well as 10d and adult. Although the fold-changes at E19 versus 1d were not impressive, four (miR-19a, miR-19b, miR-363, and miR-367) out of the seven microRNAs were highly upregulated at 10d when compared to adult.

Figure 14: microRNAs Putatively Targeting Prc1 Significantly Expressed at the Beginning and End of the Perinatal Cardiac Period. Merging exon and microRNA microarray data to further analyze Prc1 expression. **A)** Exon microarray normalized (RMA) mean expression signal of Prc1 from wild-type mouse hearts at E19, 1d, 3d, 5d, 7d, 10d and adulthood, with the corresponding standard error (±Std. Err.). **B)** Mouse microRNAs (mmu-miR) significantly changing (p-value≤0.05) within Illumina normalized (Log2) microRNA microarray data that putatively target Prc1 (TargetScan). microRNAs were found to be solely significantly changing at E19 versus 1 day and 10 day versus adult.

A.

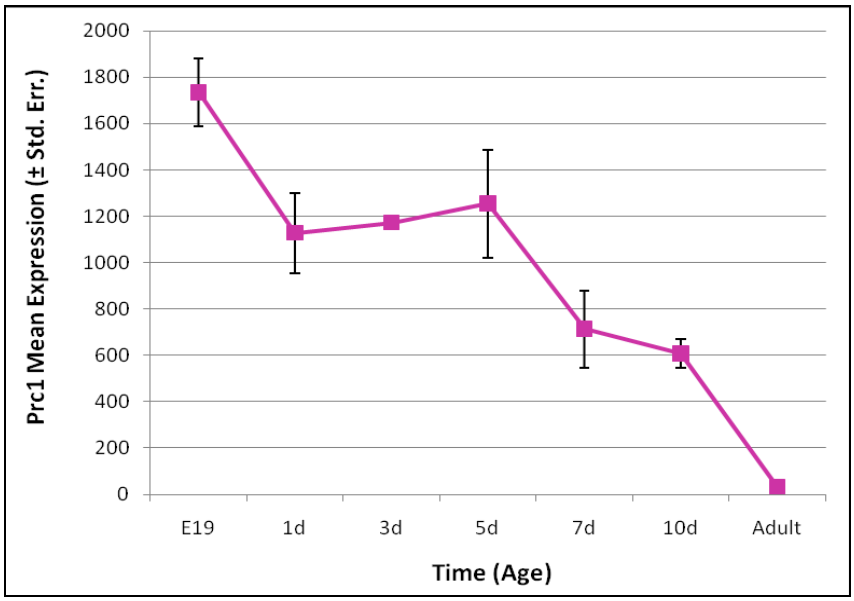

B.

Contrast	Mouse microRNA	p-value	Fold-Change
E19 vs. 1 day	mmu-miR-25	0.019	1.06
	mmu-miR-92a	0.0043	1.15
10 day vs. Adult	mmu-miR-19a	0.0001	9.30
	mmu-miR-19b	0.0001	5.63
	mmu-miR-25	0.00074	-1.11
	mmu-miR-363	0.028	4.25
	mmu-miR-367	0.000025	3.08
	mmu-miR-466l	0.01	1.36
	mmu-miR-92a	0.001	-1.20

To better understand heart maturation, cardiac proteins were isolated, immunoblotted and probed for cell cycle checkpoints throughout the transitional period. This allowed us to determine at what stage the majority of cardiomyocytes are within cell cycle at E19, 1d, 3d, 4d, 5d, 6d, 7d, 10d, and adulthood. In addition, Prc1 expression was overlaid with cell cycle markers to assess if Prc1 expression changes with cell cycle withdrawal. **Figure 15** depicts expression patterns of cardiac protein during hyperplastic- to hypertrophic-based growth. First off, HL-1, as well as adult mouse brain and skeletal muscle were used as positive or negative controls. Undifferentiated HL-1 had endogenous expression of RB, pRB(Ser780), CDC2, and pCDC2(Tyr15), detected at 5μg. RB, pRB(Ser780), CDC2, and Cyclin B1 were detected in adult mouse brain. Furthermore, adult mouse skeletal muscle showed expression of CDC2, pCDC2(Tyr15) and Cyclin B1. As the loading control, MHC proved to be equally expressed at E19 and 1day then increases and stabilizes from 3d to adult. RB, pRB(Ser780) and CDC2 had similar patterns within the heart whereby a strong signal at E19 eventually decreases through the perinatal program and becomes absent at adult, however with a burst in expression at 5d. Phosphorylated CDC2(Tyr15) illustrated a bell curve distribution with the peak at 5d and the extremities at E19 and adult. Conversely, Cyclin B1 expression oscillated with the highest expression at E19, 1d and 10d and near depletion at adult.

Overall, cardiac cells seemed to exit cell cycle and enter senescence. PRC1 increased and stabilized in expression from E19 to adult; therefore PRC1 did not seem to be dependent upon cell cycle progression and withdrawal.

In order to determine if Prc1 acts through interactors within the perinatal cardiogenomic program, GeneMANIA was utilized. GeneMANIA is a bioinformatic tool that employs a large set of functional association data (genetic interactions, pathways, co-expression, co-localization and protein domain similarity) to link genes of interest to a set of genes in the database (Warde-Farley et al., 2010). **Figure 16A** depicts the *in silico* interactors to Prc1, through co-expression, co-localization, or predicted interaction. **Panel B** summarizes the expression profiles of each putative interactor as determined by the exon microarray data. Fascinatingly, all the genes (Bub1, Ccna2, Racgap1, Cdc2a, Dlgap5, Ccnb2, Birc5, and Trim2) which are predicted to interact with Prc1 follow the same pattern as Prc1 with the exception of Trim37 and 1110008P14Rik which in fact are not significantly changing throughout perinatal cardiac development.

Figure 15: Perinatal Heart Maturation Involves Cell Cycle Withdrawal. Immunoblotting analysis for changes in cell cycle markers and Prc1 in perinatal cardiac development (N≥3). Wild-type mouse hearts aged at E19, 1d, 3d, 4d, 5d, 6d, 7d, 10d and adult were probed with markers for cell cycle checkpoints (RB, pRB(Ser780), CDC2, pCDC2(Tyr15), Cyclin B1) and PRC1. Five micrograms were loaded for PRC1, RB, pRB(Ser780) and Cyclin B1. Ten micrograms were loaded for CDC2 and pCDC2(Tyr15). Undifferentiated HL-1 as well as wild-type adult mouse brain and skeletal muscle protein samples were used as positive and/or negative controls at 5μg each. After transferring, gels were stained with Coomassie-Blue to visualize MHC as loading control (image represents a 10μg loaded gel).

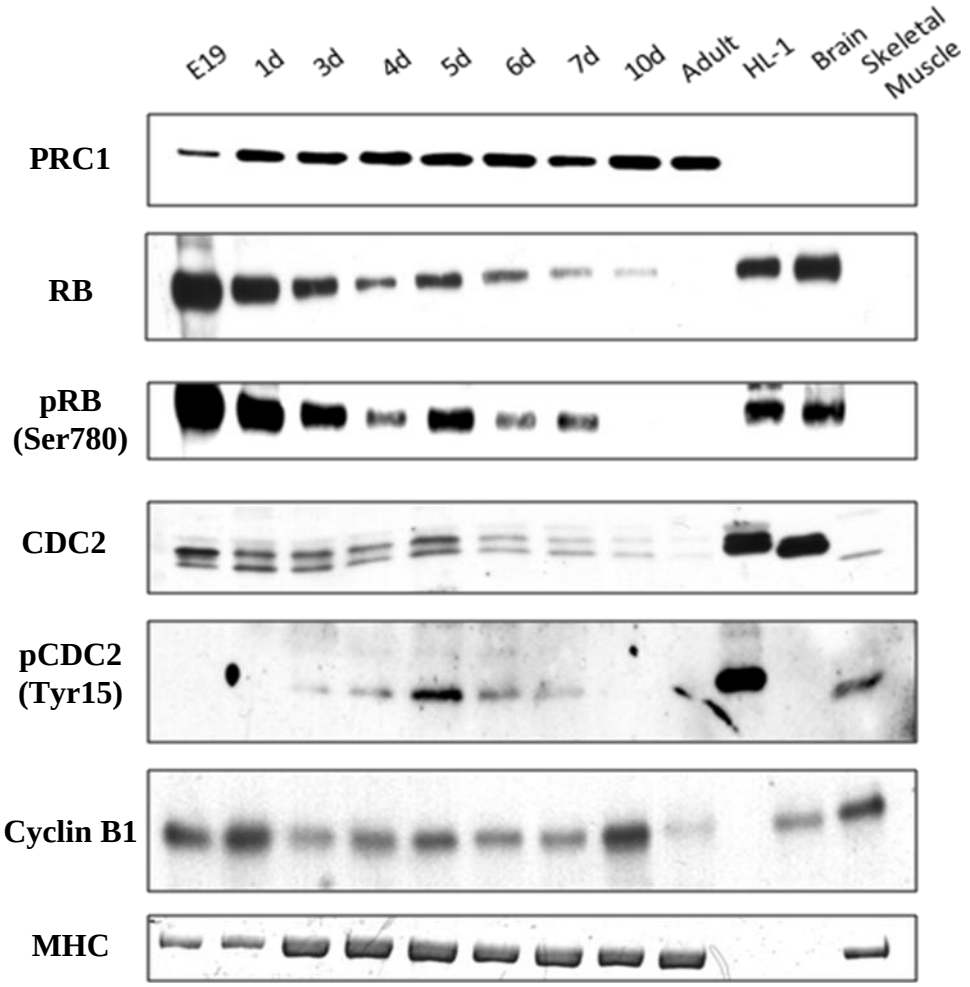
E19
1d
3d
4d
5d
6d
7d
10d
Adult
HL-1
Brain
Skeletal Muscle
PRC1
RB
pRB (Ser780)
CDC2
pCDC2 (Tyr15)
Cyclin B1
MHC

Figure 16: Genes Interacting *In Silico* with Prc1 Have the Same Expression Profile as Prc1. Genes putatively interacting with Prc1, as determined by GeneMANIA, follow the same normalized (RMA) mean expression pattern as Prc1 as found on the exon microarray. **A)** Gene interaction map generated by GeneMANIA demonstrating the different interactions linked to Prc1. The interactions entail: co-expression (Bub1, Ccna2, Racgap1, Cdc2a, Dlgap5, Ccnb2, Birc5); co-localization (Bub1, Ccna2, Cdc2a, Dlgap5, Ccnb2); and predicted interaction (Trim37, Racgap1, Dlgap5, Ccnb2, Trim2, 1110008P14Rik) (see **Appendix – Suppl. Figure 4** for extensive reference list). **B)** Normalized (RMA) mean expression signal, with corresponding standard error bars (±Std. Err.), of all genes found to interact with Prc1 as determined by GeneMANIA. Exon microarray data resulted from E19, 1d, 3d, 5d, 7d, 10d and adult wild-type mouse heart transcripts.

A.

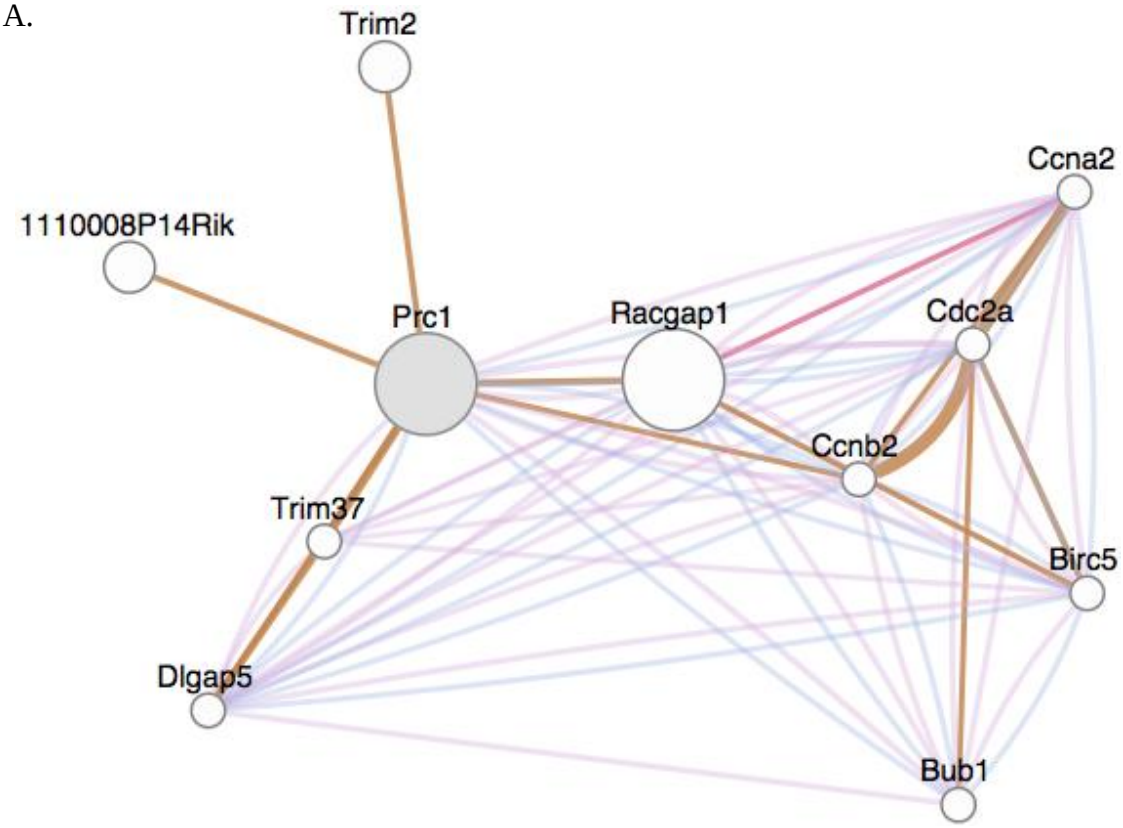
Trim2
Ccna2
1110008P14Rik
Prc1
Racgap1
Cdc2a
Ccnb2
Trim37
Birc5
Dlgap5
Bub1

B.

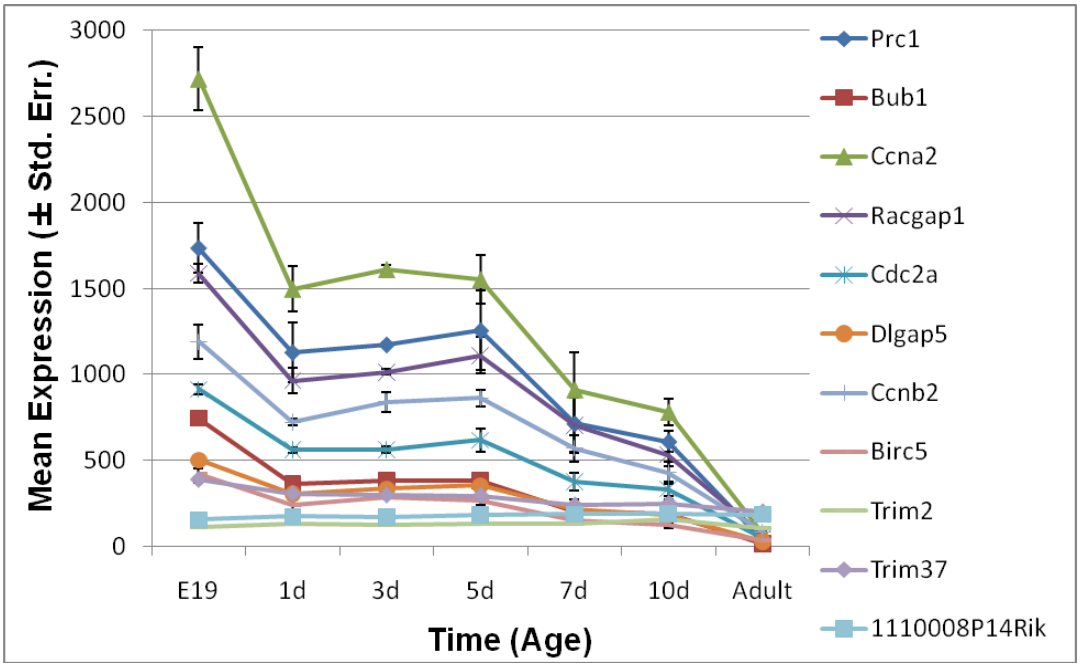
Mean Expression (± Std. Err.)
3000
2500
2000
1500
1000
500
0
E19
1d
3d
5d
7d
10d
Adult
Time (Age)
Prc1
Bub1
Ccna2
Racgap1
Cdc2a
Dlgap5
Ccnb2
Birc5
Trim2
Trim37
1110008P14Rik

DISCUSSION

Very little research has been conducted on the perinatal period of heart development in which the heart transitions from the fetal heart gene program to the adult heart gene program. It has been established that cardiomyocyte proliferation is high during fetal development and cardiomyocytes have a decreased proliferative capacity after birth. Furthermore, cells undergo a final round of DNA synthesis and karyokinesis in the absence of cytokinesis, causing binucleation (Li et al. I and II, 1997). This perinatal cardiac program summarizes a hyperplastic growth phase and a subsequent hypertrophic development, that spans between embryonic day 19 and day 10 (Soonpaa et al., 1997). The transitional period in the mouse occurs within this perinatal period.

Cardiogenesis is principally studied at the embryonic, fetal, and adult stages of development. The importance of the transitional program between the prenatal and adult stages remains largely unconsidered. Microarrays allowed us to assess the physiological manifestations through molecular changes and lead us to determine potential factors in the cardiac perinatal transitional program. We chose to study the whole heart in order to determine the transcriptional profiles in their organic environment. Previous reports have indicated the importance of studying genetic expression patterns in heart development given their highly dynamic nature (Chen et al., 2004; Sehl et al., 2000). Chen et al. claim to be the first to introduce the perinatal cardiogenomic expression profiles utilizing murine cDNA microarrays (6144 mouse EST); however they solely focused on hearts aged at day 0, 7, 14 and adulthood. Our study further identifies the perinatal cardiogenomic expression profile through embryonic day 19, postnatal day 1, 3, 5, 7, and 10, as well as adulthood, at both the transcriptional and microRNA level. Microarray profiling experiments were performed to

clarify the molecular relationship between microRNAs and mRNAs and to define the switch from a prenatal to an adult heart.

In order to gain confidence in our microarray results, validation experiments were accomplished. First, we elucidated Ppia as a previously unidentified reference gene for the cardiac perinatal transitional program as Gapdh and Pgk2 expression varied considerably (**Figure 9**). Moreover, Ppia is highly but consistently expressed within neonatal heart development. Afterwards, ten genes (Rxrγ, Pln, Mad2l1, Epas1, Asb15, Cdk4, Hif3α, Fbxw7, Pfkm, and Prc1) were quantified by RT-PCR and/or Real-Time PCR. At an FDR of 20%, expression profiles mimicked the microarray data (**Figure 10**).

Initial analysis of transcripts was accomplished by profiling of the Affymetrix GeneChip Mouse Exon 1.0 ST Array data (**Figure 4**). Volcano plots demonstrate differential gene patterning whereby the variability in gene expression subsides between 1d and 3d as well as between 5d and 7d. This suggests that a 1 and a 5 day heart is relatively similar to a 3 and 7 day heart, respectively. This correlates with an unchanging heart mass between 1d and 3d as well as 5d and 7d, as seen in **Figure 1E**.

Genes are more differentially expressed at E19 than for neonates, as previously described by Sehl et al. (Sehl et al., 2000). In particular, E19 has more genes downregulated than 1d, which may be the genetic pattern required prior to birth. A 7d and a 10d heart also proved to be different with a large number of genes up- and downregulated. Finally the largest difference is seen between a 10d and an adult heart, which is not surprising since a 10 day heart is still developing while an adult heart has reached maturity.

Analyzing the microRNA microarray data illustrates similar trends whereby expression profiles show asymmetric murine microRNA expression over time (**Figure 5**). As with transcript expression, microRNA variability is reduced when comparing 5d to 7d, while microRNAs are highly dynamic between a 10d and an adult heart. On the contrary, E19 versus 1d, 1d versus 3d, 3d versus 5d, and 7d versus 10d have more microRNAs significantly upregulated than downregulated ($p \leq 0.05$). Given that one of the main functions of microRNA is to downregulate their target genes, an increase in microRNA expression may be leading to a corresponding decrease in target gene expression, as depicted in **Figure 4**. Conversely, enhanced microRNA expression may result in the upregulation of previously suppressed genes, either by decreasing the expression of inhibitory protein and/or transcription factors or indirectly inhibiting the expression levels of inhibitory microRNAs (Divakaran & Mann, 2008). **Table 4** summarizes the microRNAs with the highest significant fold-changes ($p \leq 0.05$) and those previously shown to play a role in heart development and disease; these microRNAs may possess formerly unidentified roles in the cardiac perinatal transition.

Note that during the perinatal program, the genetic fluctuations parallel with anatomical and physiological changes such as an increase in heart rate (Wu & Wu, 2009), stroke volume and cardiac output (Hopkins et al., 1973) as well as changing ejection fraction (EF) (Dowell, 1984). The genetic expression profiles may be required for a functional heart. Additional investigations are required to explain the role of microRNAs in mRNA patterning.

To determine which factors may be involved in the perinatal transition, we focused on the genes and microRNAs that are significantly differentially expressed instead of those with consistent expression. The number of changing transcripts and microRNAs were plotted to visualize possible trends (**Figure 6A**). In fact, the temporal expression pattern of mRNAs and microRNAs uncovered an inflection point between 5 and 7 days post-birth representing a previously undescribed perinatal cardiogenomic switch. This switch demonstrates that mRNA expression changes slightly prior to 5 and 7 days, at which point a large number of genes are dramatically fluctuating into adulthood. On the other hand, microRNA expression shows a temporary reduction between 5 and 10 days but then displays a burst in expression after 10 days. Knowing that microRNAs cause gene silencing, the observed increase in mRNA expression at 7 to 10 days may be the product of decreased inhibitory microRNA expression. In addition, the general downregulation of microRNAs during the switch may be allowing for the establishment of the adult program. Additional investigation in microRNA target regulation is required to draw a definite conclusion.

We next sought out to identify transcription factor trends within cardiac development (**Figure 6B**). As described by McKinsey and Olson, cardiac development entails signaling pathways regulated by transcription factors (TFs) binding to DNA in promoter regions of cardiac growth and remodeling genes through an activating or repressive capacity (McKinsey & Olson, 2005). The gene expression profiling experiment revealed that 42% of known mouse transcription factors are significantly variable between embryonic day 19 and 10 days post-birth ($p \leq 0.05$), suggesting a highly dynamic cardiogenomic transitional program. This includes the following heart-related TFs changing on the arrays: Gata4,

Gata6, Nkx2-3, Nkx2-4, Nkx2-5, Tbx4, Tbx5, Tbx6, Tbx18, Tbx20, Hey2, Irx3, Rxrγ, Hif3α and Evx1. Out of the 258 TFs significantly changing on the exon array, 107 fluctuate in expression at least during two timepoints in the study. Interestingly transcription factor profiling behaves differently than global gene expression patterning, resulting in an M and W pattern, respectively ($p \leq 0.05$). Therefore, we propose that in order to switch from the fetal to the adult cardiogenomic program, certain stages of development require more TFs to be downregulated while others require an increase in TF expression. The aforementioned cardiogenomic switch period (between 5 and 7 days) appears to have the highest genetic variability whereby out of the 1226 genes significantly changing, there is nearly three times more TFs down- than upregulated. However, as observed in the volcano plots, the least number of transcriptional factors (mRNAs and miRNAs) are significantly changing is at 5d versus 7d. This suggests that the transcriptional machinery may be subsiding prior to the burst in transcriptional activity. On the contrary, this may simply be a result of a smaller cohort of genes that distinguishes a 5d from a 7d heart. The dramatic increase in TFs expression at 7 day may be the precursor to the increase in gene expression that follows at 10 days. Consequently, particular profiles have been determined as possible genetic mechanisms that lead to the formation of a functional heart during development.

Subsequently, by filtering the gene lists, we were able to define pathways involved in the perinatal cardiogenomic program. **Figures 7** and **8** demonstrate the gene ontologies differentially expressed, illustrated as Forest Plots and Pie Charts. The Forest Plots (**Figure 7**) highlight the genes up- and downregulated while the Pie Charts summarize total Biological Processes (BP) (**Figure 8**), at each contrasting point. When studying GO profiles,

it is important to assess the level at which the results will be studied, either through overall genetic processes or by discriminating between genes up- and downregulated throughout processes, because different results may emerge. The BP that are recurrent at each contrasting point include: Cellular Process, Metabolic Process, and Biological Adhesion; while other processes of interest are Developmental Process, Biological Regulation, and Multicellular Organismal Process.

Biological Adhesion and Developmental Process are systems that are significantly changing however this may be a result of cardiac remodeling. Moreover, Biological Adhesion solely encompasses *cell adhesion*. Since Biological Adhesion, Developmental Process and Biological Regulation did not reveal any leading or promising pathways, we focussed on Cellular Process, Metabolic Process and Multicellular Organismal Process (MOP).

Certain networks were anticipated to be influenced during the cardiac perinatal program. First, we would have expected to see changes in thyroid hormone receptors, however no change was observed in accordance with the Sehl et al. study in rats (Sehl et al., 2000). Metabolic and Cellular processes did prove to be required for perinatal heart development.

Analyzing the Metabolic Process, we notice that each contrasting age shows strong representation of the BP. The Metabolic Processes significantly changing during the transitional program reconfirm the well-established shift from a glycolytic to a fatty acid metabolism, making these profiles indispensible for proper maturation of the heart (Taegtmeyer et al., 2010). The metabolic switch is most evident with a downregulation of

genes at E19, where the Metabolic Process encompasses the functional groups: *lipid metabolic process, oxidation reduction, and lipid catabolic process*. Metabolic Process remains significantly overrepresented throughout the contrasts, in particular at 7d versus 10d where it represents nearly 50% of the BP. Interestingly the genes included in Metabolic Processes are significantly and predominantly up at 1d versus 3d, down at 3d versus 5d, up at 5d versus 7d, then down at 7d versus 10d but equally expressed at E19 versus 1d and 10d versus adult. Therefore, this expression profile of up- and downregulated genes within Metabolic Processes may be a result of normal heart development.

Next, Cellular Processes play a fundamental role in cardiac development knowing that cardiomyocytes are rapidly proliferating near birth and eventually pass through a last round of cell cycle during early hypertrophy (Soonpaa et al., 1996). Similar to Metabolic Process, Cellular Process has specific patterns. Genes within Cellular Process are solely significantly up at 1d versus 3d and 5d versus 7d, but down at 7d versus 10d, then return up at 10d versus adult, whereas E19 versus 1d and 3d versus 5d have genes both significantly up- and downregulated. Cellular Process particularly influences the contrasts 5d versus 7d and 10d versus adult. When comparing 5d to 7d, Cellular Process is composed of functional groups with very strong enrichment scores (ES). Thus the genes that are upregulated at 5d within this process may suggest that 5 days post-birth is a pivotal point in cardiomyocyte cell cycle activity. Genes upregulated at 10d include those involved in *cell proliferation*, *chromosome segregation*, and *actin-filament-based process*, which are events that may summarize cardiomyocyte binucleation. The increase in Cellular Process activity at 10d as compared to adult may substantiate the fact that cell cycle remains active at 10d while it is inexistent or limited at adulthood (Brooks et al., 1997; Poolman & Brooks, 1998).

Moreover, a 10d heart is finalizing multinucleation of cardiomyocytes to exit the transitional program while an adult heart loses the ability to regenerate (Li et al., I & II, 1997). And so, Cellular Processes are critical at 5 and 10 days post-birth.

The last Biological Process of interest is Multicellular Organismal Process (MOP). MOP is present at E19 versus 1d, 3d versus 5d, 7d versus 10d and 10d versus adult within the Forest Plots (**Figure 7**), but only found at E19 versus 1d and 3d versus 5d in the Pie Charts (**Figure 8**). MOP can be further stratified into *System Process* → *Neurological System Process* → *Cognition* → *Sensory Perception*. The MOP GO root revealed that olfactory receptor genes are a large representation of this BP. That is, ten out of the eighteen genes that make up *Sensory Perception* are olfactory receptors and the rest are channel-related. This represents ectopic expression of olfactory receptor genes within the heart, a non-olfactory tissue. Over 900 olfactory receptor genes (OR) are found in the human and nearly 1500 in mice (Niimura & Nei, 2003). Olfactory receptor genes have been previously shown to have nonconventional expression within the heart. Similar to our results, OR genes were detected in postnatal cardiogenesis (Drutel et al., 1995) but were absent in adult heart (Feingold et al., 1999). Therefore, OR genes may hold an alternative function, especially in heart development, but further experiments are required.

In search of a factor(s) with a potential role in cardiomyocyte binucleation, we identified Prc1 as a gene highly and differentially expressed at pivotal ages in the perinatal cardiac transitional program (E19 versus 1d, 5d versus 7d, 10d versus adult). In particular, Prc1 displays one of the highest fold-changes at 10d as compared to adult. **Figure 11**

summarizes the microarray-generated expression profile of Prc1 with the corresponding fold-changes and p-values for each contrast.

Protein Regulator of Cytokinesis (Prc1) was first described in 1998 by Jiang et al. PRC1 amino acid sequence has strong conservation (at 40%) with yeast anaphase spindle elongation factor, Ase1p (Jiang et al., 1998). Ase1p is known to mediate spindle assembly, elongation and disassembly in mitosis (Juang et al., 1997; Pellman et al., 1995). Similar to Ase1p, PRC1 protein is highly expressed during S and G_2/M but depleted after mitosis and during G_1 (Jiang et al., 1998). PRC1 sequence is highly conserved among eukaryotic species at residues 273 to 486, which is illustrated to be necessary for microtubule binding and bundling activity (Mollinari et al., 2002). The human Prc1 transcript encodes a protein of 620 amino acids (aa) at 71kDa, whereas mouse Prc1 produces a protein of 603aa at 70kDa (Jain et al., 2009; Jiang et al., 1998; The UniProt Consortium, 2010). The PRC1 protein constituents were assessed through consensus and mutagenesis analysis (Jiang et al., 1998; Mollinari et al., 2002). Human PRC1 is comprised of: β-sheets and turns in the carboxy-terminus; two CDK consensus phosphorylation sites at Thr470 and Thr481 (TPSKRRGLAPNTPGKARKL), two nuclear localization signals, two destruction boxes, and one KEN box, in the center; and α-helices and coiled-coil motifs in the amino-terminus (**Figure 17A**; Mollinari et al., 2002). PRC1 protein truncation experiments revealed that the N-terminal region of PRC1 is required for its association to the cleavage furrow and the center of the midbody.

In HeLa cells, PRC1 expression is nuclear during interphase, gets localized to mitotic spindle poles during prophase, associates to the entire mitotic spindle in metaphase and early anaphase, and moves to the spindle midzone and cleavage furrow during mid- and

late-anaphase. During cytokinesis, PRC1 is localized at the midbody of post-mitotic bridges and remains visible after cytokinesis (**Figure 17B**; Jiang et al., 1998).

PRC1 is phosphorylated at Thr470 and Thr481 by Cdc2 in early mitosis (Jiang et al., 1998; Mollinari et al., 2002; Zhu & Jiang et al., 2005). PRC1 is a non-motor microtubule binding protein therefore it binds to kinesin, KIF4, to be shuttled to the midline of the central spindle which is regulated through the dephosphorylation of Thr481 by phosphatase Cdc14 after metaphase (Jiang et al., 1998; Zhu & Jiang, 2005). Therefore, the phosphorylated state of PRC1 at Thr481 by Cdc2 regulates PRC1 localization through KIF4. Inactivating phosphorylation at Thr470 through site-directed mutagenesis caused disorganization of the central spindle during mitosis. Moreover, phosphorylation of PRC1 at Thr470 does not affect microtubule interaction but is required for PRC1 oligomerization which in turn is essential for the initiation of central spindle organization in mitotic progression (Fu et al., 2007).

Mollinari et al. proved that PRC1 is a microtubule binding and bundling protein through up- and downregulation experiments. Overexpressing PRC1 caused extensive bundling of microtubules within the mitotic spindle in early mitosis, preventing mitotic progression. Conversely, inhibiting PRC1 expression had no effect upon mitotic progression in metaphase and through chromatid segregation in anaphase but cells had defective anaphase spindle morphology. In the absence of PRC1, cells exhibit dispersed microtubules which are absent from the two half spindles. Interestingly, some cells displayed midzone microtubules but remained disorganized, causing the chromosomes to rotate perpendicular to the spindle equator. Although cells were deficient in microtubules, furrowing was still present but regressed prior to cleavage leaving cells binucleated (Mollinari et al., 2002).

Strickingly, inhibition of PRC1 in HeLa cells prevented cellular division without affecting karyokinesis causing more than 50% of cells to be binucleated (**Figure 17C**; Jiang et al., 1998). Briefly, the cleavage furrow appeared in late anaphase but it was interrupted and created cells with two nuclei, suggesting that PRC1 is involved in cellular cleavage.

Furthermore, PRC1 expression is increased in cancers including cholangiocarcinomas, colon cancers, breast cancer, and non-small cell lung cancers and pancreatic cancers (Kikuchi et al., 2003; Lin et al., 2002; Nakamura et al., 2004; Obama et al., 2005). In accordance, knockdown of Prc1 by siRNA demonstrated decreased breast cancer colony formation (Shimo et al., 2007). This may suggest that PRC1 mediates rapid cell growth.

In summary PRC1 downregulation causes binucleation in HeLa cells while its upregulation is found in rapidly growing cells; therefore PRC1 may be highly expressed during hyperplasia to allow for cardiomyocyte proliferation but may be subsequently depleted during late perinatal development permitting cardiomyocyte binucleation and consequently hypertrophy.

Figure 17: PRC1 is a Highly Conserved Protein Essential for Cytokinesis. PRC1 analysis through site-directed mutagenesis, localization, and inhibition experiments. **A)** Human PRC1 protein sequence is composed of: β-sheets and turns (C-terminus); two Cdk phosphorylation sites (Thr470 and Thr481); two nuclear localization signals; two destruction boxes (D); one KEN box (K); α-helices and coiled-coil motifs (N-terminus). The percentage of homology (residues 240 to 440) is determined by comparision to *Homo sapiens*, *Mus musculus*, *Drosophila melanogaster*, *Nicotiana tabacum*, *Arabidopsis thaliana*, using ClustalW. [Adapted from Mollinary et al., 2002, Originally published in *J CELL BIOL*, doi:10.1083/jcb.200111052.] **B)** HeLa cells endogeneously expressing PRC1 throughout mitosis, visualized by confocal laser scanning microscopy. Unsynchronized cells were grown on glass coverslips and incubated with primary (affinity-purified rabbit polyclonal PRC1 and mouse monoclonal α-tubulin) and corresponding secondary antibodies (FITC-conjugated goat anti-rabbit and Texas Red-conjugated goat anti-mouse). PRC1 (green) along with tubulin (red) localization was studied through interphase (a), prophase/metaphase (b, c, d), anaphase (e, f), and telophase (g, h, i). Scale bar represents 10mm. **C)** PRC1 inhibition in live HeLa cells visualized through a fluorescence microscope. HeLa cells were microinjected with 3.8mg/mL affinity-purified anti-PRC1 antibody and fluorescein-dextran, cultured in the presence of Hoechst stain, then fixed and stained 20 hours post-injection with FITC-conjugated goat anti-rabbit secondary antibody (N=2). [Panels **B** and **C** adapted from *Molecular Cell*, Vol. 2, Issue 6, Jiang, W., Jimenez, G., Wells, N., Hope, T., Wahl, G., Hunter, T., and Fukunaga, R., PRC1: A human mitotic spindle-associated CDK substrate protein required for cytokinesis, Pages 877-885, 1998, with permission from Elsevier.]

A.

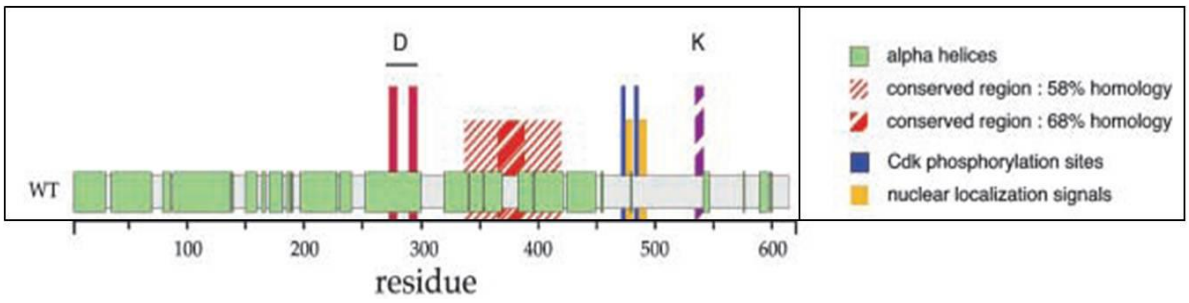
D
K
WT
100
200
300
400
500
600
residue
alpha helices
conserved region : 58% homology
conserved region : 68% homology
Cdk phosphorylation sites
nuclear localization signals

B.

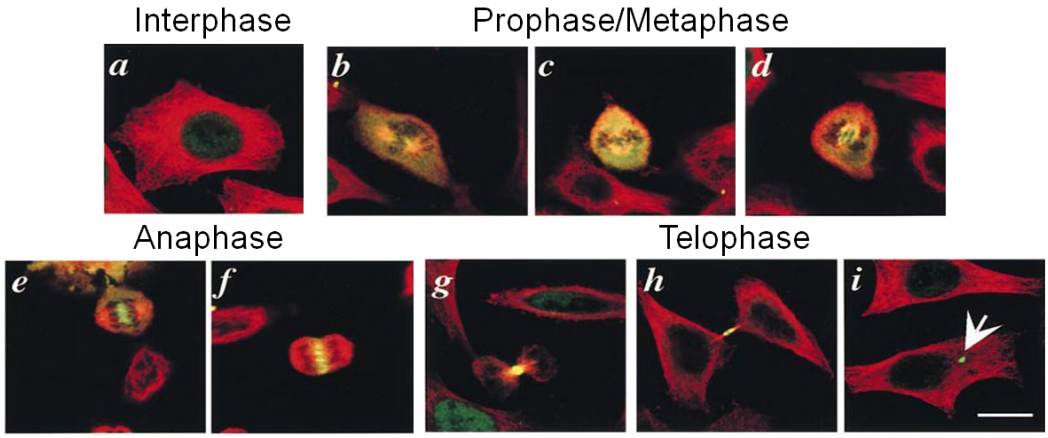
Interphase
Prophase/Metaphase
a
b
c
d
Anaphase
Telophase
e
f
g
h
i

C.

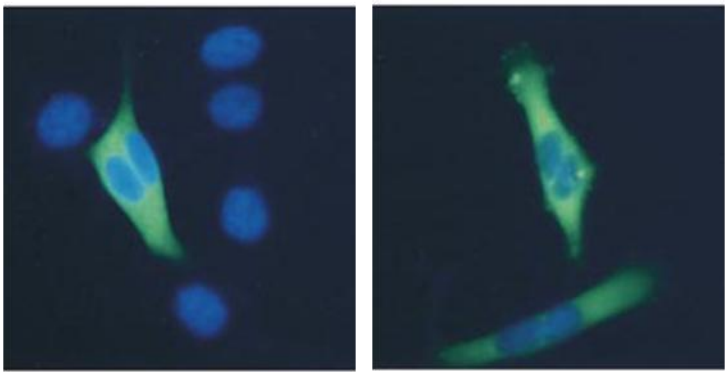

To date, Prc1 has not been examined in the heart however the analysis of GEO datasets demonstrates similar Prc1 expression patterns as compared to our study. Concurrently, Prc1 is highly expressed in embryonic development (GDS627 – 1423774 and 1423774) and decreases throughout neonatal development to eventually become virtually undetectable through adolescence and adulthood (GDS40) (**Appendix – Suppl. Figure 2**).

Knowing that inhibited PRC1 in HeLa cells causes binucleation, we investigated its expression during the perinatal cardiac transitional program whereby cardiomyocytes transition from hyperplasic to hypertrophy growth with characteristic binucleation. We were particularly intrigued because Prc1 transcript expression, according to the microarray data, is high during hyperplastic phases but then decreases when cardiomyocytes enter hypertrophy. This significant downregulation of Prc1 expression throughout neonatal development may fit with the role of cell cycle regulators. Cell cycle progression is well-defined to be modulated by cyclin-CDK complexes (Nigg, 1995); however determining the factors regulating cell cycle within the transitional program remains in its infancy.

After validating Prc1 transcript expression with RT-PCR and quantitative PCR (**Figure 10**), protein expression analysis in the heart was performed (**Figure 12**). Through peptide neutralization experiments, the Abcam rabbit monoclonal antibody appeared to be specific to endogenous cardiac PRC1. HL-1 cell lysates were loaded as a putative control knowing that they serve as a good cell model for adult cardiomyocytes, all while retaining the ability to divide (Claycomb et al., 1998). PRC1 protein is present within the heart but absent in undifferentiated HL-1 cells as well as adult mouse brain and skeletal muscle, suggesting that Prc1 may have a limited or no role in the latter samples. Prc1 expression has been previously shown to be undetected in adult mouse brain (Tarabykin et al., 2000) and

skeletal muscle (GEO Dataset, GDS1490/95032_at/Prc1/Mus musculus) but not yet established in HL-1 cells. Myosin Heavy Chain (MHC) is present in cardiac and skeletal muscle but absent in HL-1 and adult mouse brain, at 5μg.

A discrepancy exists between **Figures 11** and **12** as PRC1 protein expression increases through maturation instead of decreasing as demonstrated with transcript expression. Several reasons may explain this unexpected result. First, since this study entails temporal analysis, some results may be time-sensitive. For example, the half-life of cardiac protein in humans is between 3 to 5 days (Fuster & King, 2008), and the pattern may be the same in mice. Therefore PRC1 protein abundance may simply be a result of remnant and stable protein within the cell. Alternatively, it is important to note that in order to compensate for cardiac hypertrophy as a result of increased hemodynamic load, the efficiency of cardiac protein synthesis is markedly increased (Nagatomo et al., 1999). Hence, the unforseen abundance of PRC1 in adult may be a product of hypertrophic-induced cardiac protein synthesis which may suggest Prc1 has alternate roles within adult cardiomyocytes. Fundamentally, PRC1 is subjected to phosphorylation and dephosphorylation events in order to convey its role in cytokinesis. The immunoblotting experiment illustrates total PRC1 expression and not the cytokinetically-active form, thus we cannot conclude that highly expressed PRC1 protein signifies that an active form is acting on cytokinesis. Pulse-chase experiments and/or generation of a murine-specific antibody to phosphorylated PRC1 are vital to further understand the role of Prc1 in heart development and adaptability.

To determine the localization of Prc1 within cardiomyocytes, immunofluorescence experiments were performed; however, after several attempts, images were inconclusive due

to high autofluorescence of the heart. Conversely, immunofluorescence experiments in HeLa and HL-1 cells were successful (**Appendix – Suppl. Figure 3**).

To assess if transcript and protein abundance changes with age, the amount of total isolated cardiac mRNA and protein were plotted at each age. **Figure 13** conveys the dissimilar amounts of mRNA and protein with maturation. Interestingly, the amount of mRNA isolated returns to baseline at adulthood while the protein abundance increases drastically (**Panel A**). The difference is further distinguishable with the ratio of protein to mRNA (**Panel B**). As a result, protein expression increases with age while mRNA peaks at 10d and subsides at adulthood. This may imply that the heart reaches a steady-state in transcript expression at adulthood to maintain normal cardiac activity while protein expression increases to sustain hypertrophic cardiomyocytes.

Taking advantage of the wealth of microarray data, we searched to see if microRNAs may play a role in Prc1 expression. Our analysis revealed four microRNAs (miR-19a, miR-19b, miR-363, and miR-367) that putatively target Prc1, to be highly and significantly upregulated at 10d as compared to adult (p-value$\leq$0.05) (**Figure 14**). miR-19a and b belong to a polycistronic microRNA cluster (miR-17-5p, miR-17-3p, miR-18a, miR-19a, miR-19b, miR-20a, miR-92a) which has previously been linked to heart development (Bonauer & Dimmeler, 2009). The miRNAs may be expressed acutely at 10d and may lead to the eventual depletion of Prc1; however the role of microRNAs on Prc1 have yet to be determined.

To further understand the role of Prc1 in cardiomyocyte binucleation, we overlaid PRC1 with cell cycle checkpoint immunoblots (**Figure 15**). RB, pRB(Ser780), CDC2, pCDC2(Tyr15) and Cyclin B1 immunoblots illustrated at which point cardiomyocytes were found within cell cycle. Similarly to Kang et al. mRNA levels were not significantly variable according to the microarray data, but protein expression was inconsistent (Kang et al., 1997).

HL-1, as well as adult mouse brain and skeletal muscle protein extracts served as positive and/or negative controls. Since HL-1 cells retain the capacity to proliferate, it is anticipated to find HL-1 cells within all stages of cell cycle, with the exception of the Cyclin B1 blot, which may simply be a consequence of low detection. Adult mouse brain cells appear to be present in G_1, S, and M and absent from G_2. Adult mouse skeletal muscle was solely detected during G_2/M, which suggests that the cells are exiting cell cycle. MHC protein was used as a loading control by Coomassie Blue staining following immunoblotting analysis as previously published (Poolman & Brooks, 1998). Although the α- and β-MHC genetic isoforms were unchanged in the microarray study, it is clear that there is a discrepancy when we compare protein from E19 and 1d to the other timepoints. This result may demonstrate the switch in α- and β-MHC during heart development. The MHC isoform expression is suggested to rely on the level of mechanical performance and efficiency required by the heart (Taegtmeyer et al., 2010). Both isoforms are known to decrease in expression between day 19 and 21 post-coitus followed by a marked increase in α-MHC during postnatal development (Ng et al., 1991; Kang et al., 1997). Therefore low expression of MHC at E19 and 1d may be a product of decreased α- and β-MHC which may then give rise to increased α-MHC at 3d through adulthood.

RB and pRB(Ser780) are checkpoints for G_1/S while CDC2, pCDC2(Tyr15) and Cyclin B1 are G_2/M checkpoints. Moreover, RB is unphosphorylated during G_1 while the phosphorylated form is in S phase (Poznic, 2009). Cyclin B1 is responsible for the transition from G_2 to M (Bicknell et al., 2004). Lastly, phosphorylated CDC2 at residue tyrosine 15 maintains the cell in G_2 but once unphosphorylated the cell enters M phase (Morgan, 2007). According to **Figure 15**, cardiomyocytes exit cell cycle as the heart matures. First, RB and pRB(S780) are highly expressed at E19 until day 3, which signifies that the majority of cardiomyocytes are found within G_1/S phase. The retinoblastoma protein decreases in expression with age as previously shown (Soonpaa et al., 1996), but with a spike at day 5. Simultaneously, CDC2 expression pattern mimics that of retinoblastoma protein. Alternatively, pCDC2(Tyr15) expression profile portrays a bell curve whereby the expression peaks at 5 day. Consequently, between E19 and 4 days post-birth, the heart is majorly found in G1, S, and M phase. At 5 days post-birth, there appears to be a last push in cell cycle activity, which coincides with increased Cellular Processes (**Figures 7** and **8**). Finally, after day 5 the cellular activity subsides. On the contrary, Cyclin B1 expression varies, which may indicate a continuous transition between G_2 and M, ending at adulthood. Also, the heart may require enhanced Cyclin B1 expression in order to proceed through complete binucleation at 10d. Likewise, Chen et al. put forward the possibility that Cyclin B1 may be involved in binucleation. Bicknell et al. further proposed that the loss of Cyclin B1 and Cdc2 complex regulates hypertrophic growth.

The cell cycle checkpoint temporal profiles are confirmed with the literature. First, Cyclin B1 expression has been shown to oscillate, whereby the expression is highest at day 0, then decreases at day 7 and adulthood (Chen et al., 2004). Concurrently, CDC2 decreases

within the transitional period (Poolman & Brooks, 1998). Lastly, Kang et al. concluded that Cyclins and CDKs are highly expressed during embryonic development but then G_1/S and G_2/M Cyclins and CDKs decreased with age. Thus, depletion of CDKs and Cyclins may be responsible for cardiomyocyte cell cycle withdrawal and resulting binucleation. There were inconclusive results for RB and pRB(Ser780). Knowing that E2F initiates transcription when unbound to RB, through the phosphorylation of RB, increased abundance of phosphoRB eventually leads to increased transcription (Poznic, 2009). As a result, high expression of pRB during early transition may be involved in the coincidentally large cohort of genes at E19 (**Figure 6**).

Overall, cell cycle regulators (CDKs and Cyclins) and oncogenes (RB and pRB) are highly expressed during embryonic development but subside at different points in heart maturation. Therefore, as the heart progresses through maturation, cardiomyocytes increasingly withdraw from cell cycle and cytokinesis.

Finally, Prc1 may be exerting its role on binucleation through a network of genes. To determine putative interactors of Prc1, an algorithm was run using GeneMANIA (**Figure 16A**; Warde-Farley et al., 2010). As a result, eleven genes (Prc1, Bub1, Ccna2, Racgap1, Cdc2a, Dlgap5, Ccnb2, Birc5, Trim2, Trim37, 1110008P14Rik) were mapped into an interaction network, either through co-expression, co-localization, or as predicted interactions. The expression profiles of the eleven genes were extracted and plotted from the exon microarray data to assess if their expression reveals a pattern (**Figure 16B**). As a result, the genes predicted to interact with Prc1 are significantly changing (excluding Trim37 and 1110008P14Rik) during the transition. In particular, Bub1, Ccna2, Racgap1, Cdc2a, Dlgap5,

Ccnb2, and Birc5 follow a similar expression pattern to Prc1, with the highest fold-changes at 10d versus adult. We propose that these genes are required for a 10d heart but have a limited or absent role during adulthood. Furthermore, the seven genes have been previously shown to be involved in: spindle checkpoint function (Bub10) (Goto et al., 2011); cardiomyocyte mitosis (Ccna2) (Chaudhry et al., 2004); microtubule function in cytokinesis (Racgap1) (Jones et al., 2010); G_1/S and G_2/M phase transition (Cdc2a) (Gavet & Pines, 2010); central spindle formation (Dlgap5) (Uehara & Goshima, 2010); the control of G_2/M transition (Ccnb2) (RefSeq, 2011); and, microtubule binding through the chromosomal passenger complex (Birc5) (Ruchaud et al., 2007). These functions further support the belief that Prc1 and its factors may mediate cardiomyocyte binucleation. Ccna2 may appear to have the largest variability in expression, however once the normalized data is run through a 1-way ANOVA, Prc1 remains the gene with the highest fold-change.

In conclusion, depletion of Prc1 may mediate binucleation of cardiomyocytes through or in conjunction with Bub1, Ccna2, Racgap1, Cdc2a, Dlgap5, Ccnb2, and Birc5. Further experiments will determine the role of these factors in cardiac maturation.

CONCLUSION

A diseased or injured adult heart compensates through hypertrophy as it is incapable of regenerating muscle. To better understand the underlining effectors in cardiac disorders, the mechanisms or factors mediating the transition to a hypertrophic heart need to be elucidated. A normal murine heart transitions from a hyperplastic to a hypertrophic growth between E19 and 10 days post-birth. This transition is characterized by a switch from a prenatal to an adult gene program.

Microarray analysis proved that gene and microRNA expression are highly regulated and dynamic processes during the **cardiac perinatal transitional program**. Temporal expression patterning of mRNAs and microRNAs uncovered a point of inflection centered around 5 and 7 days post-birth, representing a previously undescribed **perinatal cardiogenomic switch**. We believe that the transitional heart program is initiated at birth and is required for the normal neonatal maturation of the fetal heart into the adult heart.

The largest cohort of transcriptional factors (mRNAs and microRNAs) is present when comparing E19 to 1d, 7d to 10d, and 10d to adult. Furthermore, total gene expression pattern differs from that of transcription factors. Approximately 40% of known mice transcription factors are significantly ($p \leq 0.05$) fluctuating between embryonic day 19 and 10 days post-birth.

Gene Ontology analysis demonstrated an interplay between Cellular and Metabolic Processes as a result of a developing heart progressing through the transition. Although 5d versus 7d displays the smallest list of genes significantly changing, the genes that form the Biological Processes have the strongest Enrichment Scores.

Validation of the microarrays by PCR quantification was successful at an FDR of 20%. Ppia proves to be a reliable reference gene when studying perinatal heart growth.

Progression of the heart through the perinatal period includes cardiomyocyte withdrawal from cell cycle. In particular, cell cycle regulator (Cyclins and CDKs) and oncogene (RB) expression decreases with perinatal cardiac development with a secondary peak at 5 days post-birth. In addition, the depletion of Prc1 and its interactors may promote cardiomyocyte binucleation.

The mechanistic switch between physiological and pathological heart development still remains unclear. This study provides a temporal analysis of factors and processes mediating different perinatal growth patterns. Understanding the perinatal period and how the fetal heart gene program is downregulated may uncover key mechanistic clues into cardiomyocyte cell cycle re-entry and myocyte regeneration.

Figure 18: Potential Model of the Processes and Factors Regulating Cardiomyocyte Maturation during the Cardiac Perinatal Transitional Program. A) Normal progression through cell cycle demonstrates increased Prc1 expression during M phase and has limited to absent expression during G1/S phase (Jiang et al., 1998). **B)** The cardiac perinatal transitional program encompasses the switch from hyperplasia and mononucleation to hypertrophy and binucleation. The transition entails Cellular and Metabolic Processes as well as dynamic genomic programs. As cardiomyocytes proceed through the cardiac perinatal transitional program (from birth unto adulthood), cell cycle activity decreases with age, with peaked expression at 5 days. Knowing the role that Prc1 plays in cytokinesis and with our perinatal cardiogenomic expression analysis, we propose that Prc1 may play a role in cardiomyocyte binucleation whereby the expression of Prc1 during the transition from a hyperplastic to a hypertrophic heart entails a depletion of Prc1 and its interactors (Bub1, Ccna2, Racgap1, Cdc2a, Dlgap5, Ccnb2, and Birc5). In addition, upregulated microRNA expression at adulthood may play an important role in hypertrophic growth. These processes are believed to mediate heart maturation through the perinatal cardiac transitional program.

A.

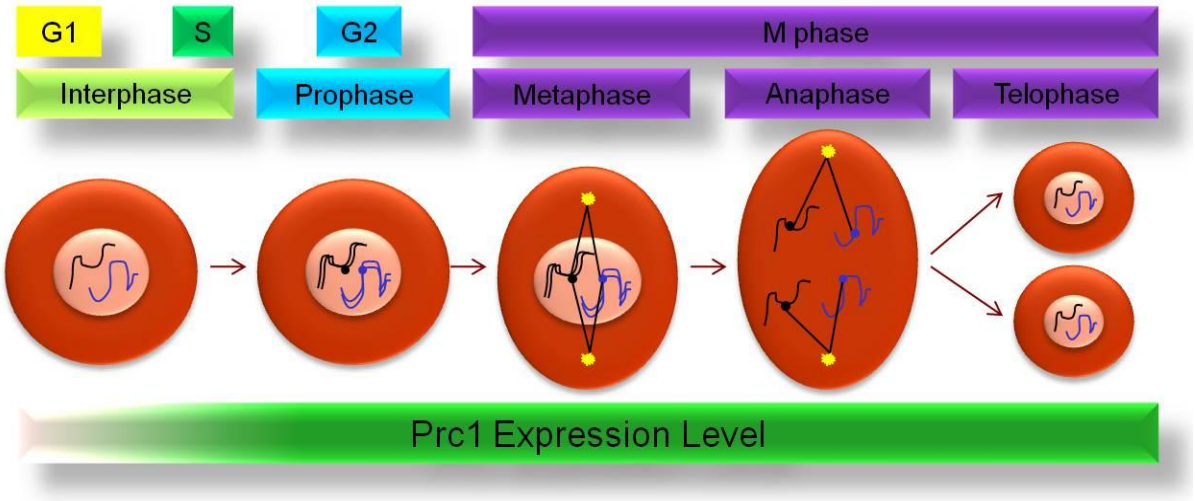
G1
S
G2
M phase
Interphase
Prophase
Metaphase
Anaphase
Telophase
Prc1 Expression Level

B.

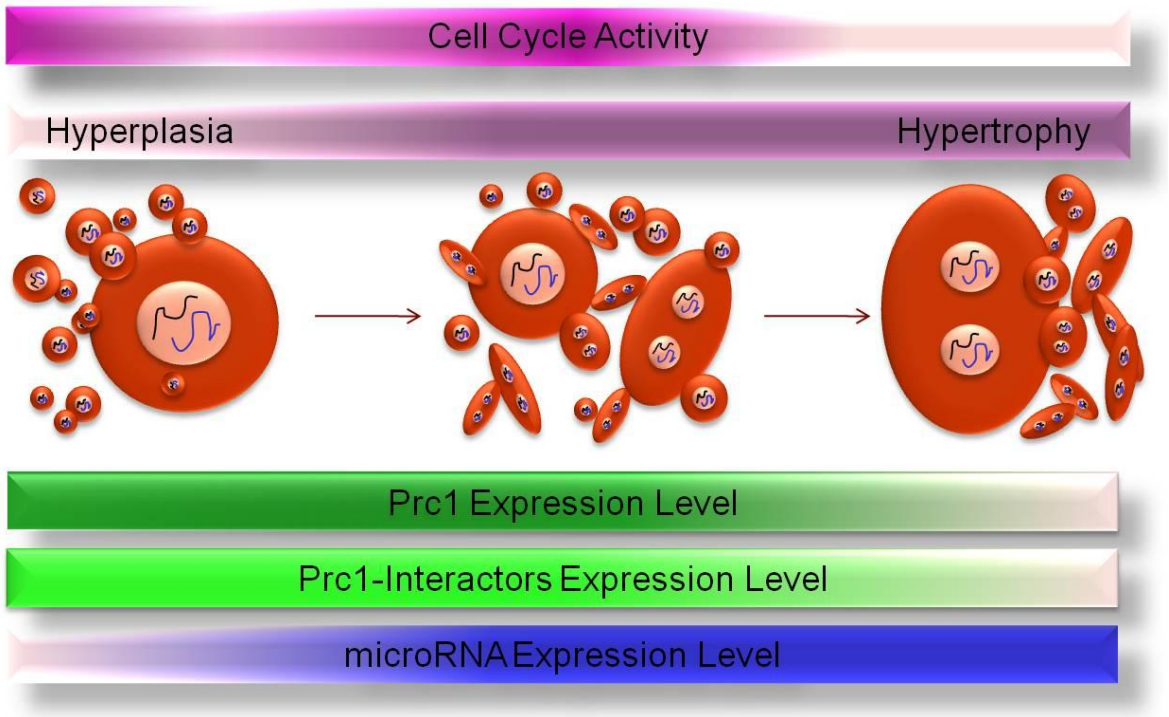
Cell Cycle Activity
Hyperplasia
Hypertrophy
Prc1 Expression Level
Prc1-Interactors Expression Level
microRNA Expression Level

REFERENCES

Ahuja, P., Sdek, P., & Maclellan, W. R. (2007). Cardiac Myocyte Cell Cycle Control in Development, Disease, and Regeneration. *Physiol Rev* , 521-544.

Ai, D., Fu, X., Wang, J., Lu, M., Chen, L., Baldini, A., et al. (2007). Canonical Wnt signaling functions in second heart field to promote right ventricular growth. *PNAS , 104*, 9319-9324.

Akazawa, H., & Komuro, I. (2003). Roles of cardiac transcription factors in cardiac hypertrophy. *Circ Res , 92*, 1079-1088.

Allawi, H., Dahlberg, J., Olson, S., Lund, E., Olson, M., Ma, W., et al. (2004). Quantitation of microRNAs using a modified Invader assay. *RNA , 10* (7), 1153-61.

Ambros, V. (2004). The function of animal microRNAs. *Nature , 431* (7006), 350-355.

Ambros, V., & Lee, R. (2004). Identification of microRNAs and other tiny noncoding RNAs by cDNA cloning. *Methods in Molecular Biology , 265*, 131-58.

Anversa, P., & Nadal-Ginard, B. (2002). Myocyte renewal and ventricular remodeling. *Nature , 415*, 240-243.

Appasani, K., Altman, S., & Ambros, V. R. (2007). *microRNAs: From Basic Science to Disease Biology*. Cambridge: Cambridge University Press.

Armstrong, M., Lee, D., & Armstrong, P. (2000). Regulation of proliferation of the fetal myocardium. *Dev. Dyn. , 219*, 226-236.

Au, K., Kou, C., Woo, A., Chim, S., Fung, K., Cheng, C., et al. (2006). Calcyclin binding protein promotes DNA synthesis and differentiation in rat neonatal cardiomyocytes. *J Cell Biochem , 98*, 555-566.

Balsam, L., Wagers, A., Christensen, J., Kofidis, T., Weissman, I., & Robbins, R. (2004). Haematopoietic stem cells adopt mature haematopoeitic fates in ischaemic myocardium. *Nature , 428*, 668-673.

Barki-Harrington, L., Perrino, C., & Rockman, H. (2004). Network integration of the adrenergic system in cardiac hypertrophy. *Cardiovasc Res , 63*, 391-402.

Bartelds, B., Knoester, H., Smid, G., Takens, J., Visser, G., Penninga, L., et al. (2000). Perinatal changes in myocardial metabolism in lambs. *Circulation , 102*, 926-931.

Baurand, A., Zelarayan, L., Betney, R., Gehrke, C., Dunger, S., Noack, C., et al. (2007). Beta-catenin downregulation is required for adaptive cardiac remodeling. *Circ Res , 100*, 1353-1362.

Bergmann, O., Bhardwaj, R., Bernard, S., Zdunek, S., Barnabé-Heider, F., Walsh, S., et al. (2009). Evidence for cardiomyocyte renewal in humans. *Science , 324* (5923), 98-102.

Bicknell, K. A., Coxon, C. H., & Brooks, G. (2004). Forced expression of the cyclin B1-CDC2 complex induces proliferation in adult rat cardiomyocytes. *Biochem. J.* , 411-416.

Bishop, S. (1990). The myocardial cell: normal growth, cardiac hypertrophy and response to injury. *Toxicologic Pathology , 18*, 438-453.

Bolli, P., & Chaudhry, W. (2010). Molecular physiology of cardiac regeneration. *Ann N Y Acad Sci , 1211*, 113-126.

Bonauer, A., & Dimmeler, S. (2009). The microRNA-17-92 cluster: still a miRacle? *Cell Cycle , 8*, 3866-3873.

Brent, G. (2000). Tissue-specific actions of thyroid hormone: insights from animal models. *Rev Endocr Metab Disord , 1*, 27-33.

Brooks, G., Poolman, R. A., & Li, J.-M. (1998). Arresting developments in the cardiac myocyte cell cycle: Role of cyclin-dependent kinase inhibitors . *Cardiovascular Research* , 301-311.

Brooks, G., Poolman, R., McGill, C., & Li, J.-M. (1997). Expression and activities of cyclins and cyclin-dependent kinases in developing rat ventricular myocytes. *J Mol Cell Cardiol , 29*, 2261-2271.

Capasso, J., Bruno, S., Cheng, W., Li, P., Rodgers, R., Darzynkiewicz, Z., et al. (1992). Ventricular loading is coupled with DNA syntesis in adult cardiac myocytes after acute and chronic myocardial infarction in rats. *Circ Res , 71*, 1379-1389.

Carmena, M., & Riparbelli, M. M. (1998). Drosophila polo kinase is required for cytokinesis. *J Cell Biol , 143*, 659-671.

Cartwright, E., Schulh, K., & Neyses, L. (2005). Calcium transport in cardiovascular health and disease - the sarcolemmal calcium pump enters the stage. *J. Mol. Cell Cardiol.* , 403-406.

Chaudhry, H., Dashoush, N., Tang, H., Zhang, L., Wang, X., Wu, E., et al. (2004). Cyclin A2 mediates cardiomyocyte mitosis in the postmitotic myocardium. *J Biol Chem , 279*, 35858-35866.

Chen, H.-W., Yu, S.-L., Chen, W.-J., Yang, P.-C., Chien, C.-T., Chou, H.-Y., et al. (2004). Dynamic changes of gene expression profiles during postnatal development of the heart in mice. *Heart , 90*, 927-934.

Chen, J., Callis, T., & Wang, D. (2009). microRNAs and Muscle Disorders. *J Cell Sci , 122*, 13-20.

Chen, J., Murchison, E., Tang, R., Callis, T., Tatsuguchi, M., Deng, Z., et al. (2008). Targeted deletion of Dicer in the heart leads to dilated cardiomyopathy and heart failure. *Proc Natl Aca Sci USA , 105* (6), 2111-6.

Chen, J., Murchison, E., Tang, R., Callis, T., Tatsuguchi, M., Deng, Z., et al. (2008). Targeted deletion of Dicer in the heart leads to dilated cardiomyopathy and heart failure. *Neuroscience , 105* (6), 2111-2116.

Chen, X., Shevtsov, S., Hsich, E., Cui, L., Haq, S., Aronovitz, M., et al. (2006). The beta-catenin/T-cell factor/lymphocyte enhancer factor signaling pathway is required for normal and stress-induced cardiac hypertrophy. *Mol Cell Biol , 26*, 4462-4473.

Chien, K. (2004). Lost in Translation. *Nature , 428*, 607-608.

Chu, C., & Rana, T. (2007). Small RNAs: Regulators and Guardians of the Genome. *Journal of Cellular Physiology , 213*, 412-419.

Chung, C., Bien, H., Sobie, E., Dasari, V., McKinnon, D., Rosati, B., et al. (2010). Hypertrophic phenotype in cardiac cell assemblies solely by structural cues and ensuing self-organization. Epub ahead of print.

Claycomb, W., Lanson, N. J., Stallworth, B., Egeland, D., Delcarpio, J., Bahinski, A., et al. (1998). HL-1 cells: A cardiac muscle cell line that contracts and retains phenotypic characteristics of the adult cardiomyocyte. *Proc. Natl. Acad. Sci.* , 2979-2984.

Clubb, F. J., & Bishop, S. (1984). Formation of binucleated myocardiac cells in the neonatal rat: An index for growth hypertrophy. *Lab. Invest.* , 571-577.

Cohen, E., Wang, Z., Lepore, J., Lu, M., Taketo, M., Epstein, D., et al. (2007). Wnt/Beta-catenin signaling promotes expansion of Isl-1-positive cardiac progenitor cells through regulation of FGF signaling. *J Clin Invest, 117*, 1794-1804.

Condorelli, G., & Dimmeler, S. (2008). MicroRNAs: components of an integrated system controlling cardiac development, physiology, and disease pathogenesis. *Cardiovasc. Res.* , 551-2.

Conlon, R., Reaume, A., & Rossant, J. (1995). Notch1 is required for the coordinate segmentation of somites. *Development , 121*, 1533-1545.

Danzi, S., & Klein, I. (2004). Thyroid hormone and the cardiovascular system. *Minerva Endocrinol , 29*, 139-150.

D'Avino, P., Savoian, M., & Glover, D. (2005). Cleavage furrow formation and ingression during animal cytokinesis: a microtubule legacy. *J Cell Sci , 118*, 1549-1558.

DeBry, R., & Seldin, M. (1996). Human/mouse homology relationships. *Genomics , 33*, 337-351.

Divakaran, V., & Mann, D. (2008). The Emerging Role of MicroRNAs in Cardiac Remodeling and Heart Failure. *Circ Res , 103*, 1072-1083.

Donovan, J., Kordylewska, A., Jan, Y., & Utset, M. (2002). Tetralogy of fallot and other congenital heart defects in Hey2 mutant mice. *Curr Biol , 12*, 1605-1610.

Dowell, R. (1984). Metabolic and contractile function enhancement during rat heart postnatal development. *Mech Ageing Dev , 25*, 307-321.

Drechsel, D., Hyman, A., Hall, A., & Glotzer, M. (1997). A requirement for Rho and Cdc42 during cytokinesis in Xenopus embryos. *Curr Biol , 7*, 12-23.

Drutel, G., Arrang, J., Diaz, J., Wisnewsky, C., Schwartz, K., & Schwartz, J. (1995). Cloning of OL1, a putative olfactory receptor and its expression in the developing rat heart. *Receptors and Channels , 3*, 33-40.

Duarte, A., Hirashima, M., Benedito, R., Trindade, A., Diniz, P., & Bekman, E. (2004). Dosage-sensitive requirement for mouse Dll4 in artery development. *Genes Dev , 18*, 2474-2478.

Eppig, J., & Nadeau, J. (1995). Comparative maps: The mammalin jigsaw puzzle. *Curr. Opin. Genet. Dev. , 5*, 709-716.

Feingold, E., Penny, L., Nienhuis, A., & Forget, B. (1999). An olfactory receptor gene is located in the extended human beta-globin gene cluster and is expressed in erythroid cells. *Genomics , 61*, 15-23.

Field, L. (2004). Modulation of the cardiomyocyte cell cycle in genetically altered animals. *Ann NY Acad Sci , 1015*, 160-170.

Fischer, A., Schumacher, N., Maier, M., Sendtner, M., & Gessler, M. (2004). The Notch target genes Hey1 and Hey2 are required for embryonic vascular development. *Genes Dev , 18*, 901-911.

Fischer, A., Steidl, C., Wagner, T., Lang, E., Jakob, P., & Friedl, P. (2007). Combined loss of Hey1 and HeyL causes congenital heart defects because of impaired epithelial to mesenchymal transition. *Circ Res , 100*, 856-863.

Forssmann, W., Nokihara, K., Gagelmann, M., Hock, D., Feller, S., Schulz-Knappe, P., et al. (1989). The heart is the center of a new endocrine, paracrine, and neuroendocrine system. *Arch. Histol. Cytol. , 52*, 293-315.

Francis, G., & McDonald, K. (1992). Left ventricular hypertrophy: An initial response to myocardial injury. *The American Journal of Cardiology , 69* (18), 3-9.

Fu, C., Yan, F., Wu, F., Wu, Q., Whittaker, J., Hu, H., et al. (2007). Mitotic phosphorylation of PRC1 at Thr470 is required for PRC1 oligomerization and proper central spindle organization. *Cell Res , 17*, 449-457.

Fuster, V., & King, S. B. (2008). *Hurst's The Heart* (12th ed. ed.). New York: McGraw-Hill Medical.

Gavet, O., & Pines, J. (2010). Progressive activation of CyclinB1-Cdk1 coordinates entry to mitosis. *Dev Cell , 18*, 533-543.

Gessler, M., Knobeloch, K., Helisch, A., Amann, K., Schumacher, N., & Rohde, E. (2002). Mouse gridlock: no aortic coarctation of deficiency, but fatal cardiac defects in Hey2-/- mice. *Curr Biol , 12*, 1601-1604.

Glotzer, M. (2005). The molecular requirements for cytokinesis. *Science , 307*, 1735-1739.

Gonzalez, S., Pisano, D., & Serrano, M. (2008). Mechanistic principles of chromating remodeling guided by siRNAs and miRNAs. *Cell Cycle , 7* (16), 2601-8.

Goto, G., Mishra, A., Abdulle, R., Slaughter, C., & Kitagawa, K. (2011). Bub1-mediated adaption of the spindle checkpoint. *PLoS Genet , 7*, e1001282.

Gould, K., Taffet, G., Michael, L., Christie, R., Konkol, D., Pocius, J., et al. (2001). Heart failure and greater infarct expansion in middle-aged mice: a relevant model for postinfarction failure. *Am J Physiol Heart Circ Physiol , 282*, H615-21.

Grego-Bessa, J., Luna-Zurita, L., Del, M., Bolos, V., Melgar, P., & Arandilla, A. (2007). Notch signaling is essential for ventricular chamber development. *Dev Cell , 12*, 415-429.

Griffiths-Jones, S., Saini, H., van Dongen, S., & Enright, A. (2008). miRBase: tools for microRNA genomics. *NAR , 36*, D154-D158.

Grigoryan, T., Wend, P., Klaus, A., & Birchmeier, W. (2008). Deciphering the function of canonical Wnt signals in development and disease: conditional loss- and gain-of-function mutations of beta-catenin in mice. *Genes Dev.* , 2304-41.

Gu, J., Anand, V., Shek, E., Moore, M., Brady, A., Kelly, W., et al. (1998). Sodium induces hypertrophy of cultured myocardial myoblasts and vascular smooth muscle cells. *Hypertension , 31*, 1083-1087.

Hopkins, S. J., McCutcheon, E., & Wekstein, D. (1973). Postnatal changes in rat ventricular function. *Circ Res, 32*, 685-691.

Huang, J., Lu, M., cheng, Y. L.-J., Zhu, X., Stout, A., Chen, M., et al. (2009). Myocardin is required for cardiomyocyte survival and maintenance of heart function. *PNAS , 106*, 18734-18739.

Hunter, T., & Pines, J. (1991). Cyclins and Cancer. *Cell , 66*, 1071-1074.

Hunter, T., & Pines, J. (1994). Cyclins and Cancer II Cyclin D and cdk inhibitors come of age. *Cell , 79*, 573-582.

Jain, E., Bairoch, A., Duvaud, S., Phan, I., Redaschi, N., Suzek, B., et al. (2009). Infrastructure for the life sciences: design and implementation of the UniProt website. *BMC Bioinformatics , 10*, 136-155.

Jiang, W., Jimenez, G., Wells, N., Hope, T., Wahl, G., Hunter, T., et al. (1998). PRC1: A human mitotic spindle-associated CDK substrate protein required for cytokinesis. *Molecular Cell , 2*, 877-895.

Jiang, Z., Zacksenhaus, E., Gallie, B., & Phillips, R. (1997). The retinoblastoma gene family is differentially expressed during embryogenesis. *Oncogene , 14*, 1789-1797.

Jones, W., Chao, A., Zavortink, M., Saint, R., & Bejsovec, A. (2010). Cytokinesis proteins Tum and Pav have a nuclear role in Wnt regulation. *J Cell Sci , 123*, 2179-2189.

Juang, Y., Huang, J., Peters, J., McLaughlin, M., Tai, C., & Pellman, D. (1997). APC-mediated proteolysis of Ase1 and the morphogenesis of the mitotic spindle. *Science , 275*, 1311-1314.

Kahaly, G., & Dillmann, W. (2005). Thyroid hormone action in the heart. *Endocr Rev , 226*, 704-728.

Kajstura, J., Pertoldi, B., Leri, A., Beltrami, C., Deptala, A., Darzynkiewicz, Z., et al. (2000). Telomere shortening is an in vivo marker of myocyte replication and aging. *Am J Pathol , 156*, 813-819.

Kanamori, M., Konno, H., Osato, N., Kawai, J., Havashizaki, Y., & Suzuki, H. (2004). A genome-wide and nonredundant mouse transcription factor database. *Biochem Biophys Res Commun , 322*, 787-793.

Kang, M. J., & Koh, G. Y. (1997). Differential and Dramatic Changes of Cyclin-Dependent Kinase Activities in Cardiomyocytes During the Neonatal Period. *J Mol Cell Cardiol* , 1767-1777.

Kang, M., Kim, J., Chae, S., Koh, K., & Koh, G. (1997). Cyclins and cyclin dependent kinases during cardiac development. *Mol Cells , 7*, 360-366.

Kikuchi, T., Daigo, Y., Katagiri, T., Tsunoda, T., Okada, K., Kakiuchi, S., et al. (2003). Expression profiles of non-small cell lung cancers on cDNA microarrays: identification of genes for prediction of lymph-node metastasis and sensitivity to anti-cancer drugs. *Oncogene , 22*, 2192-2205.

Kim, K., Soopaa, M., Daud, A., Koh, G., JS, K., & Field, L. (1994). Tumor suppressor gene expression during normal and pathologic myocardial growth. *J Biol Chem , 269*, 22607-22613.

Kioussi, C., Briata, P., Baek, S., Rose, D., Hamblet, N., Herman, T., et al. (2002). Identification of a Wnt/Dv1/beta-Catenin-Pitx2 pathway mediating cell-type-specific proliferation during development. *Cell , 111*, 673-685.

Klaus, A., Saga, Y., Taketo, M., Tzahor, E., & Birchmeier, W. (2007). Distinct roles of Wnt/beta-catenin and Bmp signlaing during early cardiogenesis. *PNAS , 104*, 18531-18536.

Krebs, L., Iwai, N., Nonaka, S., Welsh, I., Lan, Y., & Jiang, R. (2003). Notch signaling regulates left-right asymmetry determination by inducing Nodal expression. *Genes Dev , 17*, 1207-1212.

Krek, A., Grun, D., Poy, M., Wolf, R., Rosenberg, L., Epstein, E., et al. (2005). Combinatorial microRNA target predictions. *Nature Genetics* , 495-500.

Kwon, C., Arnold, J., Hsiao, E., Taketo, M., Conklin, B., & Srivastava, D. (2007). Canonical Wnt signaling is a positive regulator of mammalian cardiac progenitors. *PNAS , 104*, 10894-10899.

Lahmers, S., Wu, Y., Call, D., Labeit, S., & Granzier, H. (2004). Developmental control of titin isoform expression and passive stiffness in fetal and neonatal myocardium. *Circ Res , 94*, 505-513.

Lee, I., Ajay, S., Yook, J., Kim, H., Hong, S., Kim, N., et al. (2009). New class of microRNA targets containing simultaneous 5'UTR and 3'UTR interaction sites. *Genome Res , 19*, 1175-1183.

Lees, E. (1995). Cyclin dependent kinase regulation. *Curr Opin Cell Biol , 7*, 773-780.

Leri, A., Malhotra, A., Liew, C.-C., Kajstura, J., & Anversa, P. (2000). Telomerase activity in rat cardiac myocytes is age and gender dependent. *J Mol Cell Cardiol , 32*, 385-390.

Leu, M., Ehler, E., & Perriard, J. (2001). Characterisation of postnatal growth of the murine heart. *Anat Embryol , 204*, 217-224.

Li, F., Wang, X., & Bunger, P. G. (1997). Formation of binucleated cardiac myocytes in rat heart. I. Role of actin-myosin contractile ring. *J Mol Cell Cardiol , 29*, 1541-1551.

Li, F., Wang, X., & Gerdes, A. (1997). Formation of binucleated cardiac myocytes in rat heart. II. Cytoskeletal organisation. *J Mol Cell Cardiol , 29*, 1553-1565.

Li, F., Wang, X., Capasso, J., & Gerdes, A. (1996). Rapid transition of cardiac myocytes from hyperplasia to hypertrophy during postnatal development. *J Mol Cell Cardiol , 28*, 1737-1746.

Li, J., Poolman, R., & Brooks, G. (1998). Role of G1 phase cyclins and cyclin-dependent kinases during cardiomyocyte hypertrophic growth in rats. *Am J Physiol , 275*, H814-H822.

Lickert, H., Kutsch, S., Kanzler, B., Tamai, Y., Taketo, M., & Kemler, R. (2002). Formation of multiple hearts in mice following deletion of beta-catenin in the embryonic endoderm. *Dev Cell , 3*, 171-181.

Liebner, S., Cattelino, A., Gallini, R., Rudini, N., Iurlaro, M., Piccolo, S., et al. (2004). Beta-catenin is required for endothelial-mesenchymal transformation during heart cushion development in the mouse. *J Cell Biol , 166*, 359-367.

Lin, L., Cui, L., Zhou, W., Dufort, D., Zhang, X., Cai, C., et al. (2007). Beta-Catenin directly regulation Islet1 expression in cardiovascular progenitors and is required for multiple aspects of cardiogenesis. *PNAS , 104*, 9313-9318.

Lin, Y., Furukawa, Y., Tsunoda, T., Yue, C., Yang, K., & Nakamura, Y. (2002). Molecular diagnosis of colorectal tumors by expression profiles of 50 genes expressed diffrerntially in adnomas and carcinomas. *Oncogene , 21*, 4120-4128.

Liu, Z., Yue, S., Chen, X., Kubin, T., & Braun, T. (2010). Regulation of cardiomyocyte polyploidy and multinucleation by cyclin G1. *Circ Res , 106*, 1498-1506.

Mackay, A., Ainsztein, A., Eckley, D., & Earnshaw, W. (1998). A dominant mutant of inner centromere protein (INCENP), a chromosomal protein, disrupts prometaphase congression and cytokinesis. *J Cell Biol , 140*, 991-1002.

MacLellan, W., Garcia, A., Oh, H., Frenkel, P., Jordan, M., Roos, K., et al. (2005). Overlapping roles of pocket proteins in the myocardium are unmasked by germ line deletion of p130 plus heart-specific deletion of Rb. *Mol Cell Biol , 25*, 2486-2497.

Mallory, G., White, P., & Salcedo-Salgar, J. (1939). The speed of healing of myocardial infarction: A study of the pathologic anatomy. *Am Heart J , 18*, 647-671.

Mastronarde, D., McDonald, K., Ding, R., & McIntosh, J. (1993). Interpolar spindle microtubules in PTK cells. *J Cell Biol , 123*, 1475-1489.

McCollum, D. (2004). Cytokinesis: the central spindle takes center stage. *Curr Biol , 14*, R953-R955.

McCright, B., Gao, X., Shen, L., Lozier, J., Lan, Y., & Maguire, M. (2001). Defects in development of the kidney, heart and eye vasculature in mice homozygous for a hyppomorphic Notch2 mutation. *Development , 128*, 491-502.

McCright, B., Lozier, J., & Gridley, T. (2002). A mouse model of Alagille syndrome: Notch2 as a genetic modifier of Jag1 haploinsufficiency. *Development , 129*, 1075-1082.

McGill, C., & Brooks, G. (1995). Cell cycle control mechanism and their role in cardiac growth. *Cardiovasc Res , 30*, 557-569.

McKinsey, T., & Olson, E. (2005). Toward transcriptional therapies for the failing heart: chemical screens to modulate genes. *J Clin Invest , 115*, 538-546.

McMullen, J., Shioi, T., Huang, W., Zhang, L., Tarnavski, O., Bisping, E., et al. (2004). The Insulin-like Growth Factor 1 receptor induces physiological heart growth via the phosphoinositide 3-kinase (P110alpha) pathway. *J Biol Chem , 279*, 4782-4793.

Molkentin, J., & Dorn, I. (2001). Cytoplasmic signaling pathways that regulate cardiac hypertrophy. *Annu Rev Physiol , 63*, 391-426.

Mollinari, C., Kleman, J.-P., Jiang, W., Schoehn, G., Hunter, T., & Margolis, R. (2002). Prc1 is a microtubule binding and bundling protein essential to maintain the mitotic spindle midzone. *J Cell Biol , 157*, 1175-1186.

Montgomery, R., Davis, C., Potthoff, M., Haberland, M., Fielitz, J., Qi, X., et al. (2007). Histone deacetylases 1 and 2 redundantly regulate cardiac morphogenesis, growth, and contractility. *Genes Dev , 21*, 1790-1802.

Morgan, D. (1995). Principles of CDK regulation. *Nature , 374*, 131-134.

Morgan, D. (2007). *The Cell Cycle: Principles of Control.* Oxford: Oxford University Press.

Morkin, E. (2000). Control of cardiac myosin heavy chain gene expression. *Microsc Res Tech , 50*, 522-531.

Murray, A., & Hunt, T. (1993). *The Cell Cycle.* New York, NY: W.H. Freeman and Company.

Murry, C., Soonpaa, M., Reinecke, H., Nakajima, H., Nakajima, H., Rubart, M., et al. (2004). Haematopoietic stem cells do not transdifferentiate into cardiac myocytes in myocardial infarcts. *Nature , 428*, 664-668.

Nag, A., Healy, C., & Cheng, M. (2005). DNA synthesis and mitosis in adult amphibian cardiac muscle cells in vitro. *Science , 1979*, 1281-1282.

Nagatomo, Y., Carabello, B., Hamawaki, M., Nemoto, S., Matsuo, T., & McDermott, P. (1999). Translational mechanisms accelerate the rate of protein synthesis during canine pressure-overload hypertrophy. *Am J Physiol, 277*, H2176-2184.

Nakamura, T., Furukawa, Y., Nakagawa, H., Tsunoda, T., Ohigashi, H., Murata, K., et al. (2004). Genome-wide cDNA microarray analysis of gene expression profiles in pancreatic cancers using populations of tumor cells and normal epithelial cells selected for purity by laser microdissection. *Oncogene , 23*, 2385-2400.

NCBI. (2011, Feb 6). *Gene - Genes and mapped phenotypes*. Retrieved Feb 10, 2011, from NCBI: http://www.ncbi.nlm.nih.gov/gene

NCBI GEO Dataset. (n.d.). GDS1490/95032_at/Prc1/Mus musculus.

Nemer, M. (2008). Genetic insights into normal and abnormal heart development. *Cardiovasc Pathol , 17*, 48-54.

Nemir, M., & Pedrazzini, T. (2008). Functional role of Notch signaling in the developing and postnatal heart. *J. Mol. Cell Cardiol.* , 495-504.

Ng, W., Grupp, I., Subramaniam, A., & Robbins, J. (1991). Cardiac myosin heavy chain mRNA expression and myocardial function in the mouse heart. *Circ Res , 68*, 1742-1750.

Nigg, E. (1995). Cyclin-dependent protein kinases: key regulators of the eukaryotic cell cycle. *Bioessays , 17*, 471-480.

Niimura, Y., & Nei, M. (2003). Evolution of olfactory receptor genes in the human genome. *PNAS , 100*, 12235-12240.

Obama, K., Ura, K., Satoh, S., Nakamura, Y., & Furukawa, Y. (2005). Up-regulation of PSF2, a member of the GINS multiprotein complex, in intrahepatic cholangiocarcinoma. *Oncol Rep , 14*, 701-706.

Oberpriller, J., Oberpriller, J., Matz, D., & Soonpaa, M. (1995). Stimulation of proliferative events in the adult amphibian cardiac myocyte. *Ann HY Acad Sci , 752*, 30-46.

Ojamaa, K., Samarel, A., Kupfer, J., Hong, C., & Klein, I. (1992). Thyroid hormone effects on cardiac gene expression independent of cardiac growth and protein synthesis. *AM J Physiol , 263*, E534-540.

Oka, C., Nakano, T., Wakeham, A., De La Pompa, J., Mori, C., & Sakai, T. (1995). Disruption of the mouse RBP-J kappa gene results in early embryonic death. *Development , 121*, 3291-3301.

Olson, E. (2006). Gene regulatory networks in the evolution and development of the heart. *Science* , 1922-1927.

Oparil, S., Bishop, S., & Clubb, F. J. (1984). Myocardial cell hypertrophy or hyperplasia. *Hypertension* , 11138-43.

Orlic, D., Kajstura, J., Chimenti, S., Jakoniuk, I., Anderson, S., Li, B., et al. (2001). Bone marrow cells regenerate infarcted myocardium. *Nature , 410*, 701-705.

Orlic, D., Kajstura, J., Chimenti, S., Limana, F., Jakoniuk, I., Quaini, F., et al. (2001). Mobilized bone marrow cells repair the infacrted heart, improving function and survival. *PNAS , 98*, 10344-10349.

Pasumarthi, K., & Field, L. (2002). Cardiomyocyte cell cycle regulation. *Circ. Res.* , 1044-54.

Pellman, D., Bagget, M., Tu, Y., & Fink, G. (1995). Two microtubule-associated proteins required for anaphase spindle movement in Saccharomyces cerevisiae. *J Cell Biol , 130*, 1373-1385.

Poolman, R., & Brooks, G. (1996). Expression of the cip/kip family of cyclin-dependent kinase inhibitors during cardiac development. *Circulation , 94*, Suppl. 1-157.

Poolman, R., & Brooks, G. (1998). Expressions and activities of cell cycle regulatory molecules during the transition from myocyte hyperplasia to hypertrophy. *J Mol Cell Cardiol , 30*, 2121-2135.

Porrello, E., Mahmoud, A., Simpson, E., Hill, J., Richardson, J., Olson, E., et al. (2011). Transient regenerative potential of the neonatal mouse heart. *Science , 331*, 1078-1080.

Poznic, M. (2009). Retinoblastoma protein: a central processing unit. *J Biosci , 34*, 305-312.

Qu, J., Zhou, J., Yi, X., Dong, B., Zheng, H., Miller, L., et al. (2007). Cardiac-specific haploinsufficiency of beta-catenin attenuates cardiac hypertrophy but enhances fetal gene expression response to aortic constriction. *J Mol Cell Cardiol , 43*, 319-326.

Qyang, Y., Martin-Puig, S., Chiravuri, M., Chen, S., Xu, H., Bu, L., et al. (2007). The renewal and differentiation of Isl1+ cardiovascular progenitors are controlled by a Wnt/beta-catenin pathway. *Cell Stem Cell , 1*, 165-179.

Rhoades, M., Reinhart, B., Lim, L., Burge, C., Bartel, B., & Bartel, D. (2002). Prediction of plant microRNA targets. *Cell , 110*, 513-520.

Riken Transcription Factor Database (TFdb). (2004). (The Institute of Physical and Chemical Research) Retrieved 01 2010, from Riken Transcription Factor Database (TFdb): http://genome.gsc.riken.jp/TFdb/

Ruchaud, S., Carmena, M., & Earnshaw, W. (2007). Chromosomal passengers: conducting cell division. *Nat Rev Mol Cell Biol , 8*, 798-812.

Schwartz, K., Boheler, K., de la Bastie, D., Lompre, A., & Mercadier, J. (1992). Switches in cardiac muscle gene expression as a result of pressure and volume overload. *Am J Physiol , 262*, R364-R369.

Sehl, P., Tai, J., Hillan, K., Brown, L., Goddard, A., Yang, R., et al. (2000). Application of cDNA microarrays in determining molecular phenotype in cardiac growth, development, and response to injury. *Circulation , 101*, 1990-1999.

Shahi, P., Loukianiouk, S., Bohne-Lang, A., Kenzelmann, M., Kuffer, S., Maertens, S., et al. (2006). Argonaute - a database for gene regulation by mammalian microRNAs. *Nucleic Acids Res* (34), D115-8.

Sherr, C. (1994). G1 phase progression: cycling on cue. *Cell , 79*, 551-555.

Sherr, C. (1993). Mammalian G1 cyclins. *Cell , 73*, 1059-1065.

Shimo, A., Nishidate, T., Ohta, T., Fukuda, M., Nakamura, Y., & Katagiri, T. (2007). Elevated expression of protein regulator of cytokinesis 1, involved in the growth of breast cancer cells. *Cancer Sci , 98*, 174-181.

Simpson, L., Kumar, S., Okuno, S., Schaff, H., Porrata, L., Buckner, J., et al. (2008). Malignant primary cardiac tumors: review of a single institution experience. *Cancer , 112*, 2440-2446.

Skoufias, D., Mollinari, C., Lacroix, F., & Margolis, R. (2000). Human survivin is a kinetochore-associated passenger protein. *J Cell Biol , 151*, 1575-1582.

Song, L. a. (2006). MicroRNAs and Cell Differentiation in Mammalian Development. *Birth Defects Research , 78*, 140-149.

Soonpaa, M. H., Kyung Keun, K., Pajak, L., Franklin, M., & Field, L. (1996). Cardiomyocyte DNA synthesis and binucleation during murine development. *The American Journal of Physiology* , H2183-2189.

Soonpaa, M., Koh, G., Pajak, L., Jing, S., Wang, H., Franklin, M., et al. (1997). Cyclin D1 overexpression promotes cardiomyocyte DNA synthesis and multinucleation in transgenic mice. *J Clin Invest , 99*, 2644-2654.

Srivastava, D., & Cordes, K. (2009). MicroRNA Regulation of Cardiovascular Development. *Circulation Research , 104*, 724-732.

Subramanian, A., Tamayo, P., Mootha, V., Mukherjee, S., Ebert, B., Gillette, M., et al. (2005). Gene set enrichment analysis: a knowledge-based approach for interpreting genome-wide expression profiles. *PNAS , 102*, 15545-15550.

Swiatek, P., Lindsell, C., del Amo, F., Weinmaster, G., & Gridley, T. (1994). Notch1 is essential for postimplantation development in mice. *Genes Dev , 8*, 707-719.

Taegtmeyer, H., Sen, S., & Vela, D. (2010). Return to the fetal gene program: A suggested metabolic link to gene expression in the heart. *Ann NY Acad Sci , 1188*, 191-198.

Takada, M., Morii, N., Kumagai, S., & Ryo, R. (1996). The involvement of the rho gene product, a small molecular weight GTP-binding protein, in polyploidization of a human megakaryocytic cell line, CMK. *Exp Hematol , 24*, 524-530.

Tam, S., Gu, W., Mahdavi, V., & Nadal-Ginard, B. (1995). Cardiac Myocyte Terminal Differentiation: Potential for Cardiac Regeneration. *Annals New York Academy of Science* , 72-79.

Tarabykin, V., Britanova, O., Fradkov, A., Voss, A., Katz, L., Lukyanov, S., et al. (2000). Expression of PTTG and PRC1 genes during telencephalic neurogenesis. *Mech Dev , 92*, 301-304.

TargetScanMouse, 5.1: April 2009. (2006-2009). (Whitehead Institute for Biomedical Research) Retrieved 2010, from TargetScanMouse Prediction of microRNA targets: http://www.targetscan.org/mmu_50/

Tay Y, Z. J. (2008). MicroRNAs to Nanog, Oct4 and Sox2 coding regions modulate embryonic stem cell differentiation. *Nature , 455* (7216), 1124-8.

Terada, Y., Tatsuka, F., Suzuki, F., Yasuda, Y., Fujita, S., & Otsu, M. (1998). AIM-1: a mammalian mid-body-associated protein required for cytokinesis. *EMBO , 17*, 667-676.

TheUniProtConsortium. (2010). The Universal Protein Resource (UniProt) in 2010. *Nucleic Acids Res , 38*, D142-D148.

Thum, T., Catalucci, D., & Bauersachs, J. (2008). MicroRNAs: novel regulators in cardiac development and disease. *Cardiovascular Research , 79*, 562-570.

Thum, T., Galuppo, P., Wolf, C., Fiedler, J., Kneitz, S., van Laake, L., et al. (2007). MicroRNAs in the human heart - A clue to fetal gene reprogramming in heart failure. *Circulation , 116*, 258-267.

Timmerman, L., Grego-Bessa, J., Raya, A., Bertran, E., Perez-Pomares, J., & Diez, J. (2004). Notch promotes epithelial-mesenchymal transition during cardiac development and oncogenic transformation. *Genes Dev , 18*, 99-115.

Topper, J. (2000). TGF-beta in the cardiovascular system: molecular mechanisms of a context-specifc growth factor. *Trends Cardiovasc Med , 10*, 132-137.

Uehara, R., & Goshima, G. (2010). Functional central spindle assembly requires de novo microtubule generation in the interchromosomal region during anaphase. *J Cell Biol , 191*, 259-267.

Uren, A., Wong, L., Pakusch, M., Fowler, K., Burrows, F. V., & Choo, K. (2000). Survivin and the inner centromere protein INCENP show similar cell-cycle localization and gene knockout phenotype. *Curr Biol , 10*, 1319-1328.

van Rooij, E., Marshall, W., & Olson, E. (2008). Toward microRNA-Based Therapeutics for Heart Disease: The Sense in Antisense. *Circ Res , 103*, 919-928.

Van Rooij, E., Sutherland, L., Liu, N., Williams, A., Mcanally, J., Gerard, R., et al. (2006). A signature pattern of stress-responsive microRNAs that can evoke cardiac hypertrophy and heart failure. *Proc Natl Acad Sci USA, 103* (48), 18255-18260.

van Rooij, E., Sutherland, L., Thatcher, J., DiMaio, J., Naseem, R., Marshall, W., et al. (2008). Dysregulation of microRNAs after myocardial infarction reveals a role of miR-29 in cardiac fibrosis. *PNAS , 105* (35), 13027-13032.

Warde-Farley, D., Donaldson, S., Comes, O., Zuberi, K., Badrawi, R., Chao, P., et al. (2010). The GeneMANIA prediction server: biological network integration for gene prioritization and predicting gene function. *Nucleic Acids Res , 38*, W214-W220.

Watanabe, Y., Kokubo, H., Miyagawa-Tomita, S., Endo, M., Igarashi, K., & Aisaki, K. (2006). Activation of Notch1 signaling in cardiogenic mesoderm induces abnormal heart morphogenesis in mouse. *Development , 133*, 1625-1634.

Wellcome Trust Genome. (2007, 09 19). *miRBase Targets*. Retrieved 02 18, 2009, from Wellcome Trust Sanger Institute: http://microrna.sanger.ac.uk/cgi-bin/targets/v5/search.pl

Winick, M., & Noble, A. (1965). Quantitative changes in DNA, RNA, and protein during prenatal and postnatal growth in the rat. *Dev Biol , 12*, 451-466.

Wu, Y., & Wu, E. (2009). MR study of postnatal development of myocardial structure and left ventricular function. *J Mag Res Imag , 30*, 47-53.

Xiang, F., Sakata, Y., Cui, L., Youngblood, J., Nakagami, H., & Liao, J. (2006). Transcription factor CHF1/Hey2 suppresses cardiac hypertrophy through an inhibitory interaction with GATA4. *Am J Physiol Heart Circ Physiol , 290*, H1997-H2006.

Xin, M., Small, E., van, R., Qi, X., Richardson, J., & Srivastava, D. (2007). Essential roles of the bHLH transcription factor Hrt2 in repression of atrial gene expression and maintenance of postnatal cardiac function. *PNAS , 104*, 7975-7980.

Xue, Y., Gao, X., Lindsell, C., Norton, C., Chang, B., & Hicks, C. (1999). Embryonic lethality and vascular defects in mice lacking the Notch ligand Jagged1. *Hum Mol Genet , 8*, 723-730.

Yen, T., Li, G., Schaar, B., Szilak, I., & Cleveland, D. (1992). CENP-E is a putative kinetochore motor that accumulates just before mitosis. *Nature , 359*, 536-539.

Yoshizumi, M., Lee, W.-S., Hsieh, C.-M., Tsai, J.-C., Li, J., Perella, M., et al. (1995). Disappearance of cyclin A correlates with percentage withdrawal of cardiomyocytes from the cell cycle in human and rat hearts. *J Clin Invest , 95*, 2275-2280.

Zak, R. (1974). Development and proliferative capacity of cardiac muscle cells. *Cir Res , Suppl. 2*, 17-26.

Zamora, M., Manner, J., & Ruiz-Lozano, P. (2007). Epicardium-derived progenitor cells require beta-catenin for coronary artery formation. *PNAS , 104*, 18109-18114.

Zhou, J., Qu, J., Yi, X., Graber, K., Huber, L., Wang, X., et al. (2007). Upregulation of gamma-catenin compensates for the loss of beta-catenin in adult cardiomyocytes. *Am J Physiol Heart Circ Physiol , 292*, H270-H276.

Zhu, C., & Jiang, W. (2005). Cell cycle-dependent tarnslocation of PRC1 on the spindle by KIF4 is essential for midzone formation and cytokinesis. *Proc Natl Acad Sci USA , 162*, 343-348.

Zorio, E., Medina, P., Rueda, J., Millan, J., Arnau, M., Beneyto, M., et al. (2009). Insights Into the Role of microRNAs in Cardiac Diseases: From Biological Signalling to Therapeutic Targets. *Cardiovascular & Hematological Agents in Medicinal Chemistry , 7* (1), 82-90.

CONTRIBUTIONS OF COLLABORATORS

Shelley Deeke provided quantified HL-1 protein extracts and HeLa cells. microRNA profiling and microarray quality controls were performed in triplicate per timepoint by the Genetic Analysis Facility – The Center for Applied Genomics (TCAG) at The Hospital for Sick Children.

APPENDIX

Supplemental Figure 1: microRNA Microarray Quality Controls. Snapshots of controls analyses as calculated by TCAG.

A.

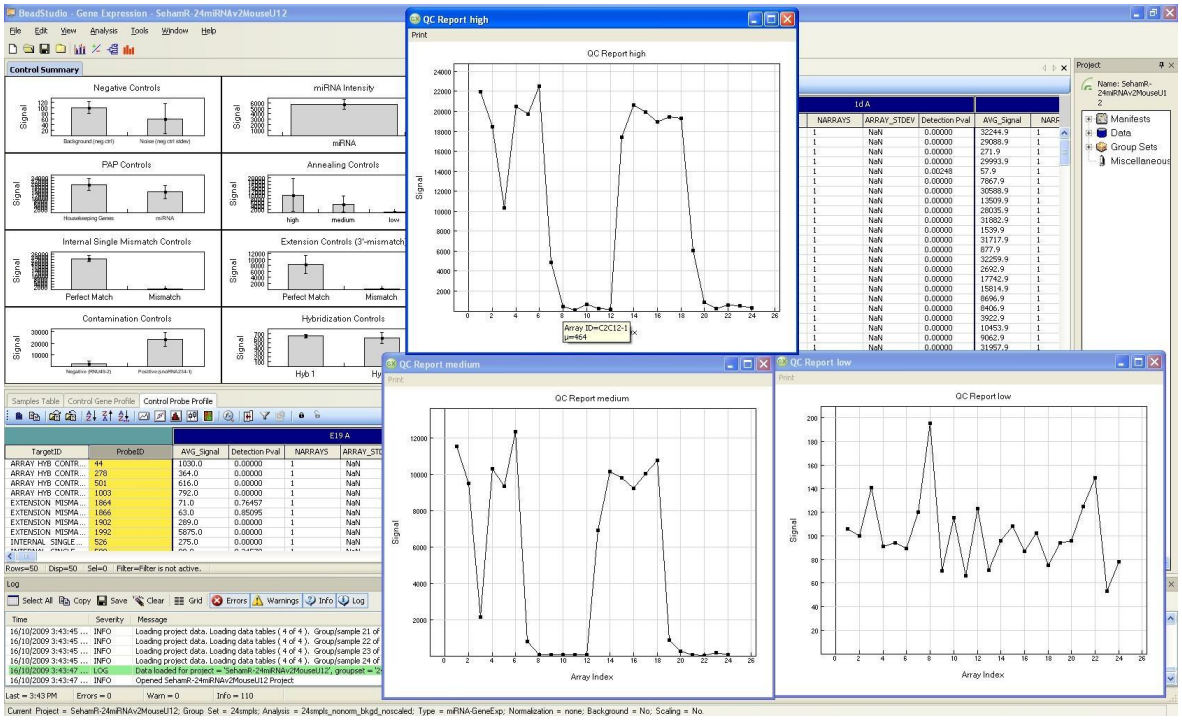
BeadStudio - Gene Expression - SehamR-24miRNAv2MouseU12
QC Report high
QC Report medium
QC Report low
Control Summary
Negative Controls
miRNA Intensity
PAP Controls
Annealing Controls
Internal Single Mismatch Controls
Extension Controls (3'-mismatch)
Contamination Controls
Hybridization Controls

B.

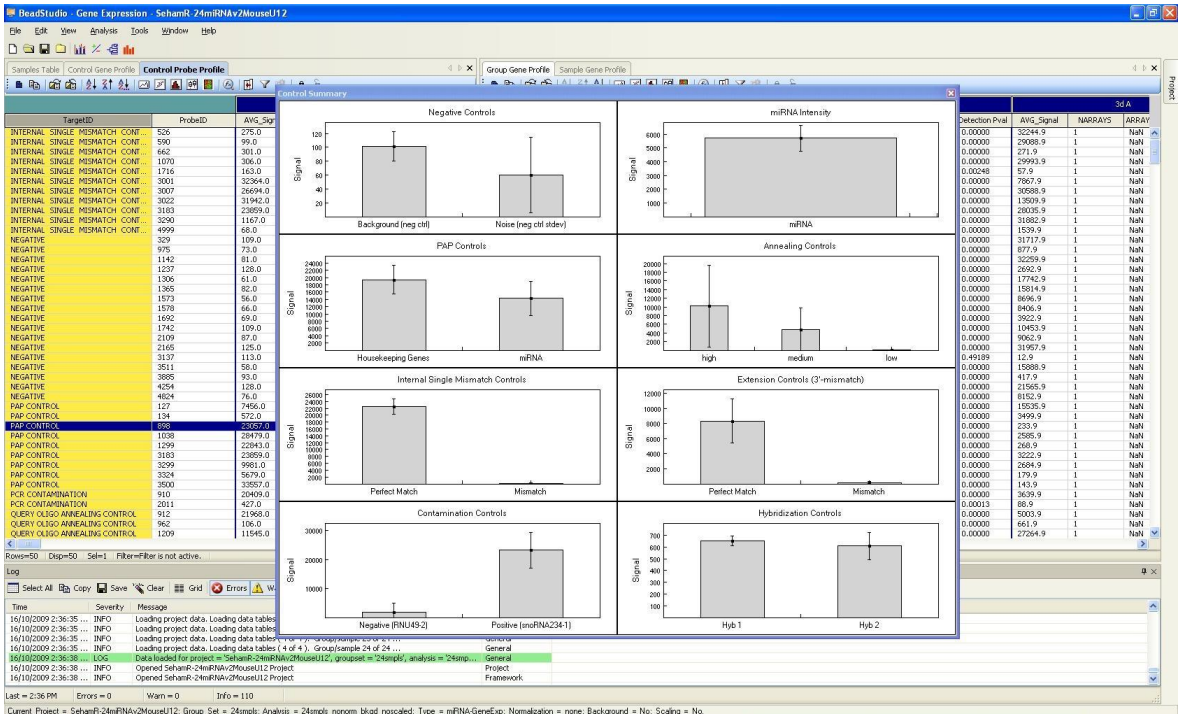
BeadStudio - Gene Expression - SehamR-24miRNAv2MouseU12
Control Summary
Negative Controls
miRNA Intensity
PAP Controls
Annealing Controls
Internal Single Mismatch Controls
Extension Controls (3'-mismatch)
Contamination Controls
Hybridization Controls

C.

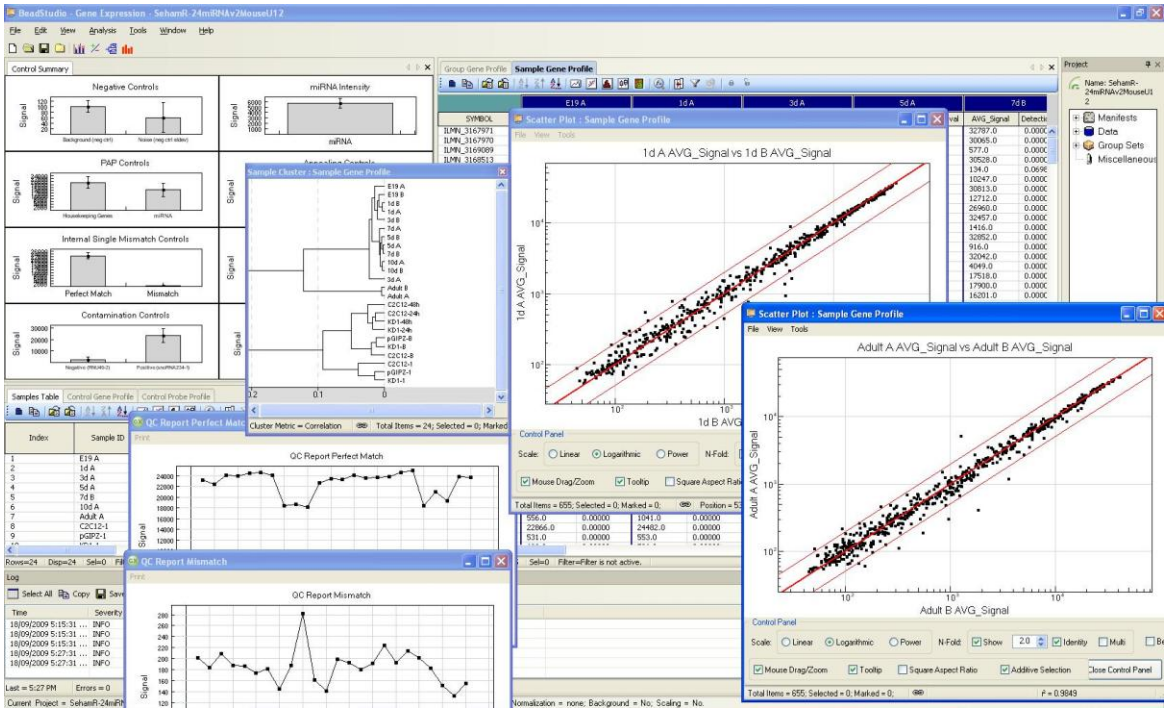
Negative Controls
miRNA Intensity
PAP Controls
Internal Single Mismatch Controls
Perfect Match
Mismatch
Contamination Controls
Sample Cluster : Sample Gene Profile
Scatter Plot : Sample Gene Profile
1d A AVG_Signal vs 1d B AVG_Signal
Adult A AVG_Signal vs Adult B AVG_Signal
QC Report Perfect Match
QC Report Mismatch

Supplemental Figure 2: Prc1 GEO Profiles. Microarray expression profiles available through NCBI Gene Expression Omnibus (GEO). **A)** Gene expression profile of murine cardiac ventricle between embryonic day 12.5, neonatal day 1, 1 week, 4 week, 3 months, 5 months and 12 months of age. (NCBI, GEO profiles, record GDS40 / 95032_at / Prc1 / Mus musculus). **B)** Mouse strain C57BL/6 embryonic expression profile of the atrial and ventricular chambers between E10.5 and E18.5. (GDS627 / 1423774_a_at / Prc1 / Mus musculus). **C)** Similar analysis to Panel B however with a different microarray platform. (GDS627 / 1423775_s_at / Prc1 / Mus musculus).

A.

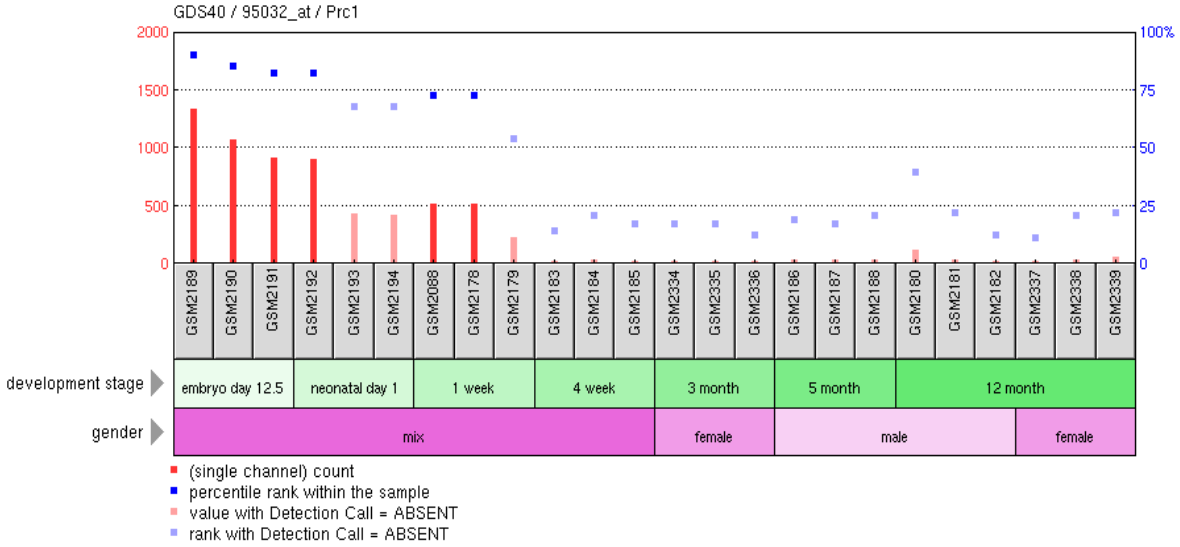
GDS40 / 95032_at / Prc1
2000
1500
1000
500
0
100%
75
50
25
0
GSM2189
GSM2190
GSM2191
GSM2192
GSM2193
GSM2194
GSM2088
GSM2178
GSM2179
GSM2183
GSM2184
GSM2185
GSM2334
GSM2335
GSM2336
GSM2186
GSM2187
GSM2188
GSM2180
GSM2181
GSM2182
GSM2337
GSM2338
GSM2339
development stage
embryo day 12.5
neonatal day 1
1 week
4 week
3 month
5 month
12 month
gender
mix
female
male
female
(single channel) count
percentile rank within the sample
value with Detection Call = ABSENT
rank with Detection Call = ABSENT

B.

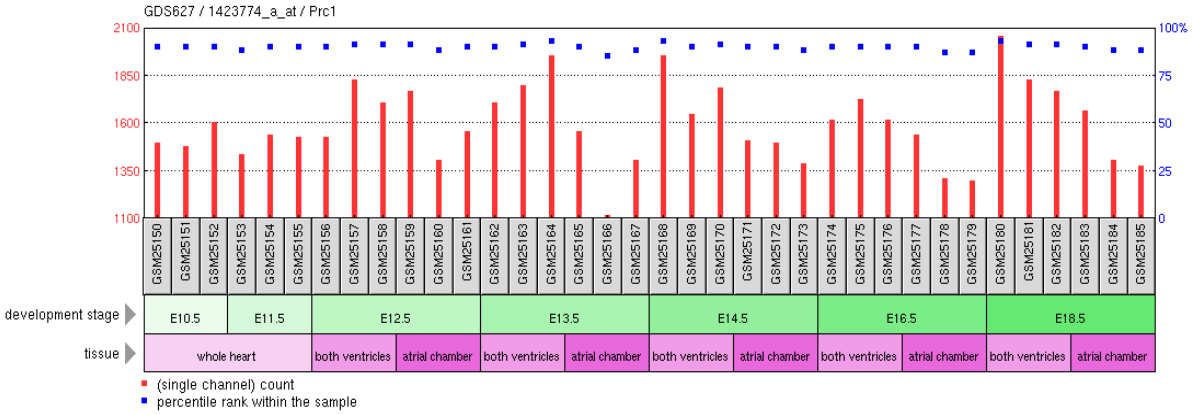
GDS627 / 1423774_a_at / Prc1
2100
1850
1600
1350
1100
100%
75
50
25
0
GSM25150
GSM25151
GSM25152
GSM25153
GSM25154
GSM25155
GSM25156
GSM25157
GSM25158
GSM25159
GSM25160
GSM25161
GSM25162
GSM25163
GSM25164
GSM25165
GSM25166
GSM25167
GSM25168
GSM25169
GSM25170
GSM25171
GSM25172
GSM25173
GSM25174
GSM25175
GSM25176
GSM25177
GSM25178
GSM25179
GSM25180
GSM25181
GSM25182
GSM25183
GSM25184
GSM25185
development stage
E10.5
E11.5
E12.5
E13.5
E14.5
E16.5
E18.5
tissue
whole heart
both ventricles
atrial chamber
both ventricles
atrial chamber
both ventricles
atrial chamber
both ventricles
atrial chamber
both ventricles
atrial chamber
(single channel) count
percentile rank within the sample

C.

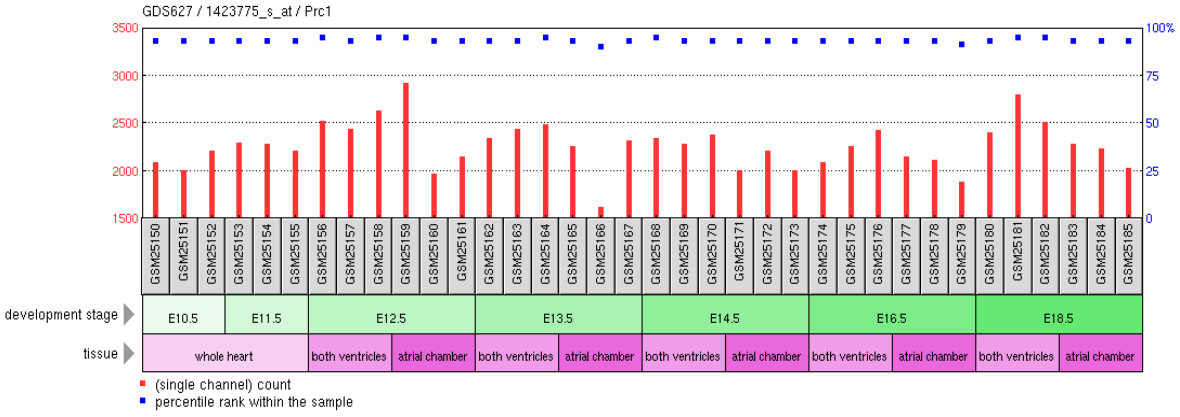
GDS627 / 1423775_s_at / Prc1
3500
3000
2500
2000
1500
100%
75
50
25
0
GSM25150
GSM25151
GSM25152
GSM25153
GSM25154
GSM25155
GSM25156
GSM25157
GSM25158
GSM25159
GSM25160
GSM25161
GSM25162
GSM25163
GSM25164
GSM25165
GSM25166
GSM25167
GSM25168
GSM25169
GSM25170
GSM25171
GSM25172
GSM25173
GSM25174
GSM25175
GSM25176
GSM25177
GSM25178
GSM25179
GSM25180
GSM25181
GSM25182
GSM25183
GSM25184
GSM25185
development stage
E10.5
E11.5
E12.5
E13.5
E14.5
E16.5
E18.5
tissue
whole heart
both ventricles
atrial chamber
both ventricles
atrial chamber
both ventricles
atrial chamber
both ventricles
atrial chamber
both ventricles
atrial chamber
(single channel) count
percentile rank within the sample

Supplemental Figure 3: Prc1 Immunofluorescence in HL-1, HeLa, and Primary Cardiomyocytes. Pre-immune rabbit serum served as a blocking control. The nucleus was stained with DAPI (blue), Prc1 with an Alexa 488 secondary (green), and the plasma membrane with wheat germ agglutinin (WGA) (red). **A)** Immunofluorescence experiments in HL-1 cells. **B)** Prc1 localization visualized in HeLa cells by immunofluorescence. Epitope blocking experiments were successful for Panel A and B. **C)** Immunofluorescence of primary mouse cardiomyocytes at 10 days post-birth.

A.

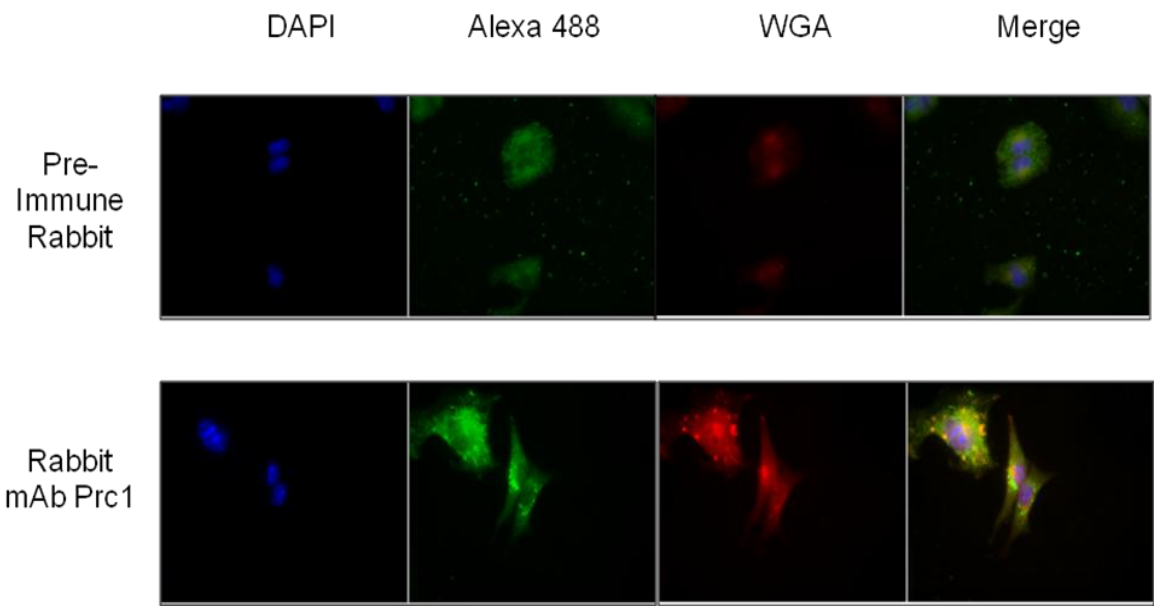
DAPI
Alexa 488
WGA
Merge
Pre-Immune Rabbit
Rabbit mAb Prc1

B.

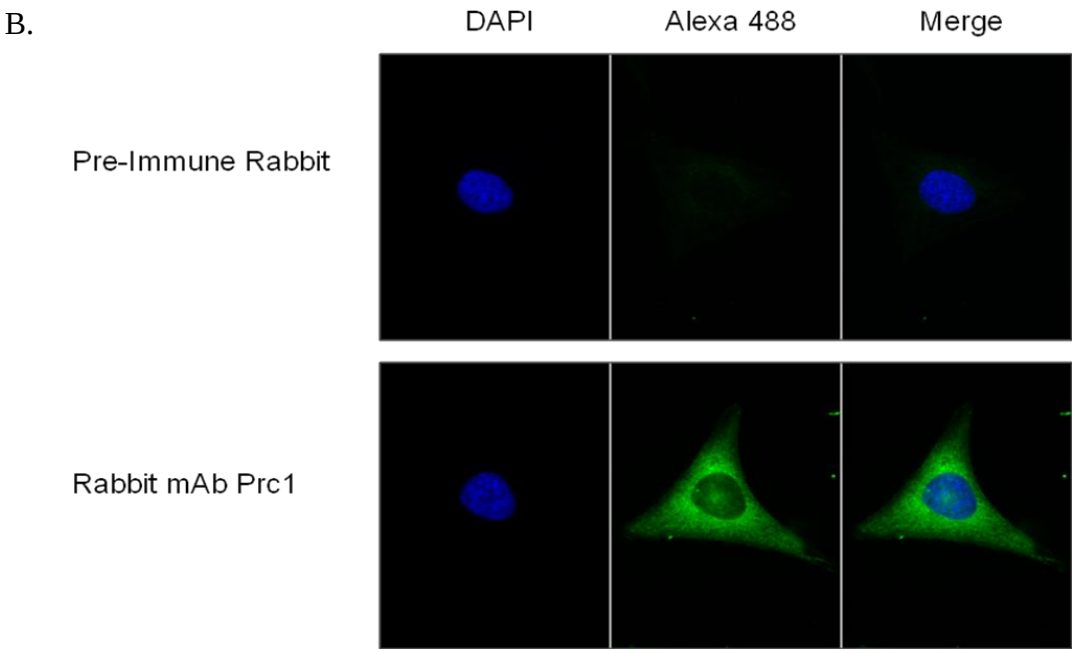
DAPI
Alexa 488
Merge
Pre-Immune Rabbit
Rabbit mAb Prc1

C.

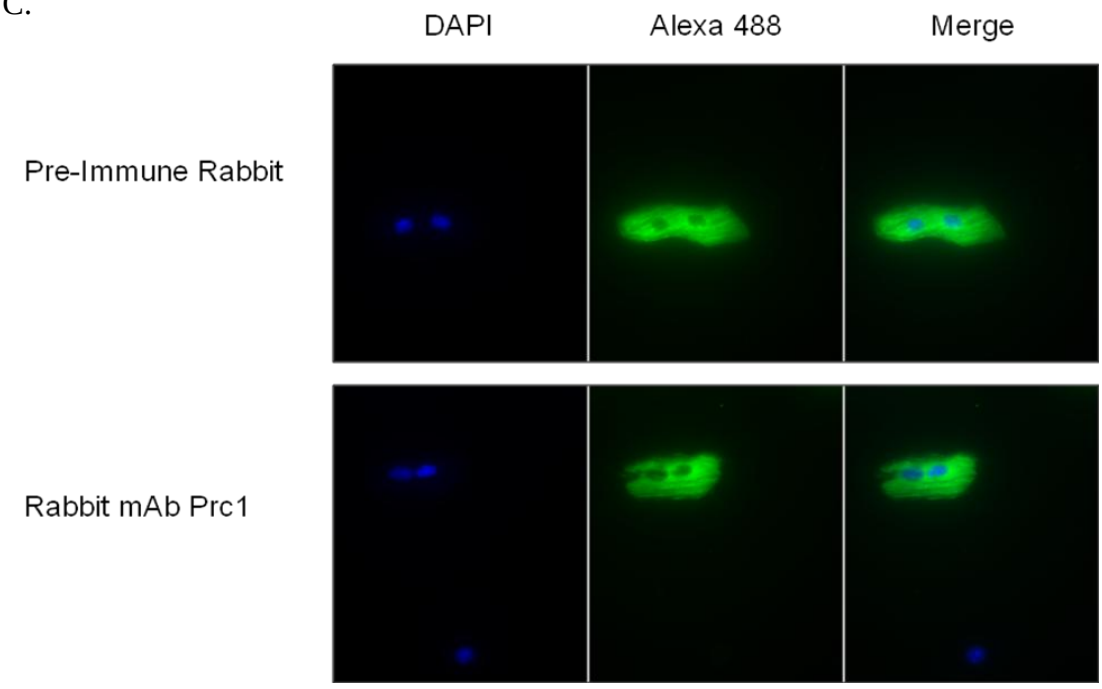

Supplemental Figure 4: GeneMANIA Prc1 Interaction Network Report. Detailed report and references of Prc1 interaction network assessed utilizing GeneMANIA.org.

GeneMANIA
fast gene function predictions

Related Genes Report

Created on: 24 Nov 2010
Last database update: 23 Sep 2010
Application version: 2.7.12

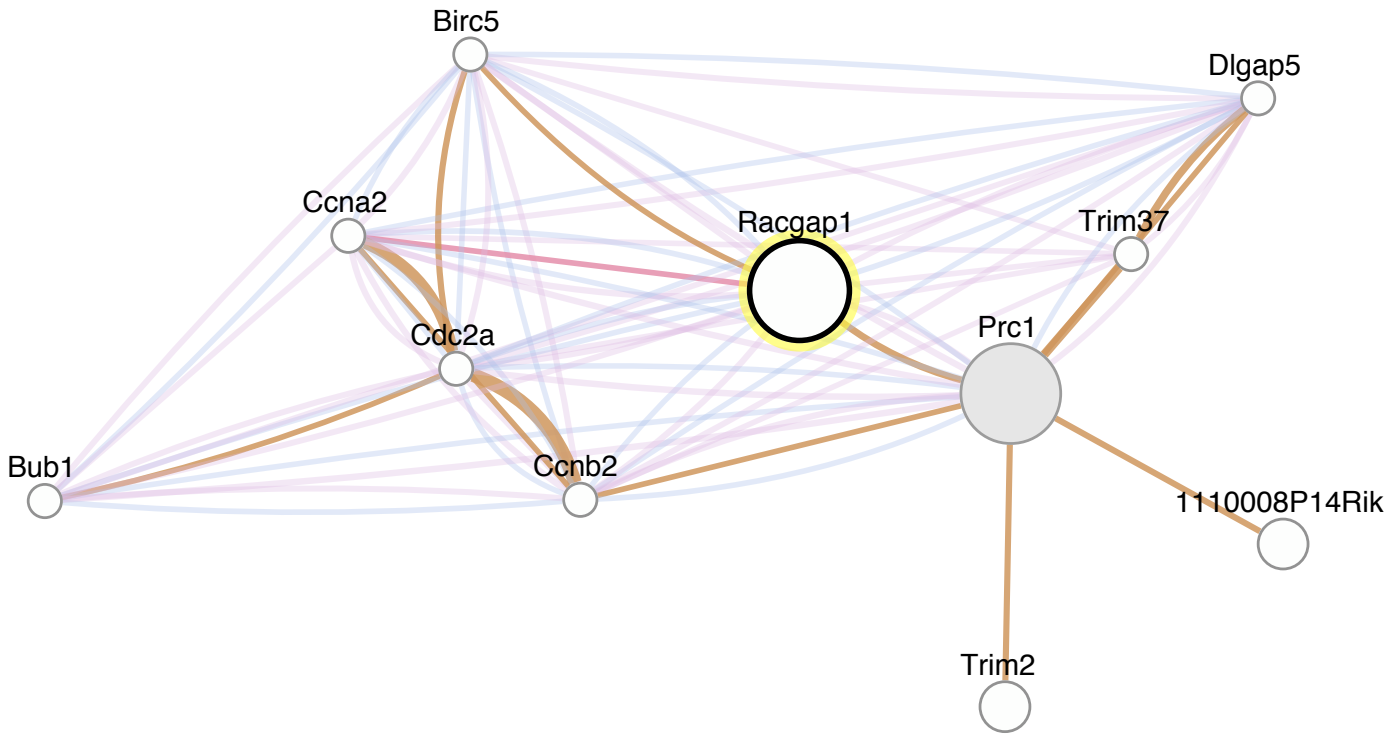

Genes

Gene	Description	Score
Prc1	protein regulator of cytokinesis 1 Gene [Source:MGI Symbol;Acc:MGI:1858961] (more at Entrez)	
Racgap1	Rac GTPase-activating protein 1 Gene [Source:MGI Symbol;Acc:MGI:1349423] (more at Entrez)	0.1
Trim2	tripartite motif-containing 2 Gene [Source:MGI (curated);Acc:MGI:1933163] (more at Entrez)	0.07
1110008P14Rik	RIKEN cDNA 1110008P14 gene Gene [Source:MGI Symbol;Acc:MGI:1920987] (more at Entrez)	0.07
Birc5	baculoviral IAP repeat-containing 5 Gene [Source:MGI (curated);Acc:MGI:1203517] (more at Entrez)	0.06
Dlgap5	discs, large (Drosophila) homolog-associated protein 5 Gene [Source:MGI Symbol;Acc:MGI:2183453] (more at Entrez)	0.06
Trim37	tripartite motif-containing 37 Gene [Source:MGI (curated);Acc:MGI:2153072] (more at Entrez)	0.06
Cdc2a	cyclin-dependent kinase 1 Gene [Source:MGI (curated);Acc:MGI:88351] (more at Entrez)	0.06
Ccnb2	cyclin B2 Gene [Source:MGI Symbol;Acc:MGI:88311] (more at Entrez)	0.06
Ccna2	cyclin A2 Gene [Source:MGI (curated);Acc:MGI:108069] (more at Entrez)	0.06
Bub1	budding uninhibited by benzimidazoles 1 homolog (S. cerevisiae) Gene [Source:MGI (curated);Acc:MGI:1100510] (more at Entrez)	0.06

Networks

Network	Description	Weight
Physical interactions		**77.4%**
Foster-Klip-2006	Direct interaction Pubmed 16396496 Tags: Cell Line; Cultured Cells; Stem Cells	18.92%
Edmondson-Ping-2002	Direct interaction Pubmed 12169683 Tags: Muscle; Signal Transduction	15.52%
Husi-Grant-2000	Direct interaction Pubmed 10862698 Tags: Brain; Signal Transduction; Nervous System	8.53%
Tomomori-Sato-Conaway-2004	Direct interaction Pubmed 14638676 Tags: Cultured Cells; Cancer; Epithelial Cells; Cell Line; Liver; Transcription Factors	8.3%

Network	Description	Weight
Ping-Bolli-2001	Direct interaction Pubmed 11139474 Tags: Muscle; Signal Transduction	6.64%
Sánchez-Vidal-2007	Direct interaction Pubmed 17296600 Tags: Transcription Factors; Cell Line; Cultured Cells; Cancer	3.97%
Mikula-Ostrowski-2006	Direct interaction Pubmed 16518874 Tags: Cultured Cells; Signal Transduction; Cancer; Cell Line; Immune System; Transcription Factors	3.75%
Berggård-James-2006	Direct interaction Pubmed 16512683 Tags: Brain; Nervous System	2.87%
Cross-Hamilton-2005	Direct interaction Pubmed 16267818 Tags: Signal Transduction; Cancer	2.7%
Daulat-Jockers-2007	Direct interaction Pubmed 17215244 Tags: Cultured Cells; Cell Line	1.74%
Shiio-Eisenman-2006	Direct interaction Pubmed 16449650 Tags: Cultured Cells; Cancer; Epithelial Cells; Cell Line; Fibroblasts; Transcription Factors	1.7%
PATHWAYCOMMONS-under-threshold	Direct interaction PATHWAY COMMONS under-threshold	0.57%
Babusiak-Vyoral-2007	Direct interaction Pubmed 17205597 Tags: BALB C	0.49%
Drakas-Baserga-2005	Direct interaction Pubmed 15602769 Tags: Development; Cultured Cells; Cell Proliferation; Cell Line; Fibroblasts; Stem Cells	0.48%
Hermjakob-Apweiler-2004	Direct interaction Pubmed 14681455	0.4%
BIOGRID	Direct interaction	0.38%
Ravasi-Hayashizaki-2010_mouse	Pubmed 20211142 Tags: Cell Proliferation; Transcription Factors	0.28%
Navarro-Lérida-Rodríguez-Crespo-2004	Direct interaction Pubmed 14760703 Tags: Brain; Nervous System	0.16%
Papin-Subramaniam-2004	Direct interaction Pubmed 15102471 Tags: Signal Transduction	0.01%

Network	Description	Weight
Co-expression		**9.89%**
Zapala-Barlow-2005	Pearson correlation Pubmed 16002470 GEO GSE3594 Tags: Development; Transcription Factors	1.34%
Shearstone-Perrin-2006	Pearson correlation Pubmed 16624518 GEO GSE5130 Tags: Immune System	0.85%
Gallardo-Castrillon-2007	Pearson correlation Pubmed 17660561 GEO GSE8249 Tags: Cell Proliferation; Transcription Factors; Ovary; Knockout; Localization	0.73%
Anderson-Neville-2007	Pearson correlation Pubmed 17338830 GEO GSE8191 Tags: Cell Proliferation; Transcription Factors	0.72%
Akerblad-Sigvardsson-2005	Pearson correlation Pubmed 16106032 GEO GSE2192 Tags: Cell Proliferation; Transcription Factors; Cultured Cells; Cell Line; Fibroblasts	0.67%
Hernandez-Novoa-Kovacs-2008	Pearson correlation Pubmed 18467653 GEO GSE11005 Tags: Knockout; C57BL; Cell Signalling	0.6%
Mutch-Williamson-2006	Pearson correlation Pubmed 16455785 GEO GSE4262 Tags: Knockout; Transcription Factors; Liver	0.48%
Moggs-Orphanides-2004	Pearson correlation Pubmed 15598610 GEO GSE2195 Tags: Development; Transcription Factors	0.44%
Burgess-Herbert-Paigen-2008	Pearson correlation Pubmed 18845850 GEO GSE10493	0.42%
Sciuto-Dillman-2005	Pearson correlation Pubmed 16300373 GEO GSE2565 Tags: Lung	0.41%
Hovatta-Barlow-2005	Pearson correlation Pubmed 16244648 GEO GSE3327 Tags: Brain	0.41%
Keeley-Abel	Pearson correlation Pubmed 16547164 GEO GSE3963 Tags: C57BL; Brain	0.33%
Zamparini-Brickman-2006	Pearson correlation Pubmed 16936074 GEO GSE5141 Tags: Development; Cell Signalling; Signal Transduction; Localization; Cell Line; Cultured Cells; Stem Cells; Transcription Factors	0.33%
Sajan-Lovett-2007	Pearson correlation Pubmed 17660535 GEO GSE7536 Tags: Signal Transduction; Localization	0.32%

Network	Description	Weight
Rosen-Lau-2007	Pearson correlation Pubmed 17681415 GEO GSE13044 Tags: Pregnancy; Development; Lung; Liver; Transcription Factors	0.32%
Lovegrove-Liles-2007	Pearson correlation Pubmed 17991715 GEO GSE7814 Tags: Apoptosis; Cell Signalling; Brain; Disease; Immune System	0.32%
Sugino-Nelson-2006	Pearson correlation Pubmed 16369481 GEO GSE2882 Tags: Brain; Localization; Nervous System; Immune System	0.32%
Barger-Prolla-2008	Pearson correlation Pubmed 18523577 GEO GSE11291 Tags: C57BL; Aging	0.31%
Cernetich-Klein-2006	Pearson correlation Pubmed 16714546 GEO GSE4324 Tags: C57BL; Cell Signalling; Immune System	0.3%
Brownstein-Mannick-2006	Pearson correlation Pubmed 16478828 GEO GSE2278 Tags: C57BL; Immune System	0.29%
Predicted		**8.76%**
PPI-OPHID	Pubmed 15657099	0.93%
I2D_Li-Vidal-2004_interolog_Worm2Mouse	Direct interaction I2D predictions of protein protein interactions for Mus musculus using Li-Vidal-2004 Caenorhabditis elegans data Pubmed 14704431 I2D INTEROLOG	0.86%
I2D_BIND_Rat2Mouse	Direct interaction I2D predictions of protein protein interactions for Mus musculus using BIND Rattus norvegicus data I2D BIND_Rat	0.76%
I2D_vonMering-Bork-2002_High_Yeast2Mouse	Direct interaction I2D predictions of protein protein interactions for Mus musculus using vonMering-Bork-2002 Saccharomyces cerevisiae data Pubmed 12000970 I2D YeastHigh	0.73%
I2D_Deribe-Dikic-2009_Human2Mouse	Direct interaction I2D predictions of protein protein interactions for Mus musculus using Deribe-Dikic-2009 Homo sapiens data Pubmed 20029029 I2D MYTH4	0.68%
I2D_vonMering-Bork-2002_Medium_Yeast2Mouse	Direct interaction I2D predictions of protein protein interactions for Mus musculus using vonMering-Bork-2002 Saccharomyces cerevisiae data Pubmed 12000970 I2D YeastMedium	0.46%
I2D_IntAct_Rat2Mouse	Direct interaction I2D predictions of protein protein interactions for Mus musculus using IntAct Rattus norvegicus data I2D IntAct_Rat	0.45%

Network	Description	Weight
I2D_Jorgensen-Pawson-2009_Human2Mouse	Direct interaction I2D predictions of protein protein interactions for Mus musculus using Jorgensen-Pawson-2009 Homo sapiens data Pubmed 20007894 I2D Jorgensen_EphR Tags: Cultured Cells; Signal Transduction; Cell Line	0.43%
I2D_Jones-MacBeath-2006_Human2Mouse	Direct interaction I2D predictions of protein protein interactions for Mus musculus using Jones-MacBeath-2006 Homo sapiens data Pubmed 16273093 I2D JonesErbB1 Tags: Cultured Cells; Cell Line	0.42%
I2D_small_scale	Direct interaction I2D predictions combined small-scale datasets I2D under_threshold	0.41%
I2D_IntAct_Fly2Mouse	Direct interaction I2D predictions of protein protein interactions for Mus musculus using IntAct Drosophila melanogaster data I2D IntAct_Fly	0.39%
I2D_HPRD_Human2Mouse	Direct interaction I2D predictions of protein protein interactions for Mus musculus using HPRD Homo sapiens data I2D HPRD	0.33%
Conservation profile-Inparanoid	Pubmed 15608241	0.3%
I2D_BIND_Human2Mouse	Direct interaction I2D predictions of protein protein interactions for Mus musculus using BIND Homo sapiens data I2D BIND	0.27%
I2D_Miller-Attisano-2009_Human2Mouse	Direct interaction I2D predictions of protein protein interactions for Mus musculus using Miller-Attisano-2009 Homo sapiens data Pubmed 19888210 I2D Miller_WntLumier Tags: Transcription Factors; Cultured Cells; Signal Transduction; Cell Line	0.23%
I2D_vonMering-Bork-2002_Low_Yeast2Mouse	Direct interaction I2D predictions of protein protein interactions for Mus musculus using vonMering-Bork-2002 Saccharomyces cerevisiae data Pubmed 12000970 I2D YeastLow	0.17%
I2D_Tarassov_PCA_Yeast2Mouse	Direct interaction I2D predictions of protein protein interactions for Mus musculus using Tarassov-Michnick-2008 Saccharomyces cerevisiae data Pubmed 18467557 I2D Tarassov_PCA Tags: Cell Proliferation	0.16%
I2D_Ingham-Pawson-2005_Human2Mouse	Direct interaction I2D predictions of protein protein interactions for Mus musculus using Ingham-Pawson-2005 Homo sapiens data Pubmed 16055720 I2D Pawson1 Tags: Cultured Cells; Cell Line; Cancer; Immune System	0.13%
I2D_IntAct_Human2Mouse	Direct interaction	0.11%

Network	Description	Weight
	I2D predictions of protein protein interactions for Mus musculus using IntAct Homo sapiens data I2D IntAct	
I2D_MINT_Human2Mouse	Direct interaction I2D predictions of protein protein interactions for Mus musculus using MINT Homo sapiens data I2D MINT	0.09%
I2D_IntAct_Yeast2Mouse	Direct interaction I2D predictions of protein protein interactions for Mus musculus using IntAct Saccharomyces cerevisiae data I2D IntAct_Yeast	0.08%
I2D_Stelzl-Wanker-2005_High_Human2Mouse	Direct interaction I2D predictions of protein protein interactions for Mus musculus using Stelzl-Wanker-2005 Homo sapiens data Pubmed 16169070 I2D StelzlHigh Tags: Transcription Factors; Nervous System	0.08%
I2D_MINT_Yeast2Mouse	Direct interaction I2D predictions of protein protein interactions for Mus musculus using MINT Saccharomyces cerevisiae data I2D MINT_Yeast	0.06%
I2D_BioGRID_Yeast2Mouse	Direct interaction I2D predictions of protein protein interactions for Mus musculus using BioGRID Saccharomyces cerevisiae data I2D BioGRID_Yeast	0.05%
I2D_Giot-Rothbert-2003-High_Fly2Mouse	Direct interaction I2D predictions of protein protein interactions for Mus musculus using Giot-Rothbert-2003 Drosophila melanogaster data Pubmed 14605208 I2D FlyHigh Tags: Cell Proliferation; Signal Transduction; Nervous System; Immune System	0.04%
I2D_Giot-Rothbert-2003-Low_Fly2Mouse	Direct interaction I2D predictions of protein protein interactions for Mus musculus using Giot-Rothbert-2003 Drosophila melanogaster data Pubmed 14605208 I2D FlyLow Tags: Cell Proliferation; Signal Transduction; Nervous System; Immune System	0.04%
I2D_Stanyon-Finley-2004-CellCycle_Fly2Mouse	Direct interaction I2D predictions of protein protein interactions for Mus musculus using Stanyon-Finley-2004 Drosophila melanogaster data Pubmed 15575970 I2D FlyCellCycle Tags: Transcription Factors	0.03%
I2D_Li-Vidal-2004_CORE_2_Worm2Mouse	Direct interaction I2D predictions of protein protein interactions for Mus musculus using Li-Vidal-2004 Caenorhabditis elegans data Pubmed 14704431 I2D CORE_2	0.03%
I2D_Rual-Vidal-2004-non_core_Human2Mouse	Direct interaction I2D predictions of protein protein interactions for Mus musculus using Rual-Vidal-2005 Homo sapiens data Pubmed 16189514 I2D VidalHuman_non_core	0.02%

Network	Description	Weight
I2D_Formstecher-Daviet-2005-Embryo_Fly2Mouse	Direct interaction I2D predictions of protein protein interactions for Mus musculus using Formstecher-Daviet-2005 Drosophila melanogaster data Pubmed 15710747 I2D FlyEmbryo Tags: Cancer	0.01%
I2D_Ptacek-Snyder-2005_Yeast2Mouse	Direct interaction I2D predictions of protein protein interactions for Mus musculus using Ptacek-Snyder-2005 Saccharomyces cerevisiae data Pubmed 16319894 I2D Yeast_Kinome	0.01%
Other		**2.51%**
Phenotype-MGI	Pubmed 17135206 Tags: Knockout; Disease	1.9%
Disease associations-OMIM	Pubmed 15608251	0.5%
Conservation profile-Phylogeny	Pubmed 14707178	0.11%
Co-localization		**1.44%**
Su-Hogenesch-2004	Pubmed 15075390	0.73%
Zhang-Hughes-2004	Pubmed 15588312	0.4%
Siddiqui-Marra-2005	Pubmed 16352711 Tags: C57BL; Development; Transcription Factors	0.3%

Query Parameters

Organism	M. musculus
Network weighting	Automatically selected weighting method (Biological process based)
Number of related genes	10
Input genes	Prc1
Networks	

Other
- Disease associations-OMIM
- Phenotype-MGI
- Conservation profile-Phylogeny

Predicted
- I2D_BIND_Human2Mouse
- I2D_BIND_Fly2Mouse
- I2D_BIND_Rat2Mouse
- I2D_BIND_Worm2Mouse
- I2D_BIND_Yeast2Mouse
- I2D_BioGRID_Yeast2Mouse
- I2D_Li-Vidal-2004_CE_DATA_Worm2Mouse
- I2D_Li-Vidal-2004_CORE_2_Worm2Mouse
- I2D_Stanyon-Finley-2004-CellCycle_Fly2Mouse

I2D_Formstecher-Daviet-2005-Embryo_Fly2Mouse
I2D_Giot-Rothbert-2003-High_Fly2Mouse
I2D_Giot-Rothbert-2003-Low_Fly2Mouse
I2D_HPRD_Human2Mouse
I2D_IntAct_Human2Mouse
I2D_IntAct_Fly2Mouse
I2D_IntAct_Rat2Mouse
I2D_IntAct_Worm2Mouse
I2D_IntAct_Yeast2Mouse
I2D_Li-Vidal-2004_interolog_Worm2Mouse
I2D_Jones-MacBeath-2006_Human2Mouse
I2D_Jorgensen-Pawson-2009_Human2Mouse
I2D_Krogan-Greenblatt-2006_Core_Yeast2Mouse
I2D_Krogan-Greenblatt-2006_NonCore_Yeast2Mouse
I2D_Miller-Attisano-2009_Human2Mouse
I2D_MINT_Human2Mouse
I2D_MINT_Fly2Mouse
I2D_MINT_Worm2Mouse
I2D_MINT_Yeast2Mouse
I2D_MIPS_Yeast2Mouse
I2D_Deribe-Dikic-2009_Human2Mouse
I2D_Li-Vidal-2004_NON_CORE_Worm2Mouse
I2D_Ingham-Pawson-2005_Human2Mouse
I2D_Wu-Li-2007_Human2Mouse
I2D_Stelzl-Wanker-2005_High_Human2Mouse
I2D_Stelzl-Wanker-2005_Low_Medium_Human2Mouse
I2D_Tarassov_PCA_Yeast2Mouse
I2D_small_scale
I2D_Rual-Vidal-2004-core_Human2Mouse
I2D_Rual-Vidal-2004-non_core_Human2Mouse
I2D_Barrios-Rodiles-Wrana-2005_Human2Mouse
I2D_Ptacek-Snyder-2005_Yeast2Mouse
I2D_vonMering-Bork-2002_High_Yeast2Mouse
I2D_vonMering-Bork-2002_Low_Yeast2Mouse
I2D_vonMering-Bork-2002_Medium_Yeast2Mouse
I2D_Yu-Vidal-2008_GoldStd_Yeast2Mouse
Conservation profile-Inparanoid
PPI-OPHID

Co-localization

Siddiqui-Marra-2005
Su-Hogenesch-2004
Zhang-Hughes-2004

Physical interactions

BIOGRID
Husi-Grant-2000
Ping-Bolli-2001
Suzuki-Hayashizaki-2001
Edmondson-Ping-2002
Tomomori-Sato-Conaway-2004
Hermjakob-Apweiler-2004
Navarro-Lérida-Rodríguez-Crespo-2004

Papin-Subramaniam-2004
Sato-Conaway-2004
Hassel-Souchelnytskyi-2004
Drakas-Baserga-2005
Babusiak-Vyoral-2005
Barrios-Rodiles-Wrana-2005
Cross-Hamilton-2005
Foster-Klip-2006
Shiio-Eisenman-2006
Berggård-James-2006
Mikula-Ostrowski-2006
Zong-Ping-2006
Gomes-Ping-2006
Qiu-Goldberg-2006
Babusiak-Vyoral-2007
Daulat-Jockers-2007
Sánchez-Vidal-2007
Vera-Jaumot-2007
PATHWAYCOMMONS-under-threshold
Ravasi-Hayashizaki-2010_mouse

Co-expression

Burgess-Herbert-Paigen-2008
Hernandez-Novoa-Kovacs-2008
Barger-Prolla-2008
Rosen-Lau-2007
Akerblad-Sigvardsson-2005
Moggs-Orphanides-2004
Brownstein-Mannick-2006
Sciuto-Dillman-2005
Sugino-Nelson-2006
Hovatta-Barlow-2005
Zapala-Barlow-2005
Keeley-Abel
Mutch-Williamson-2006
Cernetich-Klein-2006
Shearstone-Perrin-2006
Zamparini-Brickman-2006
Sajan-Lovett-2007
Lovegrove-Liles-2007
Anderson-Neville-2007
Gallardo-Castrillon-2007

PERMISSIONS

ELSEVIER LICENSE TERMS AND CONDITIONS

Feb 15, 2011

This is a License Agreement between Lara Kouri ("You") and Elsevier ("Elsevier") provided by Copyright Clearance Center ("CCC"). The license consists of your order details, the terms and conditions provided by Elsevier, and the payment terms and conditions.

All payments must be made in full to CCC. For payment instructions, please see information listed at the bottom of this form.

Supplier	Elsevier Limited The Boulevard,Langford
Registered Company Number	1982084
Customer name	Lara Kouri
Customer address	
License number	2610270744071
License date	Feb 15, 2011
Licensed content publisher	Elsevier
Licensed content publication	Molecular Cell
Licensed content title	PRC1: A Human Mitotic Spindle–Associated CDK Substrate Protein Required for Cytokinesis
Licensed content author	Wei Jiang, Gretchen Jimenez, Nicholas J Wells, Thomas J Hope, Geoffrey M Wahl, Tony Hunter, Rikiro Fukunaga
Licensed content date	December 1998
Licensed content volume number	2
Licensed content issue number	6
Number of pages	9
Start Page	877
End Page	885
Type of Use	reuse in a thesis/dissertation
Portion	figures/tables/illustrations
Number of figures/tables/illustrations	2
Format	both print and electronic
Are you the author of this Elsevier article?	No
Will you be translating?	No
Order reference number	
Title of your thesis/dissertation	Identifying Genetic Factors and Processes Involved in the Perinatal Heart Transitional Program
Expected completion date	Mar 2011
Estimated size (number of pages)	100
Elsevier VAT number	GB 494 6272 12
Permissions price	0.00 USD
VAT/Local Sales Tax	0.0 USD / 0.0 GBP
Total	0.00 USD

Terms and Conditions

INTRODUCTION

1. The publisher for this copyrighted material is Elsevier. By clicking "accept" in connection with completing this licensing transaction, you agree that the following terms and conditions apply to this transaction (along with the Billing and Payment terms and conditions established by Copyright Clearance Center, Inc. ("CCC"), at the time that you opened your Rightslink account and that are available at any time at http://myaccount.copyright.com).

GENERAL TERMS

2. Elsevier hereby grants you permission to reproduce the aforementioned material subject to the terms and conditions indicated.
3. Acknowledgement: If any part of the material to be used (for example, figures) has appeared in our publication with credit or acknowledgement to another source, permission must also be sought from that source. If such permission is not obtained then that material may not be included in your publication/copies. Suitable acknowledgement to the source must be made, either as a footnote or in a reference list at the end of your publication, as follows:
"Reprinted from Publication title, Vol /edition number, Author(s), Title of article / title of chapter, Pages No., Copyright (Year), with permission from Elsevier [OR APPLICABLE SOCIETY COPYRIGHT OWNER]." Also Lancet special credit - "Reprinted from The Lancet, Vol. number, Author(s), Title of article, Pages No., Copyright (Year), with permission from Elsevier."
4. Reproduction of this material is confined to the purpose and/or media for which permission is hereby given.
5. Altering/Modifying Material: Not Permitted. However figures and illustrations may be altered/adapted minimally to serve your work. Any other abbreviations, additions, deletions and/or any other alterations shall be made only with prior written authorization of Elsevier Ltd. (Please contact Elsevier)
6. If the permission fee for the requested use of our material is waived in this instance, please be advised that your future requests for Elsevier materials may attract a fee.
7. Reservation of Rights: Publisher reserves all rights not specifically granted in the combination of (i) the license details provided by you and accepted in the course of this licensing transaction, (ii) these terms and conditions and (iii) CCC's Billing and Payment terms and conditions.
8. License Contingent Upon Payment: While you may exercise the rights licensed immediately upon issuance of the license at the end of the licensing process for the transaction, provided that you have disclosed complete and accurate details of your proposed use, no license is finally effective unless and until full payment is received from you (either by publisher or by CCC) as provided in CCC's Billing and Payment terms and conditions. If full payment is not received on a timely basis, then any license preliminarily granted shall be deemed automatically revoked and shall be void as if never granted. Further, in the event that you breach any of these terms and conditions or any of CCC's Billing and Payment terms and conditions, the license is automatically revoked and shall be void as if never granted. Use of materials as described in a revoked license, as well as any use of the materials beyond the scope of an unrevoked license, may constitute copyright infringement and publisher reserves the right to take any and all action to protect its copyright in the materials.
9. Warranties: Publisher makes no representations or warranties with respect to the licensed material.
10. Indemnity: You hereby indemnify and agree to hold harmless publisher and CCC, and their respective officers, directors, employees and agents, from and against any and all claims arising out of your use of the licensed material other than as specifically authorized pursuant to this

license.
11. No Transfer of License: This license is personal to you and may not be sublicensed, assigned, or transferred by you to any other person without publisher's written permission.
12. No Amendment Except in Writing: This license may not be amended except in a writing signed by both parties (or, in the case of publisher, by CCC on publisher's behalf).
13. Objection to Contrary Terms: Publisher hereby objects to any terms contained in any purchase order, acknowledgment, check endorsement or other writing prepared by you, which terms are inconsistent with these terms and conditions or CCC's Billing and Payment terms and conditions. These terms and conditions, together with CCC's Billing and Payment terms and conditions (which are incorporated herein), comprise the entire agreement between you and publisher (and CCC) concerning this licensing transaction. In the event of any conflict between your obligations established by these terms and conditions and those established by CCC's Billing and Payment terms and conditions, these terms and conditions shall control.
14. Revocation: Elsevier or Copyright Clearance Center may deny the permissions described in this License at their sole discretion, for any reason or no reason, with a full refund payable to you. Notice of such denial will be made using the contact information provided by you. Failure to receive such notice will not alter or invalidate the denial. In no event will Elsevier or Copyright Clearance Center be responsible or liable for any costs, expenses or damage incurred by you as a result of a denial of your permission request, other than a refund of the amount(s) paid by you to Elsevier and/or Copyright Clearance Center for denied permissions.

LIMITED LICENSE

The following terms and conditions apply only to specific license types:
15. **Translation**: This permission is granted for non-exclusive world **English** rights only unless your license was granted for translation rights. If you licensed translation rights you may only translate this content into the languages you requested. A professional translator must perform all translations and reproduce the content word for word preserving the integrity of the article. If this license is to re-use 1 or 2 figures then permission is granted for non-exclusive world rights in all languages.
16. **Website**: The following terms and conditions apply to electronic reserve and author websites:
Electronic reserve: If licensed material is to be posted to website, the web site is to be password-protected and made available only to bona fide students registered on a relevant course if: This license was made in connection with a course, This permission is granted for 1 year only. You may obtain a license for future website posting, All content posted to the web site must maintain the copyright information line on the bottom of each image, A hyper-text must be included to the Homepage of the journal from which you are licensing at http://www.sciencedirect.com/science/journal/xxxxx or the Elsevier homepage for books at http://www.elsevier.com , and Central Storage: This license does not include permission for a scanned version of the material to be stored in a central repository such as that provided by Heron/XanEdu.
17. **Author website** for journals with the following additional clauses: All content posted to the web site must maintain the copyright information line on the bottom of each image, and he permission granted is limited to the personal version of your paper. You are not allowed to download and post the published electronic version of your article (whether PDF or HTML, proof or final version), nor may you scan the printed edition to create an electronic version, A hyper-text must be included to the Homepage of the journal from which you are licensing at http://www.sciencedirect.com/science/journal/xxxxx , As part of our normal production process, you will receive an e-mail notice when your article appears on Elsevier's online service ScienceDirect (www.sciencedirect.com). That e-mail will include the article's Digital Object Identifier (DOI). This number provides the electronic link to the published article and should be

included in the posting of your personal version. We ask that you wait until you receive this e-mail and have the DOI to do any posting. Central Storage: This license does not include permission for a scanned version of the material to be stored in a central repository such as that provided by Heron/XanEdu.

18. **Author website** for books with the following additional clauses: Authors are permitted to place a brief summary of their work online only. A hyper-text must be included to the Elsevier homepage at http://www.elsevier.com
All content posted to the web site must maintain the copyright information line on the bottom of each image You are not allowed to download and post the published electronic version of your chapter, nor may you scan the printed edition to create an electronic version. Central Storage: This license does not include permission for a scanned version of the material to be stored in a central repository such as that provided by Heron/XanEdu.
19. **Website** (regular and for author): A hyper-text must be included to the Homepage of the journal from which you are licensing at http://www.sciencedirect.com/science/journal/xxxxx. or for books to the Elsevier homepage at http://www.elsevier.com
20. **Thesis/Dissertation**: If your license is for use in a thesis/dissertation your thesis may be submitted to your institution in either print or electronic form. Should your thesis be published commercially, please reapply for permission. These requirements include permission for the Library and Archives of Canada to supply single copies, on demand, of the complete thesis and include permission for UMI to supply single copies, on demand, of the complete thesis. Should your thesis be published commercially, please reapply for permission.
21. Other Conditions:
v1.6

Gratis licenses (referencing $0 in the Total field) are free. Please retain this printable license for your reference. No payment is required.

WOLTERS KLUWER HEALTH LICENSE TERMS AND CONDITIONS

Feb 15, 2011

This is a License Agreement between Lara Kouri ("You") and Wolters Kluwer Health ("Wolters Kluwer Health") provided by Copyright Clearance Center ("CCC"). The license consists of your order details, the terms and conditions provided by Wolters Kluwer Health, and the payment terms and conditions.

All payments must be made in full to CCC. For payment instructions, please see information listed at the bottom of this form.

License Number	2610290535691
License date	Feb 15, 2011
Licensed content publisher	Wolters Kluwer Health
Licensed content publication	Circulation Research
Licensed content title	Toward MicroRNA-Based Therapeutics for Heart Disease: The Sense in Antisense
Licensed content author	Eva van Rooij
Licensed content date	Oct 24, 2008
Volume Number	103
Issue Number	9
Type of Use	Dissertation/Thesis
Requestor type	Individual
Title of your thesis / dissertation	Identifying Genetic Factors and Processes Involved in the Perinatal Heart Transitional Program
Expected completion date	Mar 2011
Estimated size(pages)	100
Billing Type	Invoice
Billing Address	
Customer reference info	
Total	0.00 USD
Terms and Conditions	

Terms and Conditions

1. A credit line will be prominently placed and include: for books - the author(s), title of book, editor, copyright holder, year of publication; For journals - the author(s), title of article, title of journal, volume number, issue number and inclusive pages.
2. The requestor warrants that the material shall not be used in any manner which may be considered derogatory to the title, content, or authors of the material, or to Wolters Kluwer/Lippincott, Williams & Wilkins.
3. Permission is granted for one time use only as specified in your correspondence. Rights herein do not apply to future reproductions, editions, revisions, or other derivative works. Once term has expired, permission to renew must be made in writing.
4. Permission granted is non-exclusive, and is valid throughout the world in the English language

and the languages specified in your original request.
5. Wolters Kluwer Health/ Lippincott, Williams & Wilkins, cannot supply the requestor with the original artwork or a "clean copy."
6. The requestor agrees to secure written permission from the author (for book material only).
7. Permission is valid if the borrowed material is original to a LWW imprint (Lippincott-Raven Publishers, Williams & Wilkins, Lea & Febiger, Harwal, Igaku-Shoin, Rapid Science, Little Brown & Company, Harper & Row Medical, American Journal of Nursing Co, and Urban & Schwarzenberg - English Language).
8. If you opt not to use the material requested above, please notify Rightslink within 90 days of the original invoice date.
9. Other Terms and Conditions:

v1.0
Gratis licenses (referencing $0 in the Total field) are free. Please retain this printable license for your reference. No payment is required.

THE AMERICAN ASSOCIATION FOR THE ADVANCEMENT OF SCIENCE LICENSE TERMS AND CONDITIONS

Mar 07, 2011

This is a License Agreement between Lara Kouri ("You") and The American Association for the Advancement of Science ("The American Association for the Advancement of Science") provided by Copyright Clearance Center ("CCC"). The license consists of your order details, the terms and conditions provided by The American Association for the Advancement of Science, and the payment terms and conditions.

All payments must be made in full to CCC. For payment instructions, please see information listed at the bottom of this form.

License Number	2623800488993
License date	Mar 07, 2011
Licensed content publisher	The American Association for the Advancement of Science
Licensed content publication	Science
Licensed content title	The Molecular Requirements for Cytokinesis
Licensed content author	Michael Glotzer
Licensed content date	Mar 1, 2005
Type of Use	Thesis / Dissertation
Requestor type	Other Individual
Format	Print and electronic
Portion	Figure
Number of figures/tables	1
Order reference number	
Title of your thesis / dissertation	Identifying Genetic Factors and Processes Involved in the Perinatal Heart Transitional Program
Expected completion date	Mar 2011
Estimated size(pages)	100
Total	0.00 USD

Terms and Conditions

American Association for the Advancement of Science TERMS AND CONDITIONS

Regarding your request, we are pleased to grant you non-exclusive, non-transferable permission, to republish the AAAS material identified above in your work identified above, subject to the terms and conditions herein. We must be contacted for permission for any uses other than those specifically identified in your request above.

The following credit line must be printed along with the AAAS material: "From [Full Reference Citation]. Reprinted with permission from AAAS."

All required credit lines and notices must be visible any time a user accesses any part of the AAAS material and must appear on any printed copies and authorized user might make.

This permission does not apply to figures / photos / artwork or any other content or materials included in your work that are credited to non-AAAS sources. If the requested material is sourced to or references non-AAAS sources, you must obtain authorization from that source as well before using that material. You agree to hold harmless and indemnify AAAS against any claims arising from your use of any content in your work that is credited to non-AAAS sources.

If the AAAS material covered by this permission was published in Science during the years 1974 - 1994, you must also obtain permission from the author, who may grant or withhold permission, and who may or may not charge a fee if permission is granted. See original article for author's address. This condition does not apply to news articles.

The AAAS material may not be modified or altered except that figures and tables may be modified with permission from the author. Author permission for any such changes must be secured prior to your use.

Whenever possible, we ask that electronic uses of the AAAS material permitted herein include a hyperlink to the original work on AAAS's website (hyperlink may be embedded in the reference citation).

AAAS material reproduced in your work identified herein must not account for more than 30% of the total contents of that work.

AAAS must publish the full paper prior to use of any text.

AAAS material must not imply any endorsement by the American Association for the Advancement of Science.

This permission is not valid for the use of the AAAS and/or Science logos.

AAAS makes no representations or warranties as to the accuracy of any information contained in the AAAS material covered by this permission, including any warranties of merchantability or fitness for a particular purpose.

If permission fees for this use are waived, please note that AAAS reserves the right to charge for reproduction of this material in the future.

Permission is not valid unless payment is received within sixty (60) days of the issuance of this permission. If payment is not received within this time period then all rights granted herein shall be revoked and this permission will be considered null and void.

In the event of breach of any of the terms and conditions herein or any of CCC's Billing and Payment terms and conditions, all rights granted herein shall be revoked and this permission will be considered null and void.

AAAS reserves the right to terminate this permission and all rights granted herein at its discretion, for any purpose, at any time. In the event that AAAS elects to terminate this permission, you will have no further right to publish, publicly perform, publicly display, distribute or otherwise use any matter in which the AAAS content had been included, and all fees paid hereunder shall be fully refunded to you. Notification of termination will be sent to the contact information as supplied by you during the request process and termination shall be immediate upon sending the notice. Neither AAAS nor CCC shall be liable for any costs, expenses, or damages you may incur as a result of the termination of this permission, beyond the refund noted above.

This Permission may not be amended except by written document signed by both parties.

The terms above are applicable to all permissions granted for the use of AAAS material. Below you will find additional conditions that apply to your particular type of use.

FOR A THESIS OR DISSERTATION
If you are using figure(s)/table(s), permission is granted for use in print and electronic versions of your dissertation or thesis. A full text article may be used in print versions only of a dissertation or thesis.

Permission covers the distribution of your dissertation or thesis on demand by ProQuest / UMI, provided the AAAS material covered by this permission remains in situ.

If you are an Original Author on the AAAS article being reproduced, please refer to your License to Publish for rules on reproducing your paper in a dissertation or thesis.

FOR JOURNALS:
Permission covers both print and electronic versions of your journal article, however the AAAS material may not be used in any manner other than within the context of your article.

FOR BOOKS/TEXTBOOKS:
If this license is to reuse figures/tables, then permission is granted for non-exclusive world rights in all languages in both print and electronic formats (electronic formats are defined below).

If this license is to reuse a text excerpt or a full text article, then permission is granted for non-exclusive world rights in English only. You have the option of securing either print or electronic rights or both, but electronic rights are not automatically granted and do garner additional fees. Permission for translations of text excerpts or full text articles into other languages must be obtained

separately.

Licenses granted for use of AAAS material in electronic format books/textbooks are valid only in cases where the electronic version is equivalent to or substitutes for the print version of the book/textbook. The AAAS material reproduced as permitted herein must remain in situ and must not be exploited separately (for example, if permission covers the use of a full text article, the article may not be offered for access or for purchase as a stand-alone unit), except in the case of permitted textbook companions as noted below.

You must include the following notice in any electronic versions, either adjacent to the reprinted AAAS material or in the terms and conditions for use of your electronic products: "Readers may view, browse, and/or download material for temporary copying purposes only, provided these uses are for noncommercial personal purposes. Except as provided by law, this material may not be further reproduced, distributed, transmitted, modified, adapted, performed, displayed, published, or sold in whole or in part, without prior written permission from the publisher."

If your book is an academic textbook, permission covers the following companions to your textbook, provided such companions are distributed only in conjunction with your textbook at no additional cost to the user:

- Password-protected website
- Instructor's image CD/DVD and/or PowerPoint resource
- Student CD/DVD

All companions must contain instructions to users that the AAAS material may be used for non-commercial, classroom purposes only. Any other uses require the prior written permission from AAAS.

Rights also extend to copies/files of your Work (as described above) that you are required to provide for use by the visually and/or print disabled in compliance with state and federal laws.

This permission only covers a single edition of your work as identified in your request.

FOR NEWSLETTERS:
Permission covers print and/or electronic versions, provided the AAAS material reproduced as permitted herein remains in situ and is not exploited separately (for example, if permission covers the use of a full text article, the article may not be offered for access or for purchase as a stand-alone unit)

FOR ANNUAL REPORTS:
Permission covers print and electronic versions provided the AAAS material reproduced as permitted herein remains in situ and is not exploited separately (for example, if permission covers the use of a full text article, the article may not be offered for access or for purchase as a stand-alone unit)

FOR PROMOTIONAL/MARKETING USES:
Permission covers the use of AAAS material in promotional or marketing pieces such as information packets, media kits, product slide kits, brochures, or flyers limited to a single print run.

The AAAS Material may not be used in any manner which implies endorsement or promotion by the American Association for the Advancement of Science (AAAS) or Science of any product or service. AAAS does not permit the reproduction of its name, logo or text on promotional literature.

If permission to use a full text article is permitted, The Science article covered by this permission must not be altered in any way. No additional printing may be set onto an article copy other than the copyright credit line required above. Any alterations must be approved in advance and in writing by AAAS. This includes, but is not limited to, the placement of sponsorship identifiers, trademarks, logos, rubber stamping or self-adhesive stickers onto the article copies.

Additionally, article copies must be a freestanding part of any information package (i.e. media kit) into which they are inserted. They may not be physically attached to anything, such as an advertising insert, or have anything attached to them, such as a sample product. Article copies must be easily removable from any kits or informational packages in which they are used. The only exception is that article copies may be inserted into three-ring binders.

FOR CORPORATE INTERNAL USE:
The AAAS material covered by this permission may not be altered in any way. No additional printing may be set onto an article copy other than the required credit line. Any alterations must be approved in advance and in writing by AAAS. This includes, but is not limited to the placement of sponsorship identifiers, trademarks, logos, rubber stamping or self-adhesive stickers onto article copies.

If you are making article copies, copies are restricted to the number indicated in your request and must be distributed only to internal employees for internal use.

If you are using AAAS Material in Presentation Slides, the required credit line must be visible on the slide where the AAAS material will be reprinted

If you are using AAAS Material on a CD, DVD, Flash Drive, or the World Wide Web, you must include the following notice in any electronic versions, either adjacent to the reprinted AAAS material or in the terms and conditions for use of your electronic products: "Readers may view, browse, and/or download material for temporary copying purposes only, provided these uses are for noncommercial personal purposes. Except as provided by law, this material may not be further reproduced, distributed, transmitted, modified, adapted, performed, displayed, published, or sold in whole or in part, without prior written permission from the publisher." Access to any such CD, DVD, Flash Drive or Web page must be restricted to your organization's employees only.

FOR CME COURSE and SCIENTIFIC SOCIETY MEETINGS:
Permission is restricted to the particular Course, Seminar, Conference, or Meeting indicated in your request. If this license covers a text excerpt or a Full Text Article, access to the reprinted AAAS material must be restricted to attendees of your event only (if you have been granted electronic rights for use of a full text article on your website, your website must be password protected, or access restricted so that only attendees can access the content on your site).

If you are using AAAS Material on a CD, DVD, Flash Drive, or the World Wide Web, you must include the following notice in any electronic versions, either adjacent to the reprinted AAAS material or in the terms and conditions for use of your electronic products: "Readers may view,

FOR MOVIES / FILM / TELEVISION:
Permission is granted to use, record, film, photograph, and/or tape the AAAS material in connection with your program/film and in any medium your program/film may be shown or heard, including but not limited to broadcast and cable television, radio, print, world wide web, and videocassette.

The required credit line should run in the program/film's end credits.

FOR MUSEUM EXHIBITIONS:
Permission is granted to use the AAAS material as part of a single exhibition for the duration of that exhibit. Permission for use of the material in promotional materials for the exhibit must be cleared separately with AAAS.

FOR TRANSLATIONS:
Translation rights apply only to the language identified in your request summary above.

The following disclaimer must appear with your translation, on the first page of the article, after the credit line: "This translation is not an official translation by AAAS staff, nor is it endorsed by AAAS as accurate. In crucial matters, please refer to the official English-language version originally published by AAAS."

FOR USE ON A COVER:
Permission is granted to use the AAAS material on the cover of a journal issue, newsletter issue, book, textbook, or annual report in print and electronic formats provided the AAAS material reproduced as permitted herein remains in situ and is not exploited separately

By using the AAAS Material identified in your request, you agree to abide by all the terms and conditions herein.

Questions about these terms can be directed to the AAAS Permissions department.

v 2 **Gratis licenses (referencing $0 in the Total field) are free. Please retain this printable license for your reference. No payment is required.**

Dear Lara,

Permission is granted with no charge.

The acknowledgement should state "reproduced / adapted with permission" and give the source journal name - the acknowledgement should either provide full citation details or refer to the relevant citation in the article reference list - the full citation details should include authors, journal, year, volume, issue and page citation.

Where appearing online or in other electronic media, a link should be provided to the original article (e.g. via DOI):-

Journal of Cell Science: jcs.biologists.org

Best wishes,
Sue Chamberlain

On 16/2/11 00:44, "Lara Kouri" wrote:

Hi Mr. Birch,

I am a graduate student writing my thesis at the University of Ottawa and I would really like to have permission to reprint a figure from the following paper: Chen, J., Callis, T., & Wang, D. (2009). microRNAs and Muscle Disorders. The Journal of Cell Science, *122*, 13-20.

Looking forward to hear from you,
Lara Kouri

CURRICULUM VITAE

Lara Kouri

Summary of Qualifications

- Master's of Science in Biochemistry
- Canadian Citizen
- Fluent in both official languages
- Great research and analytical skills
- Motivated, efficient, diligent and committed
- Effective and professional communicator

Education

M.Sc. Biochemistry June 2011
Cardiogenomic Perinatal Programming, Supervisor: Dr. Patrick Burgon
University of Ottawa Heart Institute, Ontario

B.Sc. Honours Biochemistry / Minor in Business Administration 2008
University of Ottawa, Ontario

WHMIS, Health and Safety, Animal Care, and Radiation Safety Training 2008-2010
University of Ottawa, Ontario

Ontario Secondary School Diploma - Concentration in Science 2003
Collège catholique Samuel-Genest, Ontario

Academic Awards and Achievements

- University of Ottawa Admission Scholarship
- Fellowships for Studying in French scholarship
- Two Msgr. Habib Kwaiter Scholarship Foundation scholarship
- Honour scholarship
- Merit Scholarship from the University of Ottawa
- Association of Part-Time Professors of the University of Ottawa Award
- 2nd place: 2007 Business Plan Competition hosted by the National Bank of Canada
- Dean's Honour List
- University of Ottawa graduate school Admission Scholarship
- Cash With Admission (CWA)
- Textbook and Technology Grant
- Ontario Graduate Scholarship (OGS)
- University of Ottawa National Excellence Scholarship
- CIHR Frederick Banting and Charles Best Canada Graduate Scholarship Master's Award
- Dean's Scholarship – Master's with Thesis

Employment Experience

University of Ottawa Heart Institute Summer Student Summer 2007, 2008
University of Ottawa Heart Institute Research Corporation, Ontario

- Research laboratory assistant in lipoprotein and atherosclerosis (2007, Dr. Sparks) and cardiovascular endocrinology (2008, Dr. Burgon).
- Set up and conduct biochemical experiments; operate and maintain laboratory equipment; prepare solutions, reagents, and sample formulations; compile and interpret experimental results; assist in developing and conducting sampling and analysis; optimize protocols.
- Perfected techniques: tissue culture, immunoblotting, electrophoresis (denaturing, native, lipid profiling), ELISA, radiolabelling, protein and lipid quantification, PCR, real-time PCR, sequencing, cloning, RNA extraction.

University of Ottawa Forensic Medicine Laboratory Technician May 5-6 2007
University of Ottawa, Ontario

- Research laboratory assistant: conduct a molecular biology and forensic medicine experiment to High School students in order to encourage them to study in Sciences (Dr. John Basso).

NSERC Summer Student Summer 2006

NSERC, Ontario

- Administrative tasks: enter and process applications in the database.
- Special projects: summarize information from internship files; test and comment the on-line application system; assemble company eligibility; create feedback letters; edit referee reports according to the Privacy Act.
- Program assistant for the Visiting Fellowship program: processing applications; handling daily email and telephone inquiries from international applicants; liaison between postdoctoral fellows and program coordinators working in other partner government departments.

Customer Service Specialist 2000 - 2008

Pronto-Ultramar, Ontario

- Supervisor: recognize strengths and limitations of others; plan, organize and monitor activities according to priorities; organize work autonomously or as part of a team.
- Control and adapt to interruptions, plan changes, issues and repetition without losing efficiency or composure.
- Train new employees according to the company's standards.

Mathematics Tutor 2003 - 2007

Collège catholique Samuel-Genest students, Ontario

- Work comfortably with figures.
- Identify and correct mathematical errors.
- Provide test and final exam preparation.
- Develop students' abilities to achieve higher quotas.

Skills

- Excellent knowledge of laboratory tools, data analysis, experimental design, equipment & procedures in biochemistry, genomics & molecular biology:
  - Nucleic acid (including microRNA) & protein extraction from tissue & cells
  - Primer design
  - RT-PCR, Real-Time PCR
  - Immunological methods (Western Blot, ELISA, immunohistochemistry, immunofluorescence)
  - Radioactivity assays
  - Exon & microRNA microarray experiments
  - Sequencing & cloning
  - Mammalian cell culture
- Experience working in a level 2 risk facility including hands-on experience in handling & working with mice.
- Providing training & technical guidance to students & colleagues.
- Excellent organizational, prioritization & time management skills.
- Interact, co-operate & communicate effectively & professionally with customers, the public & co-workers.
- Thorough editing & providing feedback of manuscripts for publication in peer-reviewed scientific journals & grants.
- Committed to maintaining quality & efficiency.
- Experience in contributing to multidisciplinary teams.
- Strong ability to learn & apply new information.
- Pursue goals with diligence & take pride in accomplishments.
- Experience in conducting scientific literature searches & in working with scientific data (critical evaluation, analysis, interpretation, optimization, troubleshooting).
- Preparation of clear & concise documents summarizing & analyzing key scientific information.
- Analysis & development of scientific material in the form of presentations, technical reports, protocols & theses.
- Good knowledge of statistical analysis & interpretation of microarray (gene, exon & microRNA) & common laboratory data.
- Experience in application of computer software. Software skills: Microsoft Office, Flexarray, Partek® Genomics Suite, Affymetrix® Expression Console™, NAMIS, Adobe, SigmaPlot.
- At ease with Windows & Apple operating systems.
- Comfortable with bioinformatic sites: PubMed, DAVID Bioinformatics Resources 6.7 Microarray Analysis, TargetScan, miRBase, BLAST, UCSC BLAT, Primer3, Protein Data Bank etc.

Conferences/Seminars

- Attended the "Small RNAs: Biology and Technology" symposium at the Université de Montréal, Institute for Research in Immunology and Cancer (IRIC), Montréal, Québec, June 2008.
- Poster presentation at the "Making Muscle in the Embryo and Adult" meeting at the Columbia University in New York, New York, June 2009.
- Poster presentation at "The Ottawa Conference on New Directions in Biology and Disease of Skeletal Muscle", Ottawa, Ontario, May 2010.
- Oral presentation at the "UOHI Research Day" at the University of Ottawa Heart Institute in Ottawa, Ontario, May 2010.
- Accepted abstract for poster presentation to "OzBio 2010: The Molecules of Life - from Discovery to Biotechnology", Melbourne, Australia, September 2010.

Publications

- Pandey NR, Renwick J, Rabaa S, Misquith A, **Kouri L**, Twomey E, Sparks DL. "An Induction in Hepatic HDL Secretion Associated with Reduced ATPase Expression" published by The American Journal of Pathology; October 2009, 1777-87.
- Ahmady E, Deeke SA, Rabaa S, **Kouri L**, Kenney L, Stewart AFR, Burgon P. "Identification of a novel muscle enriched a-type lamin interacting protein (MLIP)" published by The Journal of Biological Chemistry, April 2011.

Volunteer Experience

Ultimate Canadian Marathon - Carleton Cup Volunteer 2009, 2010, 2011

Canadian Cystic Fibrosis Foundation, Ontario

- Register and inform racers, collect pledges and merchandise sales, collect waivers for the CCF "Skate, Run, Drink" Triathlon.

Lanopolis 4.0 Event Logistics Assistant October 2007

University of Ottawa, Ontario

- Assist in administrative and logistical planning.
- Attend meetings to organize the event.

Canadian Cancer Society Volunteer Summer 2005

Canadian Cancer Center, Ontario

- Aid in administrative tasks at the Radiation Therapy desk and at the Blood Laboratory.
- Greet patients and connect them with the services they require.
- Quickly grasp new concepts, approaches and systems.

Networking Cocktail Representative April 27, 2005

University of Ottawa, Ontario

- Helpful resource for the recruiters and the students.

Science Career Fair Representative January 27, 2005

University of Ottawa, Ontario

- Be a resource for the recruiters and the students.

Camp Counsellor Summer 2002

Patro d'Ottawa, Ontario

- Children's monitor; assist other counsellors; provide play-time fun.
- Maintain composure, effectiveness, and flexibility under pressure.